STARS

University of Central Florida
STARS

Electronic Theses and Dissertations, 2004-2019

2010

# Patterned Cell Cultures For High Throughput Studies Of Cell Electrophysiology And Drug Screening Applications

Anupama Natarajan
*University of Central Florida*

 Part of the Medical Sciences Commons
Find similar works at: https://stars.library.ucf.edu/etd
University of Central Florida Libraries http://library.ucf.edu

This Doctoral Dissertation (Open Access) is brought to you for free and open access by STARS. It has been accepted for inclusion in Electronic Theses and Dissertations, 2004-2019 by an authorized administrator of STARS. For more information, please contact STARS@ucf.edu.

## STARS Citation

Natarajan, Anupama, "Patterned Cell Cultures For High Throughput Studies Of Cell Electrophysiology And Drug Screening Applications" (2010). *Electronic Theses and Dissertations, 2004-2019*. 1578.
https://stars.library.ucf.edu/etd/1578

# PATTERNED CELL CULTURES FOR HIGH THROUGHPUT STUDIES OF CELL ELECTROPHYSIOLOGY AND DRUG SCREENING APPLICATIONS

by

ANUPAMA NATARAJAN
B.S. University of Madras, India, 2000
M.S. Clemson University, 2003

A dissertation submitted in partial fulfillment of the requirements
for the degree of Doctor of Philosophy
in the Department of Biomedical Sciences
in the College of Medicine
at the University of Central Florida
Orlando, Florida

Summer Term
2010

Major Advisor: James J. Hickman

# ABSTRACT

Over the last decade, the field of tissue and bio-engineering has seen an increase in the development of *in vitro* high-throughput hybrid systems that can be used to understand cell function and behavior at the cellular and tissue levels. These tools would have a wide array of applications including for implants, drug discovery, and toxicology, as well as for studying cell developmental behavior and as disease models. Currently, there are a limited number of efficient, functional drug screening assays in the pharmacology industry and studies of cell-surface interactions are complicated and invasive. Most cell physiology studies are performed using conventional patch-clamp techniques or random networks cultured on silicon devices such as Microelectrode Arrays (MEAs) and Field Effect transistors (FETs).

The objective of this study was to develop high-throughput *in vitro* platforms that could be used to analyze cell function and their response to various stimuli. Our hypothesis was that by utilizing surface modification to provide external guidance cues for various cell types and by controlling the cell environment in terms of culture conditions, we could develop an *in vitro* hybrid platform for sensing and testing applications. Such a system would not only give information regarding the surface effects on the growth and behavior of cells for implant development applications, but also allow for the study of vital cell physiology parameters like conduction velocity in cardiomyocytes and synaptic plasticity in neuronal networks.

This study outlines the development of these *in vitro* high throughput systems that have varied applications ranging from tissue engineering to drug development. We have developed a simple and relatively high-throughput method in order to test the physiological effects of varying

chemical environments on rat embryonic cardiac myocytes in order to model the degradation effects of polymer scaffolds. Our results, using our simple test system, are in agreement with earlier observations that utilized a complex 3D biodegradable scaffold. Thus, surface functionalization with self-assembled monolayers combined with histological/physiological testing could be a relatively high throughput method for biocompatibility studies and for the optimization of the material/tissue interface in tissue engineering.

Traditional multielectrode extracellular recording methods were combined with surface patterning of cardiac myocyte monolayers to enhance the information content of the method; for example, to enable the measurement of conduction velocity, refractory period after action potentials or to create a functional reentry model. Two drugs, 1-Heptanol, a gap junction blocker, and Sparfloxacin, a fluoroquinone antibiotic, were tested in this system. 1-Heptanol administration resulted in a marked reduction in conduction velocity, whereas Sparfloxacin caused rapid, irregular and unsynchronized activity, indicating fibrillation. As shown in these experiments, the patterning of cardiac myocyte monolayers increased the information content of traditional multielectrode measurements.

Patterning techniques with self-assembled monolayers on microelectrode arrays were also used to study the physiological properties of hippocampal networks with functional uni-directional connectivity, developed to study the mono-synaptic connections found in the dentate gyrus. Results indicate that changes in synaptic connectivity and strength were chemically induced in these patterned hippocampal networks. This method is currently being used for studying long term potentiation at the cellular level. For this purpose, two cell patterns were optimized for cell migration onto the pattern as demonstrated by time lapse studies, and for

supporting the best pattern formation and cell survival on these networks. The networks formed mature interconnected spiking neurons.

In conclusion, this study demonstrates the development and testing of *in vitro* high-throughput systems that have applications in drug development, understanding disease models and tissue engineering. It can be further developed for use with human cells to have a more predictive value than existing complex, expensive and time consuming methods.

# ACKNOWLEDGEMENTS

I would like to thank Dr. Hickman for supporting and guiding me throughout my graduate years. He has been a true mentor. I would like to thank Dr. Molnar for providing me with invaluable ideas, suggestions and advice through the years. I would like to thank members of the Hybrid systems laboratory without whose help much of the work in this dissertation would not be possible. And last but not the least I would like to thank members of my committee for feedback, and helpful suggestions. Thank you to all.

**For Mom and Dad**

# TABLE OF CONTENTS

LIST OF FIGURES ..... ix
LIST OF TABLES ..... x
CHAPTER 1: INTRODUCTION ..... 1
References: ..... 8
CHAPTER 2: GROWTH AND ELECTROPHYSIOLOGICAL PROPERTIES OF RAT EMBRYONIC CARDIOMYOCYTES ON HYDROXYL- AND CARBOXYL-MODIFIED SURFACES ..... 10
Introduction ..... 10
Materials and Methods ..... 12
Surface modification ..... 12
Surface characterization ..... 14
Embryonic rat cardiomyocyte culture ..... 14
Histology ..... 15
Electrophysiology ..... 15
Results ..... 16
Surface modification ..... 16
Morphological characterization of cardiomyocytes on functionalized surfaces ..... 17
Electrophysiology ..... 18
Discussion ..... 18
Conclusion ..... 20
References ..... 26
CHAPTER 3: PATTERNED CARDIOMMYOCYTES ON MICROELECTRODE ARRAYS: TOWARDS THE DEVELOPMENT OF A FUNCTIONAL, HIGH INFORMATION CONTENT DRUG SCREENING PLATFORM ..... 30
Introduction ..... 30
Materials and Methods ..... 34
Surface modifications of microelectrode arrays with PEG silanes ..... 34
Laser ablation and patterning of the microelectrode arrays ..... 34
Contact angle measurements ..... 35
X-Ray photoelectron spectroscopy ..... 35
Neonatal rat cardiomyocyte culture ..... 36
Multielectrode extracellular recordings ..... 37
Results ..... 38
Surface modification of the microelectrode arrays ..... 38
Cultured neonatal rat cardiomyocytes on patterned surfaces in serum-free medium ..... 40
Extracellular recordings from patterned cardiomyocytes on the MEAs ..... 41
Electrical stimulation optimization experiments ..... 43
Pharmacology and toxin studies ..... 44
Discussion ..... 45

Surface modification, photolithographic patterning and patterned cardiac myocyte cultures on micro-electrode arrays ..... 45
Electrophysiology, toxin and drug effects ..... 46
Conclusion ..... 47
..... 55
..... 56
References ..... 57
CHAPTER 4: CREATING FUNCTIONAL NEURONAL NETWORKS ON MICROELECTRODE ARRAYS TO STUDY SYNAPTIC ..... 61
Introduction ..... 61
Materials and Methods ..... 64
Surface cleaning ..... 64
Surface modification ..... 64
Photolithographic patterning ..... 65
Surface characterization ..... 65
Cell culture ..... 66
Extracellular microelectrode recordings ..... 66
Results ..... 67
Surface modification and patterning of hippocampal neurons on microelectrode arrays ..... 67
Extracellular recordings from patterned neuronal networks ..... 69
Discussion ..... 71
References: ..... 79
CHAPTER 5: DESIGNING PATTERN FEATURES TO STUDY TWO CELL HIPPOCAMPAL NETWORKS AND CELL MIGRATION IN SERUM FREE MEDIUM ..... 82
Introduction ..... 82
Materials and Methods ..... 83
Surface cleaning ..... 83
Surface modification of the acid washed slips ..... 84
Photolithographic patterning ..... 84
Surface characterization ..... 85
Cell culture ..... 87
Time lapse recording ..... 87
Results ..... 88
Discussion ..... 90
References ..... 95
CHAPTER 6: GENERAL DISCUSSION ..... 97
References ..... 101

# LIST OF FIGURES

Figure 2-1: Surface modification of the glass coverslips..... 22
Figure 2-2: Morphology of cardiomyocyte beating clusters on the functionalized surfaces at day 5..... 23
Figure 2-3: Characterization of beating cell clusters and cell morphology..... 24
Figure 2-4: Electrophysiological characterization of cardiac myocytes grown on the functionalized surfaces at day 7 in vitro..... 25
Figure 3-1: XPS analysis..... 49
Figure 3-2: Patterned neonatal cardiomyocytes..... 51
Figure 3-3: Action potential conduction in patterned cardiac myocyte monolayers..... 52
Figure 3-4: Measurement of conduction velocity in patterned cardiac myocyte monolayers with electrical stimulation..... 53
Figure 3-5: Measurement of refractory period after cardiac action potential..... 54
Figure 3-6: Effect of the gap junction blocker 1-Heptanol..... 55
Figure 3-7: Effect of the HERG channel antagonist Sparfloxacin..... 56
Figure 4-1: XPS analysis of MEAs before and after surface modification with SAMs..... 74
Figure 4-2: Pattern design and patterned embryonic hippocampal neurons..... 75
Figure 4-3: Induction of LTP like activity in cultured hippocampal networks..... 76
Figure 4-4: Induction of LTP like activity in cultured hippocampal networks..... 77
Figure 4-5: Analysis of synaptic restructuring after ACPD addition..... 78
Figure 5-1: Chemically patterned surface chemistry characterization using XPS..... 92
Figure 5-2: Metallized image of the two-neuron circuit design with different dimensions..... 92
Figure 5-3: Characterization of the effect of feature size and line width on cellular pattern formation..... 93
Figure 5-4: Time lapse sequences over 48 hours of a two-neuron circuit formation by somal translocation mode neuron migration..... 94

# LIST OF TABLES

Table 2-1 Electrophysiological characterization of 1 week old cardiac myocyte culture grown on functionalized cultures ..... 21

# CHAPTER 1: INTRODUCTION

The idea of using cell-silicon hybrid systems for varied applications has been studied extensively over the last decade. Such a system offers a result that is three fold. Cells have a vast array of receptors and resultant downstream pathways that respond to specific compounds in certain definite ways: (a) they are capable of responding to a wide variety of bioactive chemicals and can potentially offer information on the nature and structure of an unidentified toxin or drug. (b) The effects of certain drugs or toxins on specific cell types can also be studied using such a system. (c) In addition it also gives information about the functioning of the cell itself and how and why it responds to particular chemical, electrical or other stimuli. These factors make the development of *in vitro* cell-silicon hybrid systems into high throughput tools a priority in pharmacological industries, defense companies and for understanding the basic electrophysiological properties of cells. Currently, researchers are looking at using cell-based biosensors as high throughput systems for drug discovery and clinical diagnostics as well as for toxin detection [1-2]. These cell-silicon hybrid systems could also act as a replacement for animal testing and low throughput patch-clamp electrophysiology [2].

The significance of this project therefore lies in its applications. As mentioned above, the development of such a system into a high throughput drug side effect screening platform could make drug trials more efficient. Current drug trials involve screening for side effects towards the final stages of drug testing and involve a lot of time and money [3]. Tests are also usually done on animal models and are target oriented, in that they look at the effects on specific receptors, enzymes or ion channels. There is a significant need for a fast, inexpensive tool that can be used

to study drug side effects at the cellular and tissue level. The use of human cells or cells derived from human stem cells on such a hybrid platform could add another significant advantage.

Tissue engineering is defined as the use of cells, engineering and different kinds of cell suitable materials to improve or replace biological functions of different parts of the body [4]. An important part of tissue engineering is to develop materials that can be used for delivering cells to a damaged area and allowing for cell survival, differentiation and growth. Such a microenvironment controlled by cells is maintained primarily by using 3 dimensional structures called scaffolds that are made up of materials such as different kinds of polymers. When these scaffolds degenerate over time, there will be significant effects on the cell physiology and functioning. Current methods of studying polymer degeneration effects on cardiac cells involve complex methods using hydro gels. Such systems are hard to analyze, visualize, study and can be time consuming. Cells in such systems also tend to not last over long periods of time thus constraining the experiments to understand acute effects as compared to chronic long term studies. A relatively simple system of 2 dimensional cell cultures could give quick and accurate results on the effect of scaffold degeneration byproducts on the cells.

Such hybrid systems could also be further developed to study disease models. By providing enhanced and accurate information about cell and tissue function, this platform could be used to study memory formation in neuronal systems and its basic building block, long term potantiation, and in cardiac cells the parameters QT interval and refractory period. This information could then be further utilized to understand diseases such as Alzheimer's and cardiac Arrhythmia.

This dissertation outlines the development of high throughput systems primarily by controlling and changing the surface chemistry and the interface on which the cells are grown. We hypothesized that by manipulation of surface chemistry and by providing a defined environment for the cell growth, we could develop a system that will have accurate and enhanced responses to external stimuli. We further hypothesized that these responses would give information concerning the surface effects on cell function, would provide information on cell physiology as well as any changes due to drugs and toxins and help understand basic cell developmental and network behavior. We demonstrate that these systems can be tested and validated using different chemical compounds.

This project is divided into two major objectives. The first part concerned the use of cardiomyocytes and the second half, the use of Hippocampal neurons to develop examples of high throughput devices. Cell-electrode hybrid systems are possible or effective if the cells are electrically active, form synaptic connectivity (neurons) or gap junction coupling (cardiomyocytes), communicate with each other and can mimic to a certain degree their *in vivo* behavior. Cardiomyocytes (myocardial cells or fibers or myocytes) are structurally linked by cell-to-cell contacts called gap junctions and form complex networks. The contraction of these cells produces an action potential electrical signal that can be monitored and recorded by a microelectrode array. This attachment of cardiac cells to each other enables the formation of a beating monolayer or sheet of cardiomyocytes. Previous research has shown that cardiomyocytes are sensitive to a wide range of toxins and give reproducible results [5-6]. Current research involves mainly using random monolayers of cardiomyocytes or cardiac tissue to study drug effects and physiological properties [7-9]. The use of patterned cardiomyocytes that form

connections over predetermined distances with specific orientation could allow a better understanding of important physiological properties of cardiac cells such as conduction velocity, refraction, QT interval and the effects of drugs or toxins on these parameters. In this study, the feasibility of using embryonic or neonatal rat cardiomyocytes on patterned microelectrodes as a high throughput system to study cardiac electrophysiology is examined.

The brain, the 'neural machine' responsible for the mental processes of perceiving, acting, learning, remembering and the more complex concept of consciousness, is comprised of individual nerve cells [10]. The complexity of the human thought process depends not only the different types of neuronal cells, but more importantly on the way these different cells interact with each other to form 'anatomical connections'[10]. To understand the computational mechanics of neuronal networks the electrical activity of multiple cells in a network has to be monitored and studied. The hippocampus, due to its involvement in learning and memory, is a region of interest to investigators in this field [11]. The hippocampus is located inside the temporal lobe, forms part of the limbic system and plays a part in memory and navigation. The hippocampus has three major pathways: 1) The perforant pathway 2) The mossy fiber pathway and 3) The Schaffer collateral pathway. A train of high frequency stimuli to one of these synaptic pathways leads to an increase in the amplitude of the excitatory post synaptic potential in the hippocampal neuron. This effect is called Long-term potentiation (LTP) and plays an important role in the explicit memory of mammals [10]. The study of hippocampal networks integrated with silicon devices could give new insight into LTP. In this study we used patterned neuronal networks on microelectrode arrays to analyze synaptic plasticity as well as to understand LTP in disassociated hippocampal cells as opposed to tissue slices. Different configurations of the

patterns needed were analyzed, as well as characterization of the surface chemistry that was needed for successful cell migration onto the patterns, as well as their differentiation and survival.

As mentioned earlier, an important part of cell-silicon hybrid systems is the interface between the cell and the electrode. The cells need to strongly adhere to the electrodes and the surface used for this purpose should not only facilitate this but also help in long term cell survival and differentiation. The surface chemistry and its cell friendly properties are doubly important when patterning is involved [14]. Researchers have already shown the electrical activity of hippocampal cells grown on patterns of PDL (Poly-D-Lysine) on the surface of microelectrode arrays [12, 13] and on other surfaces with extracellular matrix proteins (ECM) [15-17]. In this study we not only analyzed the use of proteins like fibronectin as viable surfaces for cell growth, survival and differentiation but also actively examine the use of self-assembled monolayers (SAMS) for this purpose.

SAMs are ordered molecular assemblies that are formed by the adsorption of a surfactant onto a solid surface and are extremely useful in modifying the surface properties of a material. They were first utilized by Nuzzo and Allar [18] and are a powerful research tool due to the fact that they are relatively easy to construct and manipulate. One of the major advantages SAM's have over traditional protein surfaces is that they can be easily changed to alter surface properties like wettability, biocompatibility and protein/cellular adhesion. SAM's can also be used to control surface properties that would aid in the differential attachment and functioning of cells. Different functional groups have been known to affect various cell types in regard to attachment, proliferation and differentiation. Cells mostly favor hydrophilic surfaces that contain amino or

carboxyl surfaces and have been shown not to grow well on certain hydrophilic (Poly-Ethylene-Glycol) or hydrophobic surfaces ($CF_3CH_3$) [19-22]. Protein adsorption onto the surface, one of the factors crucial for cell adhesion, also varies with the type of the surface [21, 22]. Cell adhesion to SAM surfaces containing adsorbed proteins has also been shown to influence differentiation [23, 24].

The use of serum-free medium in culture can also be used to control protein adsorption onto these surfaces. Since serum is absent in the medium, it facilitates the attachment of cells only in the cell adhesive regions. Serum tends to adsorb on most surfaces, making patterning almost impossible in cultures containing serum. Cells are known to deposit essential proteins needed for proper attachment and functioning in the absence of serum. But the absence of serum in the culture system decreases the number of variables that control the cell environment. Serum-free cultures on different self-assembled monolayers are a reliable way to study cell-substrate interaction in a defined system [25]. Though it is known that cell attachment is mediated by cell surface receptors and non-specific interactions, the exact mechanism by which these receptors interact with SAMs is less known and studied [26, 27]. Specific functional groups such as $NH_2$ or $NH_3$ have been shown to influence receptor mediated cell attachment to ECM in serum-free conditions [28]. Using SAMs on microelectrodes, the effect of surface on cell properties and functions can be better studied and helps in understanding the mechanisms underlying receptor-surface interactions and how cells perceive environmental changes.

This dissertation research examined the ideal surface chemistry needed for proper cell growth and survival over long periods, the right pattern features to facilitate cell migration and connectivity and the proper cell types that need to be used to develop a successful cell-electrode

hybrid system. It demonstrated the use of these techniques as applied to microelectrode arrays to not only study important cardiac electrophysiological parameters and changes when exposed to drugs and toxins but also to answer the question if neuronal networks on MEAs can be used to study synaptic plasticity. These hybrid systems are useful for applications in studying scaffold degeneration effects, neuronal networks, toxin detection, pharmacological testing, study cardiac disease models and understanding functions and behavior at the cellular level.

## References:


1. Pancrazio, J. J., Whelan, J. P., Borkholder, D. A., Ma, W., and Stenger, D. A. (1999) Development and application of cell-based biosensors, *Ann Biomed Eng 27*, 697-711.
2. Kang, G., Lee, J. H., Lee, C. S., and Nam, Y. (2009) Agarose microwell based neuronal micro-circuit arrays on microelectrode arrays for high throughput drug testing, *Lab Chip 9*, 3236-3242.
3. M. Recanatini, E. Poluzzi, M. Masetti, A. Cavalli, and F. De Ponti, "QT prolongation through hERG K(+) channel blockade: current knowledge and strategies for the early prediction during drug development," *Med Res Rev,* vol. 25, pp. 133-66, Mar 2005
4. B. K. Mann and J. L. West, "Tissue engineering in the cardiovascular system: Progress toward a tissue engineered heart," *Anatomical Record,* vol. 263, pp. 367-371, 2001.
5. Israel, D. A., Edell, D. J., and Mark, R. G. (1990) Time delays in propagation of cardiac action potential, *Am J Physiol 258*, H1906-1917.
6. Natarajan, A., Molnar, P., Sieverdes, K., Jamshidi, A., and Hickman, J. J. (2006) Microelectrode array recordings of cardiac action potentials as a high throughput method to evaluate pesticide toxicity, *Toxicol In Vitro 20*, 375-381.
7. Roy, S., Chen, M. Q., Kovacs, G. T., and Giovangrandi, L. (2009) Conduction analysis in mixed cardiomyocytes-fibroblasts cultures using microelectrode arrays, *Conf Proc IEEE Eng Med Biol Soc 2009*, 4250-4253.
8. Yeung, C. K., Sommerhage, F., Wrobel, G., Law, J. K., Offenhausser, A., Rudd, J. A., Ingebrandt, S., and Chan, M. (2009) To establish a pharmacological experimental platform for the study of cardiac hypoxia using the microelectrode array, *J Pharmacol Toxicol Methods 59*, 146-152.
9. Bussek, A., Wettwer, E., Christ, T., Lohmann, H., Camelliti, P., and Ravens, U. (2009) Tissue slices from adult mammalian hearts as a model for pharmacological drug testing, *Cell Physiol Biochem 24*, 527-536.
10. Kandel, E., Schwartz, J., and Jessell, T. (2000) *Principles of Neural Science*, 4 ed., McGraw-Hill Medical.
11. James, C. D., Spence, A. J., Dowell-Mesfin, N. M., Hussain, R. J., Smith, K. L., Craighead, H. G., Isaacson, M. S., Shain, W., and Turner, J. N. (2004) Extracellular recordings from patterned neuronal networks using planar microelectrode arrays, *IEEE Trans Biomed Eng 51*, 1640-1648.
12. Chang, J. C., Brewer, G. J., and Wheeler, B. C. (2003) A modified microstamping technique enhances polylysine transfer and neuronal cell patterning, *Biomaterials 24*, 2863-2870.
13. Gross, G. W., Harsch, A., Rhoades, B. K., and Gopel, W. (1997) Odor, drug and toxin analysis with neuronal networks in vitro: extracellular array recording of network responses, *Biosens Bioelectron 12*, 373-393.
14. Ravenscroft, M. S., Bateman, K. E., Shaffer, K. M., Schessler, H. M., Jung, D. R., Schneider, T. W., Montgomery, C. B., Custer, T. L., Schaffner, A. E., Liu, Q. Y., Li, Y. X., Barker, J. L., and Hickman, J. J. (1998) Developmental Neurobiology Implications

from Fabrication and Analysis of Hippocampal Neuronal Networks on Patterned Silane-Modified Surfaces, *Journal of the American Chemical Society 120*, 12169-12177.
15. Jacques, T. S., Relvas, J. B., Nishimura, S., Pytela, R., Edwards, G. M., Streuli, C. H., and ffrench-Constant, C. (1998) Neural precursor cell chain migration and division are regulated through different beta 1 integrins, *Development 125*, 3167-3177.
16. Liesi, P., Hager, G., Dodt, H. U., Seppala, I., and Zieglgansberger, W. (1995) Domain-Specific Antibodies against the B2 Chain of Laminin Inhibit Neuronal Migration in the Neonatal Rat Cerebellum, *Journal of Neuroscience Research 40*, 199-206.
17. Rice, D. S., and Curran, T. (2001) Role of the Reelin signaling pathway in central nervous system development, *Annual Review of Neuroscience 24*, 1005-1039.
18. Nuzzo, R. G., and Allara, D. L. (1983) Adsorption of bifunctional organic disulfides on gold surfaces, *Journal of the American Chemical Society 105*, 4481-4483.
19. Stenger, D. A., Hickman, J. J., Bateman, K. E., Ravenscroft, M. S., Ma, W., Pancrazio, J. J., Shaffer, K., Schaffner, A. E., Cribbs, D. H., and Cotman, C. W. (1998) Microlithographic determination of axonal/dendritic polarity in cultured hippocampal neurons, *J Neurosci Methods 82*, 167-173.
20. Stenger, D. A., Pike, C. J., Hickman, J. J., and Cotman, C. W. (1993) Surface determinants of neuronal survival and growth on self-assembled monolayers in culture, *Brain Res 630*, 136-147.
21. A. Galtayries, R. W.-C. M. D. N. P. M. (2006) Fibronectin adsorption on Fe-Cr alloy studied by XPS, *Surface and Interface Analysis 38*, 186-190.
22. C.D. Tidwell, D. G. C., S.L. Golledge, B.D. Ratner, K. Meyer, B. Hagenoff, and A. Benninghoven. (2001) Static ToF SIMS and XPS Characterization of Adsorbed Albunim and Fibronectin Films, *Surface and Interface Analysis 31*, 724-733.
23. Healy, K. E., Thomas, C. H., Rezania, A., Kim, J. E., McKeown, P. J., Lom, B., and Hockberger, P. E. (1996) Kinetics of bone cell organization and mineralization on materials with patterned surface chemistry, *Biomaterials 17*, 195-208.
24. Jenney, C. R., and Anderson, J. M. (2000) Adsorbed serum proteins responsible for surface dependent human macrophage behavior, *J Biomed Mater Res 49*, 435-447.
25. Schaffner, A. E., Barker, J. L., Stenger, D. A., and Hickman, J. J. (1995) Investigation of the factors necessary for growth of hippocampal neurons in a defined system, *J Neurosci Methods 62*, 111-119.
26. McClary, K. B., Ugarova, T., and Grainger, D. W. (2000) Modulating fibroblast adhesion, spreading, and proliferation using self-assembled monolayer films of alkylthiolates on gold, *J Biomed Mater Res 50*, 428-439.
27. Soekarno, A., Lom, B., and Hockberger, P. E. (1993) Pathfinding by neuroblastoma cells in culture is directed by preferential adhesion to positively charged surfaces, *Neuroimage 1*, 129-144.
28. St John, P. M., Kam, L., Turner, S. W., Craighead, H. G., Issacson, M., Turner, J. N., and Shain, W. (1997) Preferential glial cell attachment to microcontact printed surfaces, *J Neurosci Methods 75*, 171-177.

# CHAPTER 2: GROWTH AND ELECTROPHYSIOLOGICAL PROPERTIES OF RAT EMBRYONIC CARDIOMYOCYTES ON HYDROXYL- AND CARBOXYL-MODIFIED SURFACES

## Introduction

One of the most promising methods for the replacement of damaged cardiac muscle involves seeding cardiac myocytes or stem cells onto a bioresorbable scaffold. The tissue is allowed to maturate *in vitro* and then the construct is implanted at the appropriate location as prosthesis [1–4].

Poly(lactic acid) (PLA), poly(lactic-co-glycolic acid) (PLGA) and poly(glycolic acid) (PGA) are among the few biodegradable scaffold materials which have been approved for human use [5]. They have been extensively used in cardiac tissue engineering [2, 6, 7]. Degradation of PLA, PLGA and PGA *in vitro* and *in vivo* has been shown to be mediated by hydrolysis [8–12] producing degradation products with hydroxyl and carboxyl functional groups. Although PLA, PLGA and PGA have been extensively used in tissue engineering and considered biocompatible, the bioactivity of their degradation products has been much less studied, due to technical difficulties. In a recent paper, Sung *et al.* reported differential survival of cardiac myocytes when exposed to different degradation stages of PLGA scaffolds [13]. The composition of the scaffold significantly influenced the survival of the cells. In addition, degradation rate and survival of the cardiac myocytes were inversely correlated. There are several lines of evidence indicating that surface interactions are important in the development of cardiac myocytes. Clark *et al.* reported that cell–cell contact was a major determinant in the development of spontaneous activity

(beating) in adult feline cardiomyocyte cultures [14]. The culture surface had a significant role, not only in the attachment [15] of the cells, but also in cell signaling. Simpson *et al.* showed that the phenotype of cardiac myocytes was determined by the culture substrate (type I collagen) through a signaling process which involved the cardiac $\alpha$-1 or $\beta$-1 integrin chain [16].

The goal of our study was to create a simple *in vitro* test system where the chemical environment (both contact and soluble) of the cardiac myocytes could be controlled and systematically varied. We were especially interested in the physiological reaction of the cells to hydroxyl- and carboxyl-functional groups in the culture system as a model of different degradation stages of PLA or PLGA scaffolds. Our defined system consisted of a functionalized surface to determine contact interactions between the cells and the culture-surface, as well as a serum-free culture medium developed earlier in our laboratory [17, 18]. In the development of this test system we concentrated on the study of the effect of the chemical environment of the cells, although there are several lines of evidence indicating that topology of the surface/physical properties of the 3D scaffold could also be important for the determination of growth and differentiation of the cells [19–22]. The surfaces were functionalized using self-assembled monolayers (SAMs) because of the flexibility of the method [23–26]. Almost any surface can be equipped with functionalized monolayers which possess the required specific electrical, optical or chemical properties [24, 27–31]. A wide variety of functional groups are available for surface modification [32]. SAMs have already been used for the study of cell–surface interactions [33–36], cell patterning [37], control of protein adsorption [38–41] and prosthetic device biocompatibility [42–44]. Fields has suggested the use of SAMs to create bioactive surfaces with covalent protein-functionalization and controlled protein folding [45, 46].

For physiological testing of the surfaces we utilized embryonic (*vs.* the more commonly used neonatal) rat cardiac myocytes, because in earlier studies we had developed a serum-free medium formulation which was shown to support the growth and differentiation of embryonic cardiac myocytes on our defined surfaces [17]. Serum-free culture conditions were essential for the testing of surface effects on the physiology of the cells because of the fast adsorption of serum proteins to the defined surfaces [47–52].We believe this method for testing the physiological effects of the degradation products of PLA and PLGA scaffolds (modeled by the hydroxyl and carboxyl functionalized surfaces) could be generalized for *in vitro* biocompatibility testing of these materials. The interface between the engineered material and the tissue can be mimicked by specific surface functional groups and the biological effects of these surfaces can be tested independently of the biomaterial's bulk physical properties. Other applications would be in the development of clinically applicable biomaterials by surface modification of a material which already has excellent biofunctionality and bulk properties [53, 54].

## Materials and Methods

### *Surface modification*

The following surfaces were used in this study: (i) Trimethoxysilylpropyldiethylenetriamine (DETA), (ii) (3-aminopropyl)triethoxysilane (APTES), (iii) 11-mercaptoundecanoic acid (MUA, $HS(CH_2)10COOH$) and (iv) 11-mercapto-1-undecanol (MUL, $HS(CH_2)11OH$). These surfaces were used to model the hydroxyl and carboxyl groups produced during to scaffold degeneration.

*DETA surface modification:* Briefly, glass coverslips (Thomas Scientific, Swedesboro, NJ, USA; 6661F52, 22 x 22 mm, No. 1) were cleaned using an $O_2$ plasma cleaner (Harrick,

Ithaca, NY, USA; PDC-32G) for 30 min at 400 mTorr. The DETA (United Chemical Technologies, Bristol, PA, USA; T2910KG) SAM was formed by the reaction of the cleaned surface with a 0.1% (v/v) mixture of the organosilane in freshly distilled toluene (Fisher, Pittsburgh, PA, USA; T2904). The coverslips were placed in the mixture, heated to 70°C, rinsed with toluene, reheated to 70°C and then oven-dried

*APTES Surface modification:* Briefly, after $O_2$ plasma cleaning, the glass cover slips were immersed in a mixture of 1% APTES (Sigma, St Louis, MO, USA) in freshly distilled and dried toluene for 60 min inside a nitrogen-purged glove box. They were then rinsed with fresh, dried toluene three times and cured in the oven at 110°C for 30 min. The APTES-modified SAMs were immersed in absolute ethanol (Sigma) until they were used. The carboxyl- and hydroxyl-modified SAMs were prepared using the bi-functional cross-linker *N*-succinimidyl 4-maleimidobutyrate (GMBS, Pierce, Rockford, IL, USA). The APTES SAMs were immersed in a solution of 2 mM GMBS in absolute ethanol after dissolution in a minimum amount of dry dimethyl sulfoxide (DMSO, Pierce) for approx. 60 min. They were then rinsed with absolute ethanol three times. The intermediate GMBS was immersed immediately in 10 mM MUA (Aldrich 45,056-1; 95%) with a minimum amount of dry DMSO, or 10 mM MUL (Aldrich 44,752-8; 97%) with a minimum amount of dry dimethylforamide (DMF, Pierce) in absolute ethanol, for at least 1 h [56], followed by a final rinse in ethanol.

## *Surface characterization*

Surfaces were characterized by contact angle measurements using an optical contact angle goiniometer (KSV Instruments, Monroe, CT, USA; Cam 200) and by X-ray photoelectron spectroscopy (XPS) (Fisons Escalab 200i XL). XPS survey scans, as well as high-resolution S 2p, N 1s and C 1s scans, utilizing monochromatic Al K$\alpha$ excitation, were obtained [55]. The energy of the emitted electrons is measured with a hemispherical energy analyzer at pass energies ranging from 50 to 150 eV. The binding energy (BE) scale is referenced by setting the peak maximum in the Si 2p spectrum. The counts are normalized by the peak area of the Si 2p as an internal reference. Spectra were collected with the analyzer at 90°C with respect to the surface plane. A typical pressure in the analysis chamber during spectral acquisition is about 9-10 Torr.

## *Embryonic rat cardiomyocyte culture*

Cardiomyocytes were obtained from rat embryos on the 14th day of embryonic development (E14) [57] according to a protocol approved by the Institutional Animal Care and Use Committee of the University of Central Florida. Briefly, rats were killed by inhalation of an excess of $CO_2$. The hearts were removed from the embryos in Hibernate E medium (BrainBits, Springfield, IL, USA) and dissociated using type II Collagenase (Worthington, Lakewood, NJ, USA; LS004174, 125 units/g, 1 g/5 ml) in L-15 medium. The hearts in the collagenase solution were placed in the water bath (37°C, 90 rpm) for 20 min followed by gentle manual trituration.

The cell suspension was then centrifuged on a 4% bovine serum albumin (BSA, Sigma, A-3058) cushion at 300*g*, 4°C for 10 min. The cell pellet was then resuspended in the culture medium and plated on the surface-modified coverslips at a density of 1000 cells/mm$^2$. The culture medium consisted of 100 ml Ultraculture medium (Cambrex, East Rutherford, NJ, USA), 5 ml B-27 (Invitrogen, Carlsbad, CA, USA), 1 ml non-essential amino acids (Invitrogen, 11140-050), 1 ml L-glutamine (Invitrogen, 25030-164), 1 ml 1 M Hepes buffer (Sigma) and 0.375 gm dextrose (Sigma). The medium was changed on the first day after culture and thereafter every 3 days.

## *Histology*

The coverslips were fixed with 3.7% formaldehyde in phosphate-buffered saline (PBS) for 10 min and permeabilized with 0.1% Triton X-100 in PBS solution for 5 min. The fixed cells were preincubated with 1% BSA for 20–30 min. Then, fluorescent phallotoxin was added to the coverslips (BODIPY 581/591 phalloidin, Invitrogen, B3416, 1:40 dilution in PBS). The coverslips in the staining solution were then kept at room temperature for 20 min and mounted with Citofluor mounting solution (Ted Pella) onto slides. The immunostainings were visualized using a Zeiss LSM 510 confocal microscope [17].

## *Electrophysiology*

Whole-cell patch-clamp recordings were performed in a recording chamber on the stage of a Zeiss Axioscope 2FS Plus upright microscope in L-15 medium at 22°C. Patch-clamp pipettes were prepared from borosilicate glass (BF150-86-10; Sutter, Novato, CA, USA) with a Sutter P97 pipette puller and filled with intracellular solution (in mM: K-gluconate 140, EGTA 1, MgCl2 2, Na2ATP 5, Hepes 10; pH 7.2). The resistance of the electrodes was 6–8 M. Action

potentials were recorded in current clamp mode using a Multiclamp 700A amplifier (Axon, Union City, CA, USA). Signals were filtered at 2 kHz and digitized at 20 kHz with an Axon Digidata 1322A interface. Data recording and analysis was performed with pClamp 9 software (Axon). Membrane potentials were corrected by subtraction of the 15 mV tip potential, which was calculated using Axon's pClamp 9 program.

## Results

### *Surface modification*

Glass coverslips were functionalized with (i) Trimethoxysilylpropyldiethylenetriamine (DETA), (ii) (3-aminopropyl)triethoxysilane (APTES), (iii) 11-mercaptoundecanoic acid (MUA, $HS(CH_2)10COOH$) and (iv) 11-mercapto-1-undecanol (MUL, $HS(CH_2)11OH$), according to the protocol outlined in Fig. 2-1. Contact angle and XPS measurements were used for the verification of the surface modification process. Contact angle for the DETA, APTES, GMBS modified APTES, MUA and MUL surfaces was 48±3° , 45±4° , 60±2° , 66±3° and 56±3° respectively. The normalized intensity of nitrogen on APTES was 600 ± 200, calculated as the area under the high-resolution N 1s peak, divided with the internal reference peak, Si 2p. The C 1s spectra of MUA and MUL show three distinct peaks. The first is around 284.5 eV, a peak characteristic of the internal units of aliphatic carbons (C–C and C–H) from MUA and MUL, the second is around 286 eV, a characteristic peak of alcoholic carbons (C–OH) from MUL and MUA, and the third is around 288 eV, corresponding to the carboxyl carbons (COOH) from the MUA. There is a small contribution from the crosslinker as well, but it is not considered

significant. Sulfur peaks, although small, were evident in the spectra from both the MUL and MUA cross-linked surfaces. The intensity of the peaks at 286 eV is higher on the MUL surface than on MUA, as expected, but does not give a clear cut distinction between the two surfaces. However, there is a five-fold difference in intensity of the carbonyl carbon peak from MUA *vs.* that from the MUL. There is obviously some contribution from the buried carbonyl peaks due to the crosslink, but the surface functional groups, as expected, dominate the XPS spectrum. The carbon data in conjunction with the sulfur data indicate derivitization of the surfaces with the respective end-groups.

### *Morphological characterization of cardiomyocytes on functionalized surfaces*

The growth and differentiation of rat embryonic cardiomyocytes on the four functionalized surfaces (MUA, MUL, APTES and DETA) were studied over a two week period. At the early stage of the culture (1–3 days) the cells formed small, clearly separated, non-beating clusters [17]. By day 5 *in vitro* these clusters showed spontaneous beating on all surfaces. The best attachment and growth of the cardiac cells was observed on DETA, followed by those on the MUA surfaces. APTES was a close third with cell attachment and spontaneous activity almost similar to the MUA surface (Fig. 2-2). The MUL surface showed comparatively poor attachment and a significantly lower presence of beating cell clusters compared to the other three surfaces (Fig. 2-3).

Histological analysis using BODIPY-conjugated phallotoxin showed that the beating islands consisted of cardiac myocytes. The beating islands varied in diameter, from approx. 260–305 μm for each of the cell groupings, with an approximate range of 13–20 cells/island. At the single-cell level we were not able to detect any differences in the morphology of cardiac

myocytes grown on the functionalized surfaces. The measured parameters of cell size and shape were quantified by the ratio of the longest and shortest axis of the cells and measured by the NIH Image program, as shown in Fig. 2-3.

### *Electrophysiology*

Whole-cell patch-clamp experiments were performed on beating cardiac myocytes grown on the functionalized surfaces at day 7 *in vitro*. There was no significant difference in any of the measured parameters between the four groups, except in the length of the action potentials (Fig. 2-4 and Table 2-1). There was a significant fraction of cells on MUL that fired longer action potentials compared to any of the other functionalized surfaces. The differences in peak shape are shown in Fig. 2-4. The longer *average* action potential length in the MUL group was the result of the presence of a larger number of cells generating longer action potentials, as indicated in Fig. 2-4B. However, this cell population was not totally unique to the MUL surface, as this type of action potential was observed from cells on the other surface as well, but at a much lower frequency. Longer action potentials in the MUL, and less frequently in the other groups, were also observed in older

## Discussion

The interaction of cardiac myocytes with the degradation products of the commonly used scaffold materials poly(lactic acid) (PLA), poly(lactic-co-glycolic acid) (PLGA) and poly(glycolic acid) (PGA) were modeled by culturing embryonic rat cardiac myocytes on functionalized coverslips presenting carboxyl and hydroxyl groups on the surface. Contact angle

measurements and XPS indicated the successful functionalization of the glass coverslips with SAMs presenting carboxyl and hydroxyl groups on the surface. Embryonic cardiac myocytes formed beating islands on all tested surfaces, DETA, APTES, MUA and MUL, but the number of attached cells and beating patches was significantly lower on the MUL surface compared to any of the other functionalized surfaces. Also, whole-cell patch-clamp experiments indicated that the average action potential length generated by the beating cardiac myocytes were significantly longer on MUL compared to the other surfaces. The decreased number of beating cardiac myocytes on the hydroxyl-functionalized surface was in agreement with recent observations reported by Sung and co-workers [13] using 3D scaffolds. They reported that there was a decreased survival of cardiac myocytes in advanced stages of degradation of the PLGA scaffolds (higher hydroxyl/carboxyl ratio) compared to non-degraded scaffolds. In contrast to the experiments of Sung *et al.* where 3D scaffolds were used for biocompatibility studies, thus limiting systematic studies, we have developed a general method to test the effect of the chemical environment on cardiac myocytes using self-assembled monolayer-based surface modifications in a serum free environment and used Sung *et al.* results as a reference and for validation. Moreover, we were able to measure physiological parameters, not only survival, in our system, which is not possible in 3D scaffolds.

Our observation concerning the increased number of cardiac myocytes that generated long action potentials on MUL compared to the other functionalized surfaces might indicate that either (i) these long action potentials are generated by non-healthy cells and the ratio of non-healthy/healthy cells was greater on MUL, which is in agreement with the decreased viability, or (ii) the hydroxyl groups on the surface affected the differentiation of the cardiac myocytes by

inducing the development of a phenotypically separate cell population, or (iii) surface properties selectively affected the survival of atrial *vs.* ventricular myocytes, which have different electrophysiological properties, or (iv) hydroxyl groups on the surface slowed down the differentiation process in these cardiac myocytes, because the action potential duration is shortened as the normal development of cardiac myocytes progresses.

Further studies are needed to gain a deeper understanding regarding the impact of the chemical environment on the physiology of cardiac myocytes (as well as other cell types) because this information is essential for several tissue engineering applications. Our system, which consists of a serum-free culture medium and a defined surface, offers a tool for these studies. As more and more cells become available for culture under serum free conditions, our method can be extended to all of these cell types. In this study, we did not investigate the effect of substrate topography/texture on the physiology of the cells, only the chemical composition, but those important effects can also be modeled in our defined system.

## Conclusion

Our simple method that used hydroxyl- and carboxyl-functionalized surfaces to test the effect of the different chemical environments that surrounds cardiac myocytes at different stages of the degradation of PLA, PLGA or PGA scaffolds gave the same result, decreased viability in the case of hydroxyl-functionalization, than earlier experiments using a complex 3D scaffold. In our system the chemical environment affected not only the survival, but also the physiology (action potential duration) of the cardiac myocytes. Surface functionalization with self-assembled monolayers combined with histological/physiological testing could be a relatively high throughput method for biocompatibility studies and optimization

**Table 2-1 Electrophysiological characterization of 1 week old cardiac myocyte culture grown on functionalized cultures**

| Parameter | MUA | | MUL | | APTES | | DETA | |
|---|---|---|---|---|---|---|---|---|
| | Mean | SEM | Mean | SEM | Mean | SEM | Mean | SEM |
| $R_m$ (MΩ) | 35.0 | 4.00 | 34.9 | 2.77 | 51.6 | 11.32 | 28.3 | 8.30 |
| $V_m$ (mV) | −44.3 | 3.26 | −49.8 | 4.27 | −44.9 | 5.63 | −43.2 | 6.04 |
| $C_p$ (pF) | 111 | 22.20 | 77 | 23.38 | 76 | 13.23 | 135 | 25.8 |
| AP overshoot (mV) | 18.9 | 3.85 | 22.1 | 5.23 | 21.0 | 7.83 | 8.9 | 3.05 |
| AP1/2 duration (ms) | 106 | 23.60 | 231* | 63.08 | 98 | 38.77 | 89 | 28.35 |

$n = 13–19$ experiments/group;
* significantly different from all of the other groups, $P < 0.05$.

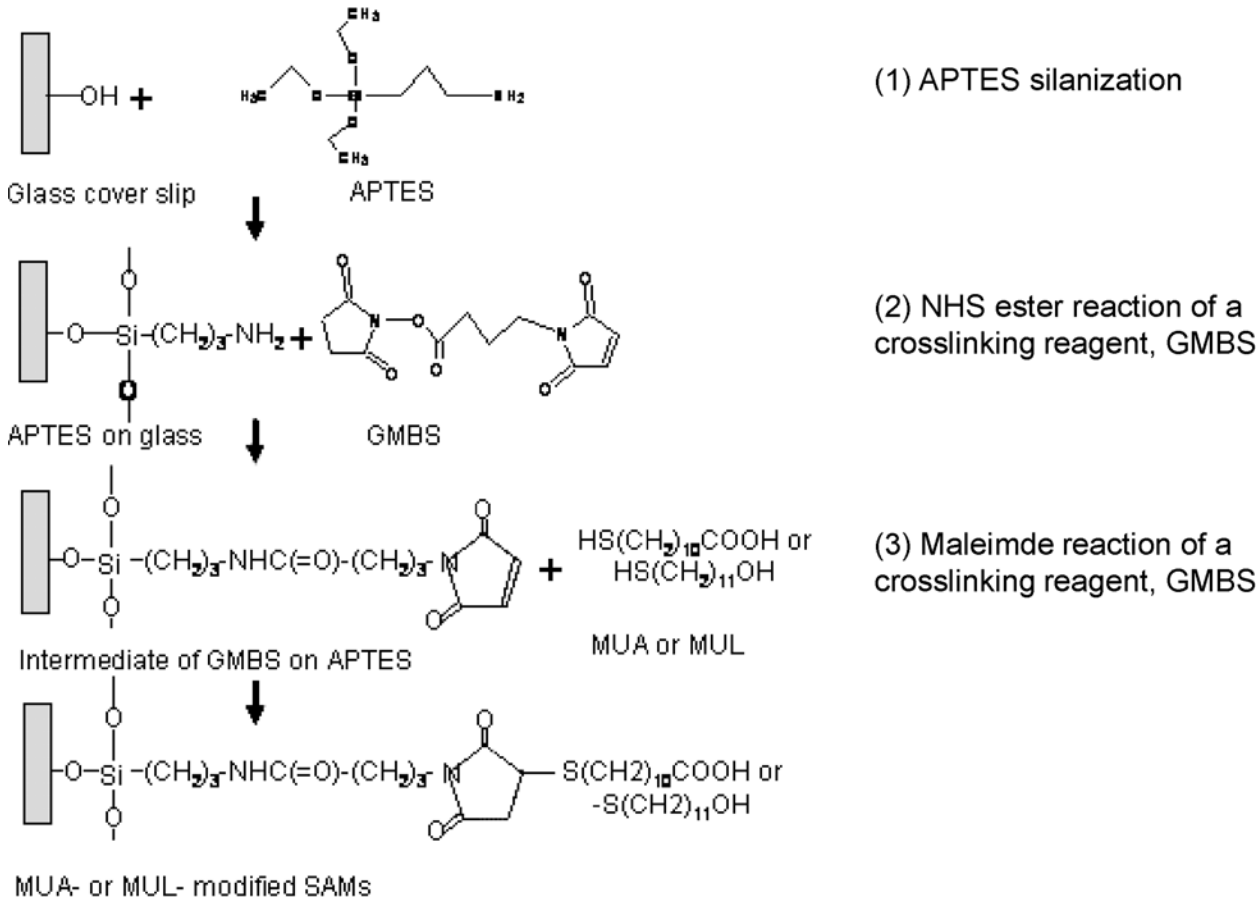


**Figure 2-1: Surface modification of the glass coverslips**

**Glass coverslips were covalently modified with the APTES SAM, MUA or MUL was then covalently attached to the APTES monolayer with a bi-functional cross-linker (GMBS).**

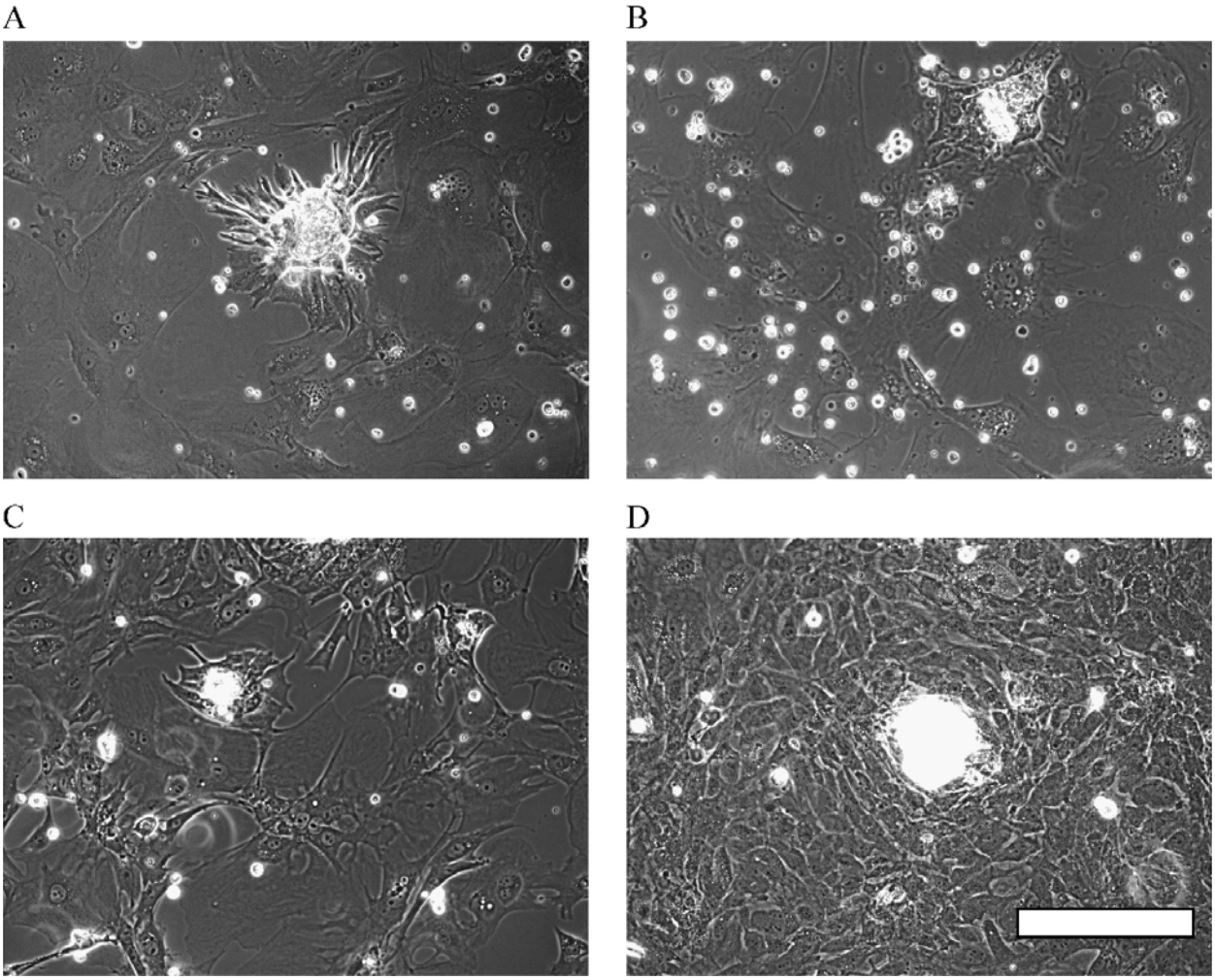


**Figure 2-2: Morphology of cardiomyocyte beating clusters on the functionalized surfaces at day 5**

**(A) MUA, (B) MUL, (C) APTES and (D) DETA. Scale bar = 100 µm.**

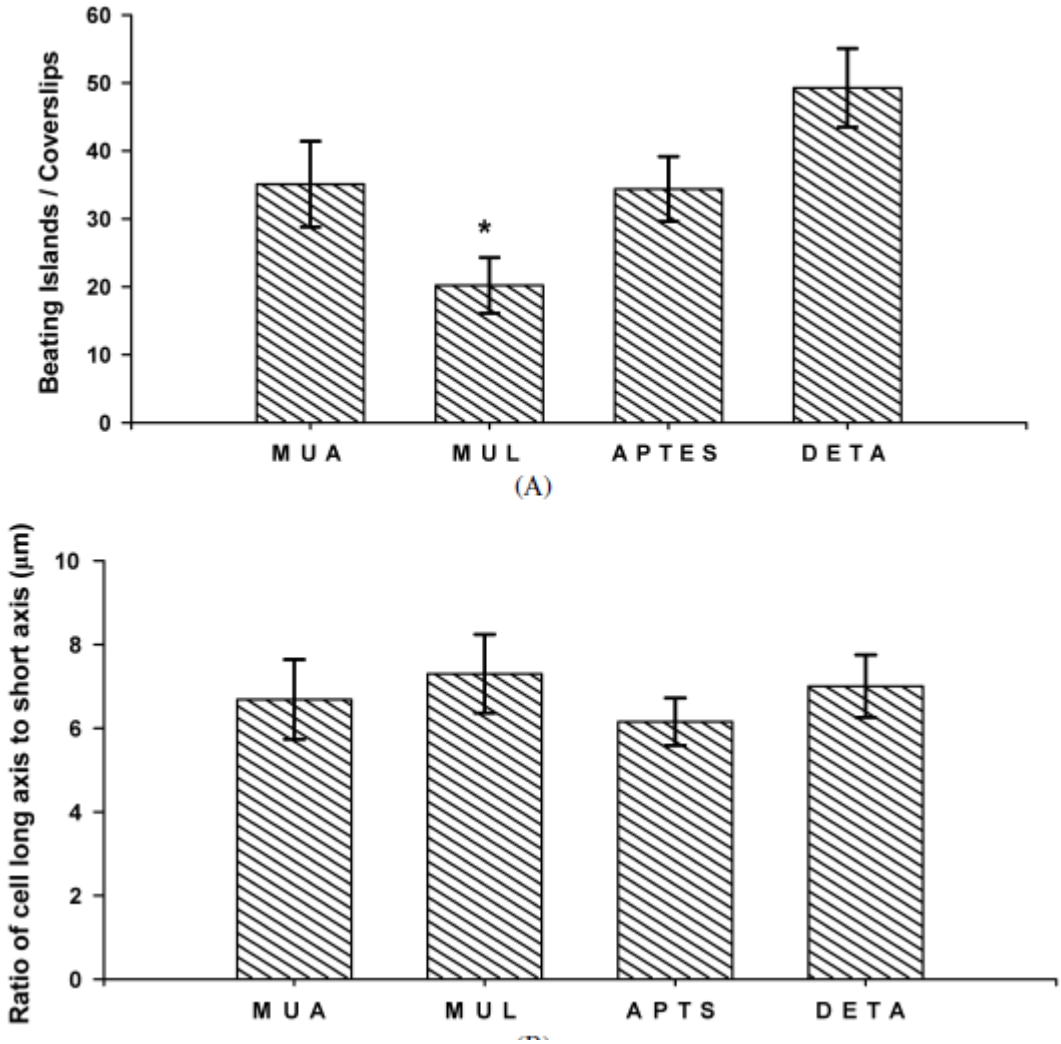


**Figure 2-3: Characterization of beating cell clusters and cell morphology**

**(A) Beating cardiomyocyteclusters/ coverslip on the functionalized surfaces. There were significantly less beating clusters on MUL surface compared to MUA, APTES or DETA. There was no significant difference between MUA, APTES or DETA. Two-sample Student's *t* -test, $p < 0.05$. 5 experiments with 3 parallel coverslips in each, mean ±SEM. (B) Ratio of the longest and shortest axis of the cells measured by the NIH Image program ImageJ.**

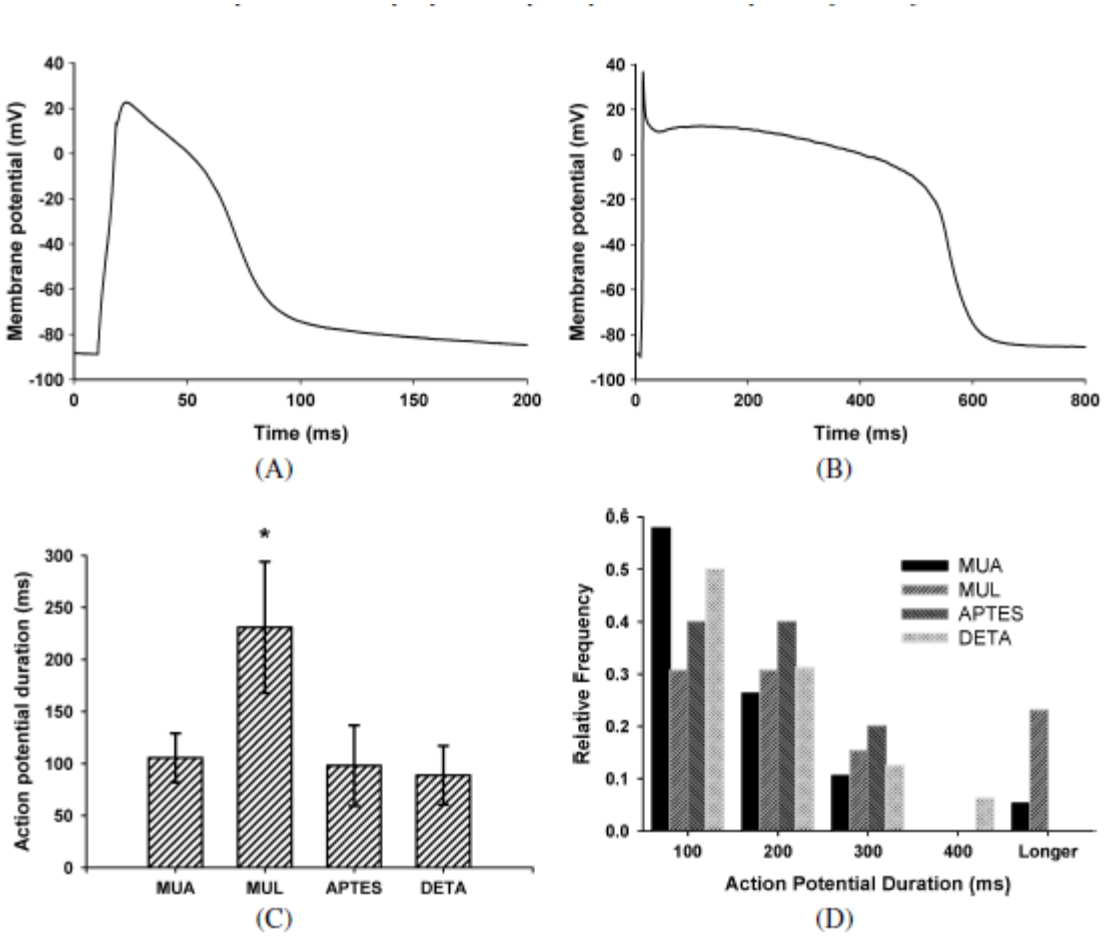


**Figure 2-4: Electrophysiological characterization of cardiac myocytes grown on the functionalized surfaces at day 7 in vitro**

**(A, B) Representative action potential shapes on MUA and MUL surfaces, respectively. Note the different time-scales. (C) Action potentials were significantly wider on the MUL surface than on any of the other surfaces. Mean of 13–19 experiments ± SEM was shown. Two-sample Student's *t* -test, p <0.05. D: The distribution of the action potential width showed that on the MUL surfaces there was a cell population generating unusually wide action potentials. Relative frequency was normalized to the total number of recorded cells on the given surface**

# References


[1] E. Rabkin and F. J. Schoen, "Cardiovascular tissue engineering," *Cardiovascular Pathology,* vol. 11, pp. 305-317, 2002.

[2] R. L. Carrier, M. Papadaki, M. Rupnick, F. J. Schoen, N. Bursac, R. Langer, L. E. Freed, and G. Vunjak-Novakovic, "Cardiac tissue engineering: Cell seeding, cultivation parameters, and tissue construct characterization," *Biotechnology and Bioengineering,* vol. 64, pp. 580-589, 1999.

[3] J. Leor, S. Aboulafia-Etzion, A. Dar, L. Shapiro, I. M. Barbash, A. Battler, Y. Granot, and S. Cohen, "Bioengineered cardiac grafts - A new approach to repair the infarcted myocardium?," *Circulation,* vol. 102, pp. 56-61, 2000.

[4] H. J. Evans, J. K. Sweet, R. L. Price, M. Yost, and R. L. Goodwin, "Novel 3D culture system for study of cardiac myocyte development," *Am J Physiol Heart Circ Physiol,* vol. 285, pp. H570-578, July 11, 2003 2003.

[5] K. A. Athanasiou, G. G. Niederauer, and C. M. Agrawal, "Sterilization, toxicity, biocompatibility and clinical applications of polylactic acid polyglycolic acid copolymers," *Biomaterials,* vol. 17, pp. 93-102, Jan 1996.

[6] B. K. Mann and J. L. West, "Tissue engineering in the cardiovascular system: Progress toward a tissue engineered heart," *Anatomical Record,* vol. 263, pp. 367-371, 2001.

[7] M. Papadaki, N. Bursac, R. Langer, J. Merok, G. Vunjak-Novakovic, and L. E. Freed, "Tissue engineering of functional cardiac muscle: molecular, structural, and electrophysiological studies," *American Journal of Physiology-Heart and Circulatory Physiology,* vol. 280, pp. H168-H178, 2001.

[8] A. Gopferich, "Polymer degradation and erosion: Mechanisms and applications," *European Journal of Pharmaceutics and Biopharmaceutics,* vol. 42, pp. 1-11, Jan 1996.

[9] A. Gopferich, "Mechanisms of polymer degradation and erosion," *Biomaterials,* vol. 17, pp. 103-114, Jan 1996.

[10] L. Lu, S. J. Peter, M. D. Lyman, H. L. Lai, S. M. Leite, J. A. Tamada, S. Uyama, J. P. Vacanti, R. Langer, and A. G. Mikos, "In vitro and in vivo degradation of porous poly(DL-lactic-co-glycolic acid) foams," *Biomaterials,* vol. 21, pp. 1837-1845, Sep 2000.

[11] Q. Cai, J. Z. Bei, and S. G. Wang, "Relationship among drug delivery behavior, degradation behavior and morphology of copolylactones derived from glycolide, L-lactide and epsilon-caprolactone," *Polymers for Advanced Technologies,* vol. 13, pp. 105-111, Feb 2002.

[12] Q. Cai, G. X. Shi, J. Z. Bei, and S. G. Wang, "Enzymatic degradation behavior and mechanism of poly(lactide-co-glycolide) foams by trypsin," *Biomaterials,* vol. 24, pp. 629-638, Feb 2003.

[13] H. J. Sung, C. Meredith, C. Johnson, and Z. S. Galis, "The effect of scaffold degradation rate on three-dimensional cell growth and angiogenesis," *Biomaterials,* vol. 25, pp. 5735-5742, Nov 2004.

[14] W. A. Clark, M. L. Decker, M. Behnke-Barclay, D. M. Janes, and R. S. Decker, "Cell contact as an independent factor modulating cardiac myocyte hypertrophy and survival in

long-term primary culture," *Journal of Molecular and Cellular Cardiology,* vol. 30, pp. 139-155, 1998.

[15] S. Boateng, S. S. Lateef, C. Crot, D. Motlagh, T. Desai, A. M. Samarel, B. Russell, and L. Hanley, "Peptides bound to silicone membranes and 3D microfabrication for cardiac cell culture," *Advanced Materials,* vol. 14, pp. 461-+, 2002.

[16] D. G. Simpson, L. Terracio, M. Terracio, R. L. Price, D. C. Turner, and T. K. Borg, "Modulation of Cardiac Myocyte Phenotype in-Vitro by the Composition and Orientation of the Extracellular-Matrix," *Journal of Cellular Physiology,* vol. 161, pp. 89-105, 1994.

[17] M. Das, P. Molnar, C. Gregory, L. Riedel, A. Jamshidi, and J. J. Hickman, "Long-term culture of embryonic rat cardiomyocytes on an organosilane surface in a serum-free medium," *Biomaterials,* vol. 25, pp. 5643-5647, Nov 2004.

[18] A. Natarajan, P. Molnar, K. Sieverdes, A. Jamshidi, and J. J. Hickman, "Microelectrode array recordings of cardiac action potentials as a high throughput method to evaluate pesticide toxicity," *Toxicology in Vitro,* vol. 20, pp. 375-381, Apr 2006.

[19] F. Berthiaume, P. V. Moghe, M. Toner, and M. L. Yarmush, "Effect of extracellular matrix topology on cell structure, function, and physiological responsiveness: Hepatocytes cultured in a sandwich configuration," *Faseb Journal,* vol. 10, pp. 1471-1484, 1996.

[20] Y. Ito, "Surface micropatterning to regulate cell functions," *Biomaterials,* vol. 20, pp. 2333-2342, 1999.

[21] C. Y. Lin, N. Kikuchi, and S. J. Hollister, "A novel method for biomaterial scaffold internal architecture design to match bone elastic properties with desired porosity," *Journal of Biomechanics,* vol. 37, pp. 623-636, May 2004.

[22] A. E. Dityatev, N. M. Chmykhova, L. Studer, O. A. Karamian, V. M. Kozhanov, and H. P. Clamann, "Comparison of the topology and growth rules of motoneuronal dendrites," *Journal of Comparative Neurology,* vol. 363, pp. 505-516, 1995.

[23] G. M. Whitesides, J. P. Mathias, and C. T. Seto, "Molecular self-assembly and nanochemistry: a chemical strategy for the synthesis of nanostructures," *Science,* vol. 254, pp. 1312-9., 1991.

[24] T. Wink, S. J. vanZuilen, A. Bult, and W. P. vanBennekom, "Self-assembled monolayers for biosensors," *Analyst,* vol. 122, pp. R43-R50, 1997.

[25] K. L. Prime and G. M. Whitesides, "Self-assembled organic monolayers: model systems for studying adsorption of proteins at surfaces," *Science,* vol. 252, pp. 1164-7., 1991.

[26] P. E. Laibinis, J. J. Hickman, M. S. Wrighton, and G. M. Whitesides, "Orthogonal Self-Assembled Monolayers: Alkanethiols on Gold and Alkane Carboxylic Acids on Alumina," *Science,* vol. 245, pp. 845-847, 1989.

[27] C. D. Bain and G. M. Whitesides, "Molecular-Level Control over Surface Order in Self-Assembled Monolayer Films of Thiols on Gold," *Science,* vol. 240, pp. 62-63, 1988.

[28] M. Mrksich, C. S. Chen, Y. N. Xia, L. E. Dike, D. E. Ingber, and G. M. Whitesides, "Controlling cell attachment on contoured surfaces with self- assembled monolayers of alkanethiolates on gold," *Proceedings of the National Academy of Sciences of the United States of America,* vol. 93, pp. 10775-10778, 1996.

[29] E. Ostuni, L. Yan, and G. M. Whitesides, "The interaction of proteins and cells with self-assembled monolayers of alkanethiolates on gold and silver," *Colloids and Surfaces B-Biointerfaces,* vol. 15, pp. 3-30, 1999.

[30] D. A. Stenger, J. H. Georger, C. S. Dulcey, J. J. Hickman, A. S. Rudolph, T. B. Nielsen, S. M. McCort, and J. M. Calvert, "Coplanar Molecular Assemblies of Aminoalkylsilane and Perfluorinated Alkylsilane - Characterization and Geometric Definition of Mammalian-Cell Adhesion and Growth," *Journal of the American Chemical Society,* vol. 114, pp. 8435-8442, 1992.

[31] G. S. Ferguson, M. K. Chaudhury, H. A. Biebuyck, and G. M. Whitesides, "Monolayers on Disordered Substrates - Self-Assembly of Alkyltrichlorosilanes on Surface-Modified Polyethylene and Poly(Dimethylsiloxane)," *Macromolecules,* vol. 26, pp. 5870-5875, 1993.

[32] A. Ulman, *Introduction to Ultrathin organic Films*. San Diego: Academic Press, Inc., 1991.

[33] J. H. Georger, D. A. Stenger, A. S. Rudolph, J. J. Hickman, C. S. Dulcey, and T. L. Fare, "Coplanar Patterns of Self-Assembled Monolayers for Selective Cell-Adhesion and Outgrowth," *Thin Solid Films,* vol. 210, pp. 716-719, 1992.

[34] A. E. Schaffner, J. L. Barker, D. A. Stenger, and J. J. Hickman, "Investigation of the factors necessary for growth of hippocampal neurons in a defined system," *Journal of Neuroscience Methods,* vol. 62, pp. 111-119, 1995.

[35] M. Mrksich, "Tailored substrates for studies of attached cell culture," *Cellular and Molecular Life Sciences,* vol. 54, pp. 653-662, 1998.

[36] M. Das, P. Molnar, H. Devaraj, M. Poeta, and J. J. Hickman, "Electrophysiological and Morphological Characterization of Rat Embryonic Motoneurons in a Defined System," *Biotechnol. Prog.,* vol. 19, pp. 1756 -1761, 2003.

[37] M. S. Ravenscroft, K. E. Bateman, K. M. Shaffer, H. M. Schessler, D. R. Jung, T. W. Schneider, C. B. Montgomery, T. L. Custer, A. E. Schaffner, Q. Y. Liu, Y. X. Li, J. L. Barker, and J. J. Hickman, "Developmental neurobiology implications from fabrication and analysis of hippocampal neuronal networks on patterned silane- modified surfaces," *Journal of the American Chemical Society,* vol. 120, pp. 12169-12177, 1998.

[38] P. Tengvall, I. Lundstrom, and B. Liedberg, "Protein adsorption studies on model organic surfaces: an ellipsometric and infrared spectroscopic approach," *Biomaterials,* vol. 19, p. 407, 1998.

[39] V. A. Liu, W. E. Jastromb, and S. N. Bhatia, "Engineering protein and cell adhesivity using PEO-terminated triblock polymers," *Journal of Biomedical Materials Research,* vol. 60, pp. 126-134, 2002.

[40] D. J. Vanderah, G. Valincius, and C. W. Meuse, "Self-assembled monolayers of methyl 1-thiahexa(ethylene oxide) for the inhibition of protein adsorption," *Langmuir,* vol. 18, pp. 4674-4680, 2002.

[41] S. K. Bhatia, J. L. Teixeira, M. Anderson, L. C. Shriver-Lake, J. M. Calvert, J. H. Georger, J. J. Hickman, C. S. Dulcey, P. E. Schoen, and F. S. Ligler, "Fabrication of surfaces resistant to protein adsorption and application to two-dimensional protein patterning," *Anal Biochem,* vol. 208, pp. 197-205., 1993.

[42] D. A. Puleo and A. Nanci, "Understanding and controlling the bone-implant interface," *Biomaterials,* vol. 20, pp. 2311-2321, 1999.
[43] M. H. Schoenfisch, M. Ovadia, and J. E. Pemberton, "Covalent surface chemical modification of electrodes for cardiac pacing applications," *Journal of Biomedical Materials Research,* vol. 51, pp. 209-215, 2000.
[44] S. Tosatti, R. Michel, M. Textor, and N. D. Spencer, "Self-assembled monolayers of dodecyl and hydroxy-dodecyl phosphates on both smooth and rough titanium and titanium oxide surfaces," *Langmuir,* vol. 18, pp. 3537-3548, 2002.
[45] G. B. Fields, "Induction of protein-like molecular architecture by self- assembly processes," *Bioorganic & Medicinal Chemistry,* vol. 7, pp. 75-81, 1999.
[46] G. B. Fields, J. L. Lauer, Y. Dori, P. Forns, Y. C. Yu, and M. Tirrell, "Proteinlike molecular architecture: Biomaterial applications for inducing cellular receptor binding and signal transduction," *Biopolymers,* vol. 47, pp. 143-151, 1998.
[47] P. Molnar, W. S. Wang, A. Natarajan, J. W. Rumsey, and J. J. Hickman, "Photolithographic patterning of C2C12 myotubes using vitronectin as growth substrate in serum-free medium," *Biotechnology Progress,* vol. 23, pp. 265-268, Jan-Feb 2007.
[48] M. Mrksich and G. M. Whitesides, "Using self-assembled monolayers to understand the interactions of man-made surfaces with proteins and cells," *Annual Review of Biophysics and Biomolecular Structure,* vol. 25, pp. 55-78, 1996.
[49] C. R. Jenney and J. M. Anderson, "Adsorbed serum proteins responsible for surface dependent human macrophage behavior," *Journal Of Biomedical Materials Research,* vol. 49, pp. 435-447, Mar 15 1999.
[50] N. Faucheux, R. Schweiss, K. Lutzow, C. Werner, and T. Groth, "Self-assembled monolayers with different terminating groups as model substrates for cell adhesion studies," *Biomaterials,* vol. 25, pp. 2721-2730, Jun 2004.
[51] L. Y. Li, S. F. Chen, J. Zheng, B. D. Ratner, and S. Y. Jiang, "Protein adsorption on oligo(ethylene glycol)-terminated alkanethiolate self-assembled monolayers: The molecular basis for nonfouling behavior," *Journal of Physical Chemistry B,* vol. 109, pp. 2934-2941, Feb 2005.
[52] I. C. Goncalves, M. C. L. Martinsa, M. A. Barbosa, and B. D. Ratner, "Protein adsorption on 18-alkyl chains immobilized on hydroxyl-terminated self-assembled monolayers," *Biomaterials,* vol. 26, p. 3891, 2005.
[53] Y. Ikada, "Surface Modification of Polymers for Medical Applications," *Biomaterials,* vol. 15, pp. 725-736, 1994.
[54] B. D. Ratner, "Surface Modification of Polymers - Chemical, Biological and Surface Analytical Challenges," *Biosensors & Bioelectronics,* vol. 10, pp. 797-804, 1995.
[55] B. Ge and F. Lisdat, "Superoxide sensor based on cytochrome c immobilized on mixed-thiol SAM with a new calibration method," *Analytica Chimica Acta,* vol. 454, pp. 53-64, Mar 2002.
[56] M. Das, C. A. Gregory, P. Molnar, L. M. Riedel, K. Wilson, and J. J. Hickman, "A defined system to allow skeletal muscle differentiation and subsequent integration with silicon microstructures," *Biomaterials,* vol. 27, pp. 4374-4380, Aug 2006.
[57] I. Harary and B. Farley, "In vitro studies on single beating rat heart cells," *Experimental Cell Research,* vol. 29, pp. 451-465, 1963.

# CHAPTER 3: PATTERNED CARDIOMMYOCYTES ON MICROELECTRODE ARRAYS: TOWARDS THE DEVELOPMENT OF A FUNCTIONAL, HIGH INFORMATION CONTENT DRUG SCREENING PLATFORM

## Introduction

The development of a high-throughput, high-information content device to study and understand cardiac electrophysiology is important in the field of cardiac physiology, tissue engineering and drug research. More than 850,000 people are hospitalized for arrhythmias each year and ventricular fibrillation (VF) is a leading cause of cardiac death [1]. Despite the intensive research in this area, the mechanism of VF is still poorly understood [2]. Past studies have indicated that VF is caused and sustained by circulating unstable wavelets originating from a sequence of wave break and re-entry [3]. Recent studies have also introduced the motor rotor hypothesis that explains VF by the presence of an excitation source that is unable to maintain a uniform conduction through the myocardium [2]. Other reasons include impairment due to local conduction blocks and slow conduction [4] caused by tissue heterogeneities [5] that stabilize re-entry. However, no clear theory has emerged as the primary cause for VF and arrhythmia.

Arrhythmia is a known side effect of commercial drugs. One of the mechanisms by which drugs could cause a potentially fatal form of ventricular tachy arrhythmia, called Torsades de pointes (Tdp), is through the prolongation of the QT interval (ECG analogue of the ventricular action potential). It has been reported that approximately 2-3% of all prescribed drugs can cause long QT syndrome [6, 7]. A broad range of cardiovascular drugs and antibiotics also have the

potential risk of causing drug induced Tdp [8,9]. At the same time, prolongation of the QT interval does not necessarily lead to Tdp; lengthening of the QT interval could even be antiarrhythmogenic, as it is considered a mechanism of action of the class III anti-arrhythmics [10,11]. Thus, a relatively high-throughput method to identify cardiac side effects and differentiate between arrhythmic and anti-arrhythmic effects at an early stage of drug development would have a significant impact.

Gap junctions play an important role in the propagation of excitation in cardiac tissue. Changes in gap junction function affect major cardiac parameters, such as conduction velocity (CV). It has been observed in several cardiovascular diseases that the expression of connexins, protein molecules that form gap junction channels, is decreased or their distribution is changed, leading to a malfunction in gap junction coupling [12] Understanding the pharmacological modulation of cardiac gap junction channels would further aid the drug development enterprise.

Introduction of a relatively high-throughput, functional, high information content *in vitro* method for cardiac side effect testing, which has high predictive value, would have a significant impact on drug development as it would reduce cost, time and the number of drugs failing in clinical trials [13]. *In vitro* testing would also reduce the need for animal testing and could be used to study drug effects with a functional assay, but at a cellular level. Other *in vitro* methods, such as whole heart experiments (Langendorff heart model) or the Purkinje fiber preparation are difficult and time consuming [13]. Traditional methods used to study QT interval prolongation at the cellular level include patch-clamp experiments. However, these experiments are time consuming, require a skilled operator and cannot be used to study cell to cell communication, cell coupling, action potential propagation or parameters such as CV and re-entry. Moreover,

evidence suggests that prolongation of QT intervals is not the best predictor of Torsades de pointes. The measurement of the length, or the variability in the length, of the refractory period after a cardiac action potential may have more relevance for predicting arrhythmic behavior [10].

Cardiac myocytes cultured on microelectrode arrays (MEAs) have several benefits compared to either traditional patch clamp electrophysiology or isolated organ methods. The use of MEA's in the investigation of cardiac side effects would provide information in a relatively high-throughput and low cost manner compared to standard patch-clamp electrophysiology. However, at this time, it is still a low information content method compared to standard methods and this has prevented its use in a wider number of applications. Cardiac myocytes on MEAs have been used in a limited number of studies to investigate the effect of toxins, such as pesticides [14] and cardioactive drugs [15] on cardiac field potentials. A commercial system has also been introduced to measure QT intervals in a relatively high-throughput fashion [16], but has seem limited application. However, cardiac myocytes can now be maintained over longer periods of time [17] thus chronic experiments such as monitoring network remodeling for disease models is now feasible. In addition, serum-free formulation for cardiac culture has also been developed [18].

This combination of factors suggests that the opportunity exists to develop the next level of sophistication for this technique. Investigating a ***patterned*** cardiac myocyte layer that is aligned with the electrodes of a MEA could solve several problems associated with the random spread of excitation in a cardiac monolayer, which makes evaluation of the obtained data, such as conduction velocity, difficult. It would also enable the development of specific open-loop or closed-loop stimulation protocols to measure critical parameters, such as the length of the

refractory period after the action potential. It could also be used to create a high-throughput, low-cost functional reentry model.

Several different methods have been developed for cell patterning. One category of this technique is based on direct placement of cells or extracellular matrix molecules on desired locations and includes patterning through microfluidic channels [19-21], microcontact printing [22] and inkjet printing [23]. Other methods utilize photolithography following surface modification using self-assembled monolayers (SAMs) [24-26]. The benefit of these methods is the compatibility of the technique with cheap automated silicon manufacturing steps and the ability of the cells to self-assemble after random plating.

SAMs are one molecule thick monolayers attached to a surface composed of organic molecules, which have been extensively used for surface patterning [24, 27]. Surface modification with SAMs is also compatible with advanced photolithography methods [25, 28]. Studies have also shown that cells survive on these surfaces for extended periods of time [29], do not migrate off the patterned areas [29] and exhibit the typical morphology and physiology of the specific cell type [18, 31, 32].

The goal of this study was the development of patterned, neonatal rat, cardiomyocyte cultures on microelectrode arrays in a serum-free medium for the study of cardiac physiology and pharmacology utilizing a high-throughput technique, but with high information content. An adsorbed fibronectin foreground was used because it supported cardiac myocyte attachment and growth and a 2-[Methoxy(Polyethyleneoxy)Propyl]TrimethoxySilane (SiPEG) self-assembled monolayer was used as the cell repellent background because of its excellent protein adsorption resistant properties [33]. The measurement of conduction velocity with the patterned cardiac

myocyte monolayers was demonstrated and illustrated the feasibility to apply different stimulation protocols to the MEA/cardiac system. The action of 1-heptanol and Sparfloxacin on the cardiac patterns was also assessed. This method could easily be adapted for use with cardiac myocytes derived from human stem cells to eliminate interspecies differences in drug side effect screening and become an alternative to the existing more complex, expensive and time consuming methods.

## Materials and Methods

### *Surface modifications of microelectrode arrays with PEG silanes*

MEA's containing 60 titanium nitride, 10 μm diameter electrodes (Multichannel Systems, Germany) were cleaned before use by soaking the arrays in a detergent solution for 2 hours followed by sonication for 10 minutes. The arrays were then oxygen plasma cleaned for 20 minutes. Surface modification was completed by incubation of the MEAs in a 3 mM PEG silane, 2-[Methoxypoly (ethyleneoxy)propyl]trimethoxysilane ($M_W$ = 460-590, Gelest), solution in toluene (with 0.35 ml of concentrated HCL) for 45 minutes at room temperature. The arrays were then rinsed once in toluene, twice in ethanol, twice in water and sonicated in water for 2 minutes to remove the non-covalently linked material [30]. The arrays were air dried with nitrogen and stored in a dessicator overnight.

### *Laser Ablation and patterning of the microelectrode arrays*

The microelectrode arrays were patterned using a deep UV (193 nm) excimer laser (Lambda Physik) at a pulse power of 230 mW and a frequency of 10 Hz for 45 seconds through

a quartz photomask (Bandwidth foundry, Eveleigh, Australia). The arrays were sterilized using 100% ethanol and then incubated with 5 μg/ml of fibronectin in a Phosphate buffered solution (Invitrogen) for 20 minutes. The solution was removed and the surface was first rinsed with PBS, followed by the plating medium, and then dried before the cells were plated.

### *Contact angle measurements*

The water contact angle was measured with a Ramé-hart goniometer (Ramé-hart Inc.). The contact angle of a static sessile drop (5 μl) of water was measured three times and then averaged.

### *X-Ray photoelectron spectroscopy*

The XPS characterization of the plasma cleaned, PEG-silane and fibronectin derivitized MEA surfaces was performed with a Thermo ESCALAB 220i-XL X-Ray photoelectron spectrometer equipped with an aluminum anode and a quartz monochromator. The surface charge compensation was achieved using a low-energy electron flood gun and, when it was necessary, by masking the samples with Al foil (a small area was left un-covered for analysis). Survey scans were recorded in order to determine the relevant elements (pass energy of 50 eV, step size = 1 eV). High resolution spectra were recorded for the Si 2p, C 1s, N 1s, and O 1s peaks (pass energy of 20 eV, step size = 0.1 eV).

The spectrometer was calibrated against the reference binding energies of clean Cu, Ag and Au samples. In addition, the calibration of the binding energy (BE) scale was made by

setting the C 1s BE in a hydrocarbon environment at 285 eV. Peak deconvolution was performed with Avantage version 3.25 software, provided by Thermo Electron Corporation.

### *Neonatal rat cardiomyocyte culture*

The neonatal rat, cardiomyocyte culture was prepared using the cardiac isolation kit from Worthington [31]. All animal work was approved by the UCF IACUC and followed NIH guidelines. Briefly, two day-old rat pups were euthanized in a precharged $CO_2$ chamber. Hearts were dissected and minced in ice cold Hanks balanced salt solution (HBSS). Cardiac myocytes were dissociated by incubation of the hearts in trypsin (100 µg/ml of HBSS) for 16 hours at 2-8°C. The hearts in the trypsin solution were briefly warmed with a trypsin inhibiter before adding collegenase (300 units/ml, L-15 medium) for 45 minutes in a water bath at 37°C followed by mechanical trituration. The cell solution was filtered to remove any remaining tissue and centrifuged at 50g for 5 minutes at 22°C. The cells were resuspended in high glucose Dulbecco's modified eagle medium (DMEM, Gibco/Invitrogen) supplemented with 10% Fetal Bovine Serum (Gibco/Invitrogen) and 1% penicillin streptomycin (Gibco/Invitrogen), preplated in Petri dishes and incubated at 37°C and 5% $CO_2$ for 45 minutes. This was necessary to eliminate the fibroblasts. The supernatant from the Petri dishes was centrifuged at 50g for 5 min at 22°C. The cells were then resuspended in the plating medium. The serum-free plating medium consisted of: 100 ml Ultraculture medium (Bio Whittaker Cambrex) supplemented with 10 ml B27, 1 ml L-glutamine (Gibco/Invitrogen), 1 ml Penicillin Streptomycin , 0.375 g dextrose (Fisher Scientific) in 800 µl water, 1 ml non-essential amino acids and 1 ml of Hepes buffer (Gibco/Invitrogen) [32]. Additional growth factors were also added to improve cell survival in the serum-free

conditions. They included 0.1 μg/ml of L-thyroxine, 10 ng/ml of Epidermal growth factor (Sigma-aldrich) and 0.5 μg/ml of Hydrocortisone (BD biosciences). Cells were plated at a density of 1000 cells/$mm^2$ on the microelectrode arrays. The medium was changed 24 hours after plating. Subsequent changing of the medium was performed every third day.

### *Multielectrode extracellular recordings*

The cardiac myocytes were cultured on patterned metal microelectrode arrays (Planar 10 μm electrodes, 200 μm separations, Multichannelsystems). A 60 channel amplifier (MEA1040, Multichannelsystems) was used to record electrical activity from the spontaneously beating cardiac cells. The same electrodes were also used for stimulation using a stimulus generator (STG 1002, Multichannel systems). The cells were stimulated utilizing 500 mV, 1 ms wide bipolar pulses at 2 Hz. The recording medium was the same as the plating medium with the pH adjusted to 7.3 using HEPES buffer. After a 30 minute incubation period, action potentials were detected and recorded using built in functions of the Multichannel System software. For drug experiments, 50 μM 1-Heptanol (Gibco/Invitrogen) was added to the bathing medium and recordings were performed before and 15 minutes after drug administration with additional recordings done at 15 minute intervals. For Sparfloxacin (Sigma-aldrich), 2 μM of the drug was added to the recording medium and recordings were taken in 15 minute intervals before and after drug administration. The data was further analyzed using software written using Matlab and Clampfit (Axon instruments).

# Results

## *Surface modification of the microelectrode arrays:*

Our laboratory routinely uses self-assembled monolayers to modify and pattern glass coverslips for cell culture applications [17, 18, 25, 37-39]. However, patterning cardiac myocytes on multielectrode arrays presented a challenge for three primary reasons. 1) The complex composition of the MEA surface made the verification of the surface modification step difficult, 2) MEAs are expensive, thus methods needed to be developed that enabled them to be cleaned and refunctionalized for repeated use and 3) patterned cardiac myocytes do not grow optimally on the standard trimethoxysilylpropyldiethylenetriamine (DETA) surfaces [17] nor on clean glass. Thus, a cell resistant background surface was needed which was also resistant to protein adsorption as this would allow fibronectin incubation on the foreground and prevent it's adherence to the background, enabling cardiac myocyte attachment. Thus, poly(ethylene glycol) (PEG) was chosen for the background because of its excellent protein adsorption resistance. X-ray Photoelectron Spectroscopy (XPS) was used to test the results of the surface modifications and throughout the entire study for quality assurance purposes.

*PEG-silane modified MEAs*: Figure 3-1 indicates a survey scan (Fig 1A) for oxygen plasma-cleaned MEA showing distinct peaks for Si 2p (103.3 eV), Si 2s (153.6 eV), N 1s (397.4 eV), and O 1s (533 eV). This elemental composition is primarily due to silicon nitride, the material used to insulate the MEA leads. The very small C 1s peak is due to interstitial carbon, most possibly from air, that could not be completely eliminated. A survey scan of a PEG modified

MEA (Fig 1B) indicates almost the same elemental composition, but with two major differences. On the PEG modified MEA the C 1s peak is much larger, indicating the incorporation of PEG on the MEA surface. Moreover, in the high resolution XPS scans (Fig 3-1A(a) and 1B inserts) it is clearly visible that on the clean MEA surface the small C 1s signal consists of a single peak, centered at about 285 eV, which is characteristic for C-C bonds, whereas the large (note the Y axis scale on each insert) C 1s signal on the PEG-modified MEA consists of 2 peaks, one centered at 285 eV (C-C peak) and the other one is shifted approximately +1.5 eV from the first peak and is characteristic of the C-O bond in PEG. This finding is in agreement with the literature [33, 34] and is indicative of the incorporation of PEG on the surface.

*Contact angle measurements of the PEG-silane*: The Contact angle measurements had an average of 38 ± 1º as expected for complete PEG coverage [33, 34] (Contact angle for clean glass is < 5 degrees and MEAs is 22 ± 3°).

*Fibronectin (FN) adsorption on the MEAs*: As in the case of the unpatterned PEG-modified MEA's, the absorption of FN on an ablated MEA surface was observed in the survey spectrum as the appearance of a large and complex C 1s signal, which was not present on the survey scan of an unmodified MEA surface (Fig 3-1A). Figures 1C and D shows a comparison of the C 1s high resolution spectra before fibronectin (C) and after fibronectin adsorption (D). The high intensity C 1s signal seen in Fig 1D was deconvoluted into three peaks centered at 285 eV (C-C), 286.4 (C-N and C-O) and 288.4 (N-C=O and O-C=O) eV, in agreement with published data[42,43]. The ratio of $C_{286.4eV}/C_{288.4eV}$ was found to be approximately 1.18 (theoretical 1.2). Fibronectin adsorption on an ablated MEA was also indicated by the appearance of an additional N 1s peak in the spectra of the MEAs after fibronectin adsorption.

The high resolution N 1s spectrum of a clean MEA (Fig 3-1E) indicates only one N 1s peak centered at 397.4 eV, and is due to the insulating material (silicon nitride) [44]. The high resolution N 1s spectrum of FN adsorbed on a an ablated MEA (Fig 1F) clearly indicates a second N 1s peak centered at 400.3 eV, characteristic for nitrogen from amine and/or amide groups [43] From the above data it could be concluded that fibronectin was adsorbed on the MEA surface in the laser ablation areas.

XPS analysis of an unpatterned PEG control coverslip incubated in fibronectin showed no fibronectin adsorption on the PEG background. XPS measurement indicates that ablation of a PEG monolayer by the laser exposure used in the patterning step was complete (data not shown). Survey scans for the MEA surface after PEG treatment followed by laser ablation indicated a carbon peak similar to a clean MEA (as on Fig 3-1A inserts (a) clean MEA and (b) after ablation). Oxygen plasma cleaning of the MEA experiments was performed both before and after surface modification. Utilizing this procedure the MEAs could be reused and refunctionalized at least 6 – 10 times without any observable degradation of the quality of the electrophysiological recordings.

### *Cultured neonatal rat cardiomyocytes on patterned surfaces in serum-free medium:*

The growth and activity of neonatal rat cardiomyocytes on the patterned MEAs was assessed for over 2 weeks. The cells attached to the fibronectin, but not to the PEG background and showed clearly delineated regions (Figure 3-2A). This allowed the beating cells to grow exclusively over specific electrodes. The cells formed monolayers by day 2 and spontaneous contraction and beating activity began on day 4 and was consistent throughout the pattern. Cell

survival and activity improved markedly with the addition of L-thyroxine, epidermal growth factor and hydrocortisone to the culture medium indicated in the Methods. In a previous publication cells were shown to maintain spontaneous beating actively for up to 2 months in vitro [17].

### *Extracellular recordings from patterned cardiomyocytes on the MEAs:*

The electrical activity of the spontaneously contracting cells patterned on the microelectrodes was extracellularly recorded using the MEA system. Cardiac myocytes formed a morphologically homogenous, integrated network of cells that communicated through gap junctions and displayed normal tissue electrophysiology. The recorded field potential (FP) signals correlated with the contraction cycle.

In random cultures the direction and speed of the propagation of excitation (action potentials) has been shown previously to depend on a number of variables, including intercellular resistance across the gap junctions and the depolarizing sodium current [45-47] [35-37]. For extracellular MEA recordings, previous research had indicated that the excitation wave could be followed through the monolayer as the increasing delay in field potential peak times and could be used to determine the pathway of the excitation as it moved away from the initiation site [48]. However, a direct determination of the conduction velocity has been difficult in unpatterned monolayers, even though the timing of field potential generation could be estimated. With ***patterning*** of the cells on the electrode array, the exact path along which a spontaneous excitation wave traveled could be determined and then calculated distances used for velocity determination. Moreover, because of the pre-determined pathway there would be no need to image the propagation of the wave, just the measurement of the start and end times of the waves

on the patterns as recorded by the microelectrodes in the array. Thus, in later high-throughput applications significantly fewer electrodes will be possible for these measurements. Figure 3-3 shows a typical recording and the direction of propagation was determined as shown in Figure 3-3A. Figure 3-3B indicates the delay between field potentials at different electrodes on the pattern, which enabled the determination of the initiating signal. The signal propagation was also visualized using an Imaging software routine written in Matlab 6.5 [49]. The program converted recordings from the electrodes into a video showing the field potential movement across an 8 x 8 grid. This program also indicated the origin of the signal, aiding in the calculation of the conduction velocity. Using the recording shown in the supplementary data (30 ms delay, 0.54 mm distance) the conduction velocity was calculated to be 0.217 m/s for **spontaneous** firing of the patterned cardiomyocytes. The average conduction velocity over eight different MEAs was 0.192 ± 0.012 m/s. Previous research has shown that *in vitro* conduction velocities ranged from 0.12 m/s [38] to 0.242 m/s [51]. In a computer simulation of action potential propagation in cardiac fibers in realistic conditions (taking into account extracellular solutions and spaces) the conduction velocity was 0.504 m/s [52]. In the human heart the action potential generated by the Sino-atrial node spread through the atria at a conduction velocity of 0.5 m/sec [53].

The conduction velocity of the signal on patterned cardiac monoloyers was also measured after **stimulation**. In these experiments, the cardiac pattern was stimulated at electrode 51 and the evoked response was recorded at electrode 72 across a distance of 0.77 mm (Figure 3-4A, B). The conduction velocity utilizing a field stimulation of 500 mV, 1 ms at 2 Hz was calculated as 0.315 ± 0.013 m/s (n = 8). Previous research has indicated that rapid electrical stimulation in cultured, neonatal rat cardiomyocytes had an effect on the expression of Connexin 43 leading to

changes in conduction properties [39], including an increase in conduction velocity. The result from this study indicates that rapid electrical stimulation at 2 Hz caused an increase in the conduction velocity as well as a more reproducible value compared to the non-stimulated or spontaneous case. These results indicate that an accurate estimation of conduction velocity and propagation paths can be determined utilizing stimulation in addition to spontaneous signals. The measurement of conduction velocities also helped in the understanding of the electrophysiological properties of the cultured, neonatal rat cardiac model. The stimulated conduction velocities were also closer to the modeled values as well as those generated by the SA node in the heart in vivo.

### *Electrical stimulation optimization experiments*

The stimulation protocol was optimized by determining a minimal threshold which reliably generated contraction from the cells. The cardiomyocytes were stimulated with 2 Hz, 500 mV, 1 ms wide bidirectional pulses at different electrodes. As seen in Figures 3-4 A and B, the time-delay between the stimulation artifact and the FP at the different electrodes is in good correlation with the distance between the stimulation and recording electrodes. The excitation wave spread evenly on branched patterns as evidenced by the zero time difference at the end of the branches.

As shown in Figure 3-5, paired pulse stimulation protocols could also be used with the defined cardiac patterns. By varying the time-delay between stimulations the absolute/relative refractory period after action potential generation could be mapped. If the stimulation delay between the two electrodes was too short, the second stimulus failed to evoke a second propagating action potential. This experiment enables new possibilities to study phenomena

difficult to measure in random (not constrained) monolayers, such as re-entry, refractory periods after action potentials and arrhythmia.

## *Pharmacology and toxin studies*

One of the most important applications of this system could be measurements to determine the effect of drugs, their side effects, and toxins on cardiac system function. Two pharmacological agents, 1-Heptanol and Sparfloxacin, were tested to demonstrate the usability of this system for pharmacological and toxicology studies. Patterned spontaneously beating cardiomyocytes were exposed to 50 μM 1-Heptanol in the recording medium and the field potentials were recorded at 15 minute intervals. A control recording was taken before the toxin application. As shown in Figure 3-5, 1-Heptanol had a marked effect on the propagation of the excitation wave; it significantly increased the delay of the FP between the two recording electrodes. The conduction velocity was calculated to be 0.006 ± 0.004, a significant decrease from 0.192 ± 0.012 m/s, the value measured before treatment. The increase in the time delay indicates a block and uncoupling of the gap junctions and this result clearly shows that the effect of a gap junction blocker can be analyzed using this system.

*Effect of Sparfloxacin: Sparfloxacin* is a fluoroquinone antibiotic and HERG channel antagonist that is known to cause QT prolongation, Tdp and ventricular fibrillation [40, 41]. Application of 2 μM of Sparfloxacin to the recording medium caused a significant change in the spontaneous beating frequency within 25 minutes, with an increased FP length, non-synchronous contractions similar to fibrillation and burst-like beating activity as shown in Figure 3-65B. The

beating frequency changed from a stable value of 0.6 Hz-1 Hz to intra-bursts with a higher frequency range of 1 Hz -1.2 Hz. The loss of synchrony between the two electrodes measured also indicated a propagation block in the monolayer.

## Discussion

### *Surface modification, photolithographic patterning and patterned cardiac myocyte cultures on micro-electrode arrays*

In this study, it was shown that the surface of commercial multielectrode arrays could be functionalized with SiPEG self-assembled monolayers. The PEG layer could be ablated and subsequently patterned using standard photolithographical techniques and that incubation of the patterns with 5 μg/ml fibronectin for 20 minutes did not affect the cell resistive properties of PEG, but significantly improved the attachment of cardiac cells to the glass surface. Surface analysis of the MEAs after modification indicated that both PEG-Silane modification and fibronectin adsorption on the ablated areas of the MEA surface was successful. The patterned commercial electrodes were re-usable 6-10 times without an observable decline in the quality of electrophysiological recordings after each cleaning. Rat neonatal, cardiac myocytes demonstrated normal physiology and formed beating monolayers on the areas designated by the patterns.

Manipulating cells, determining their attachment, growth and differentiation in cultures has become more important in applications such as tissue engineering, toxin detection, drug screening and robotics. Unfortunately, there is no generally applicable method to pattern all cell types. The method developed here using a protein adsorption resistant background, SiPEG,

followed by protein adsorption (fibronectin) to the ablated area is a relatively simple, fast and cheap solution for this problem and could be generalized for 'difficult to pattern' cells.

### *Electrophysiology, toxin and drug effects*

The patterned cells formed a confluent interconnected network of spontaneously contracting cells communicating via gap junctions. The activity of the cells could be measured using the embedded microelectrode array. The extracellular electrodes allowed not only recording, but also stimulation of the patterned cardiac myocyte monolayers. For the measurement of conduction velocity three different methods were used: 1) traditional video-monitoring of the excitation wave in the monolayer, 2) measurement of the speed of the spontaneous excitation waves on the patterns via the microelectrode array and 3) measurement of the propagation of stimulation-evoked extracellular field potential. All of these methods produced consistent results which were in reasonable agreement with published *in vivo* data. Conduction velocity increased with rapid electrical stimulation indicating that changes in cell physiology can be studied using this method. Patterning of the monolayers made conduction velocity measurements simpler, faster and more reliable. In future commercial applications this may be a more cost effective and higher throughput technique for screening fcardiac side effects for drug candidates. It would also drastically reduce the number of required electrodes.

We have also demonstrated that alternating stimulation at different electrodes on the patterns could be used to measure the refractory period after action potentials, an important parameter for determining potentially fatal pharmacological side effects. This technique could also be a valuable tool for the study of cardiac defects, such as reentrant arrhythmia. Further

development of this technology, especially for use with human cells, could significantly affect pharmaceutical drug development enabling additional paramaters for measurements in cardiac side effect screening.

Two pharmacological agents, 1-Heptanol and Sparfloxacin, were used to demonstrate the effectiveness of this method for drug screening. Both of these compounds are known to have cardiac side effects. 1-Heptanol is a gap junction blocker, whereas Sparfloxacin is an antibiotic that was taken off the market due to cardiac side effects. Our results were in agreement with the literature as 1-Heptanol drastically decreased the conduction velocity in the cardiac myocyte monolayers without completely blocking the conduction, whereas Sparfloxacin caused fibrillations which initiated a complete conduction block. These results indicated that specific drug actions can be studied using this system. 1-Heptanol affected the conduction velocity properties, while maintaining the synchronicity of the beating cells. The addition of Sparfloxacin to the cells caused a loss in rhythmicity resulting in a burst-like activity similar to fibrillations that are shown to have occurred in animal and human trials for the drug. These promising initial results support the need for further development of this system as a high-throughput, high-information content functional drug screening platform.

## Conclusion

A simple and reliable method for patterning cardiac myocytes on multielectrode arrays was developed. This method is compatible with standard silicon manufacturing steps. Patterning of the cardiac myocytes increased the information content of the traditional multielectrode array recordings by enabling measurement of conduction velocity in a fast and simple approach.

Moreover, using these stimulation protocols, the measurement of the refractory period after the action potentials became possible. Measurement of the effect of drugs, with known cardiac effects, was in agreement with the literature. Further development of this method could result in cheaper, faster, pharmaceutical side-effect screening with higher predictive value.

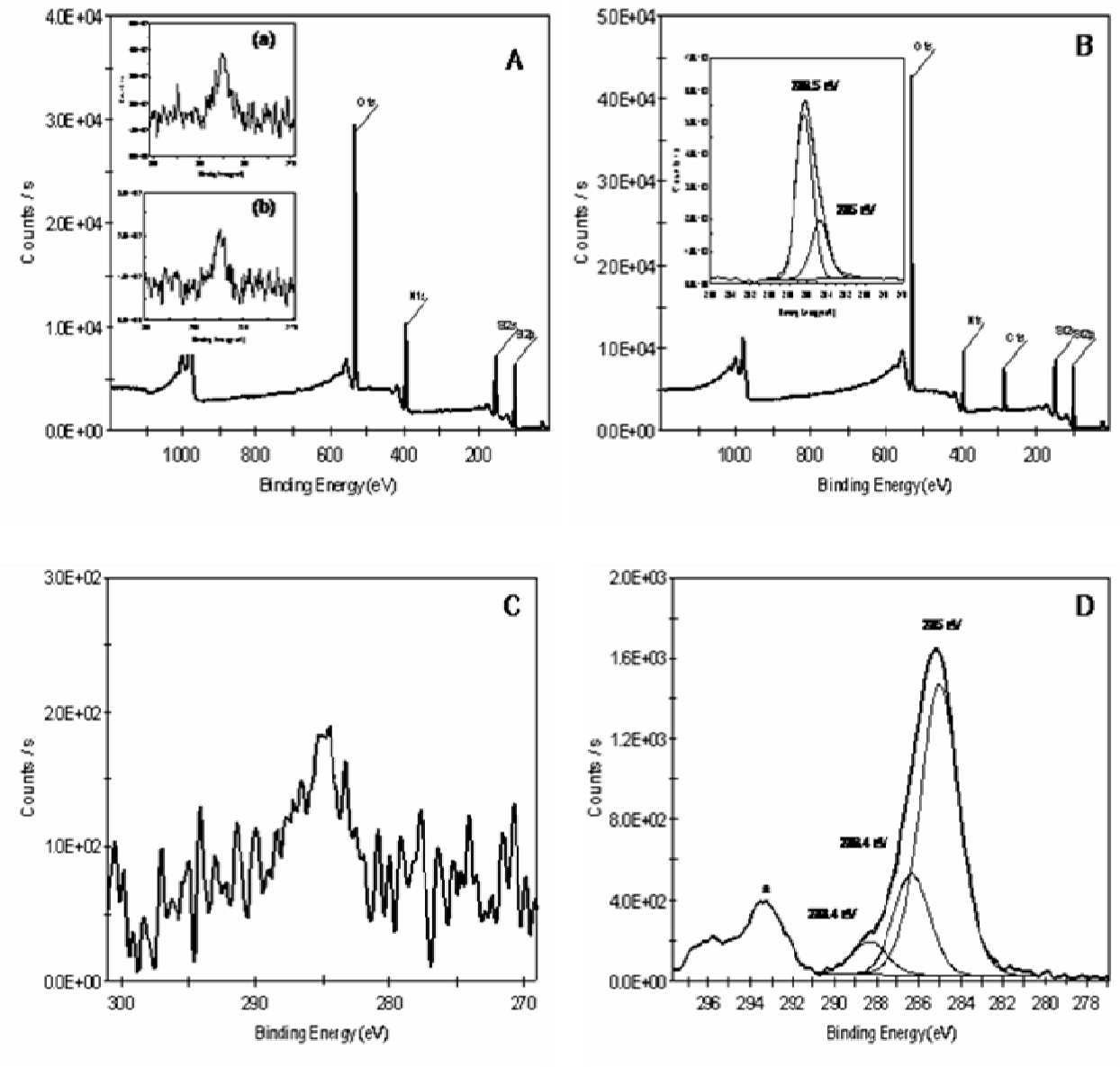


**Figure 3-1: XPS analysis**

**A: Typical XPS survey spectra of oxygen plasma-cleaned MEA; Insert: C 1s high resolution spectrum of (a) clean MEA and (b) after PEG ablation. B: XPS survey spectra of a PEG modified MEA; Insert: High resolution C1s spectrum of PEG modified MEA. C: High resolution C 1s spectra of a clean MEA. D: High resolution C1s of Fibronectin adsorbed on a laser ablated PEG modified MEA (*: K 2p peak due to PBS, solvent for Fibronectin).**

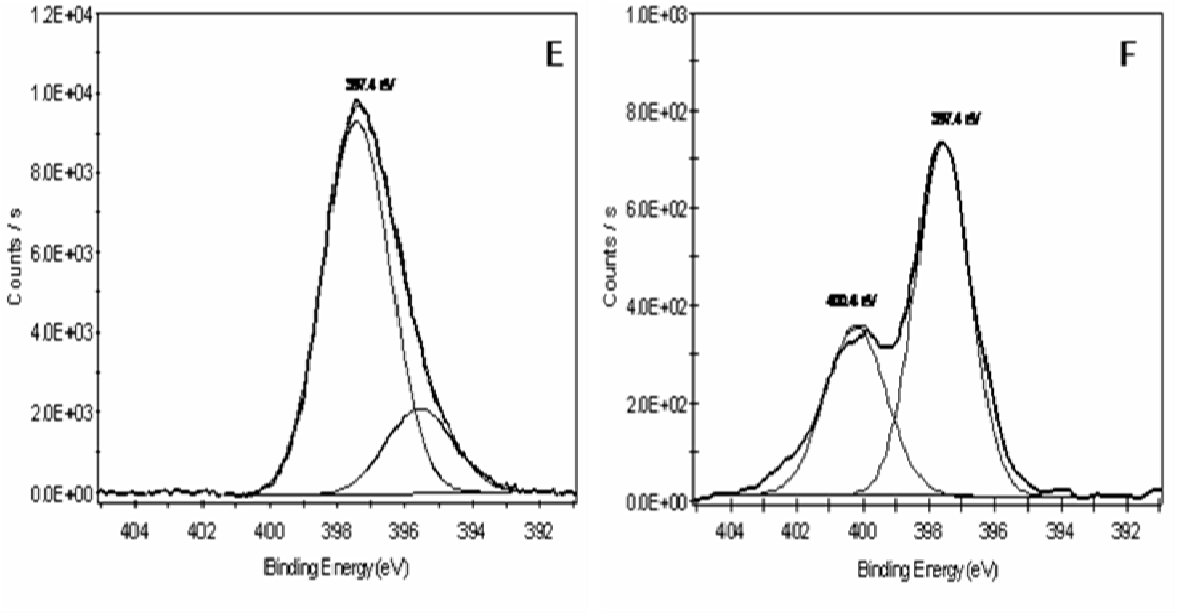


**Figure 3-1: XPS analysis**

**E: High resolution N 1s spectra of a clean MEA. F: High resolution N 1s spectra of Fibronectin adsorbed on a laser ablated PEG region on an MEA.**

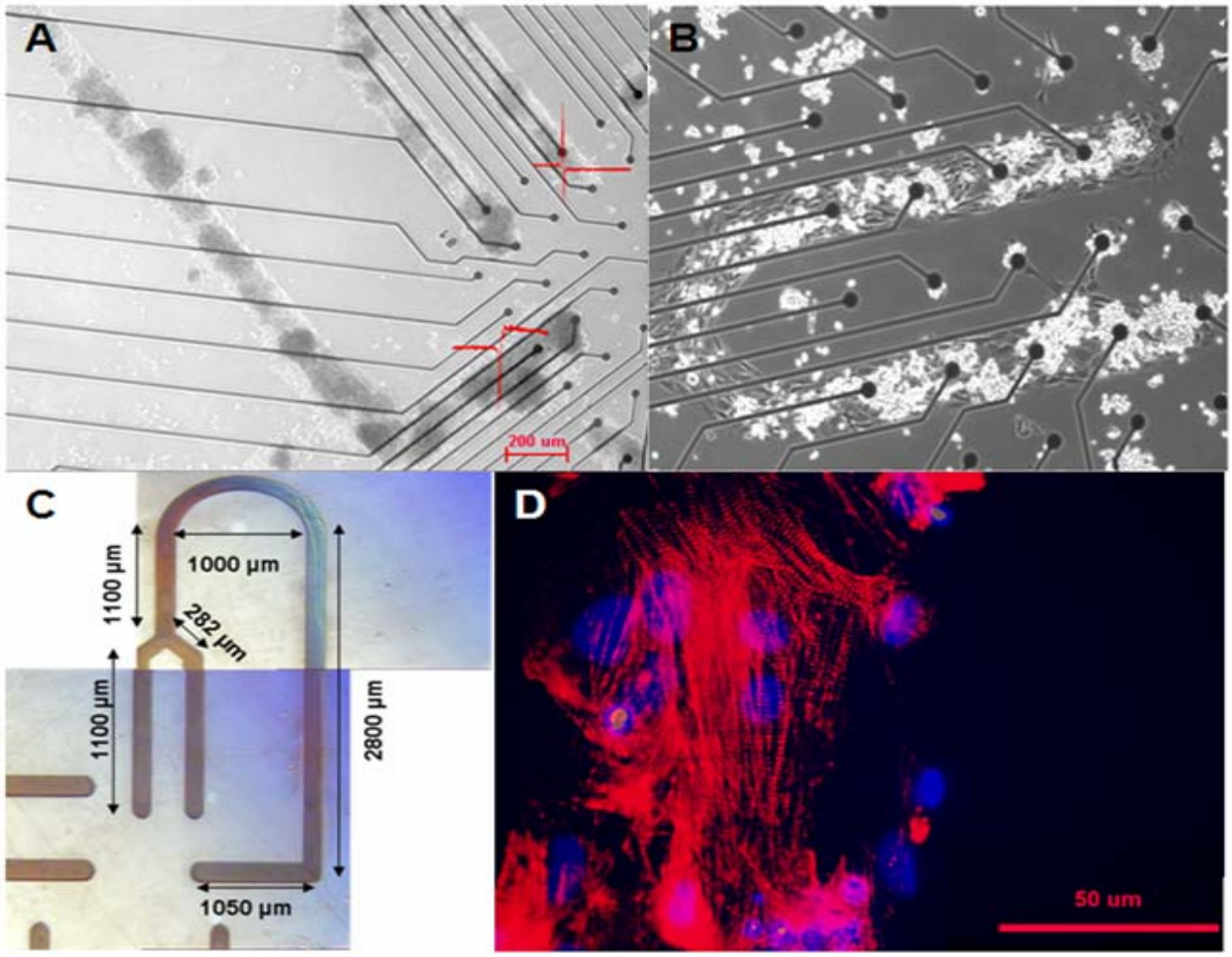


**Figure 3-2: Patterned neonatal cardiomyocytes**

**Patterned neonatal cardiomyocytes A, B: Phase contrast pictures on day 12. A: Field potentials measured at individual electrodes are marked in red. Electrode distance: 200 µm, C: Pattern design and dimensions. D: Immunostaining with Rhodamine phalloidin for F-actin indicating cardiac myofibrils (note the visible striations). Nuclei are stained with DAPI (blue).**

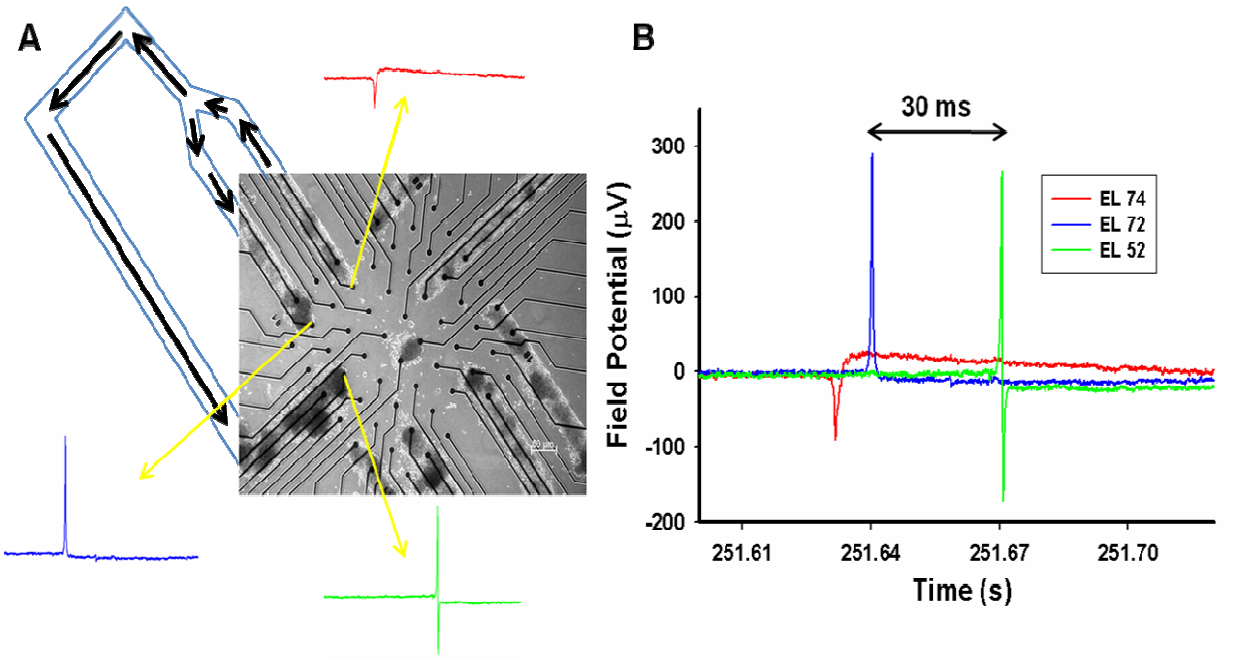


**Figure 3-3: Action potential conduction in patterned cardiac myocyte monolayers.**

**A: phase contrast picture of cardiac myocyte patterns on the top of the substrate embedded electrodes (electrode distance is 200 μm) with a sketch of the conduction pathway on the completed pattern and with the recorded extracellular signals on the given electrodes. B: Overlay of the recorded traces showing the temporal relationship of the signals. Spontaneous AP was generated in the cardiac myocyte monolayer in the right fork of the pattern, close to electrode 74. AP spread through the pattern reaching electrode 74 first, electrode 72 second and with a much longer delay (according to the longer path) electrode 52 last. Conduction velocity was determined based on the time delay in the signal between electrode 74 and 52 and the known pattern geometry. The calculated conduction velocity in this experiment was 0.192 ± 0.012 m/sec.**

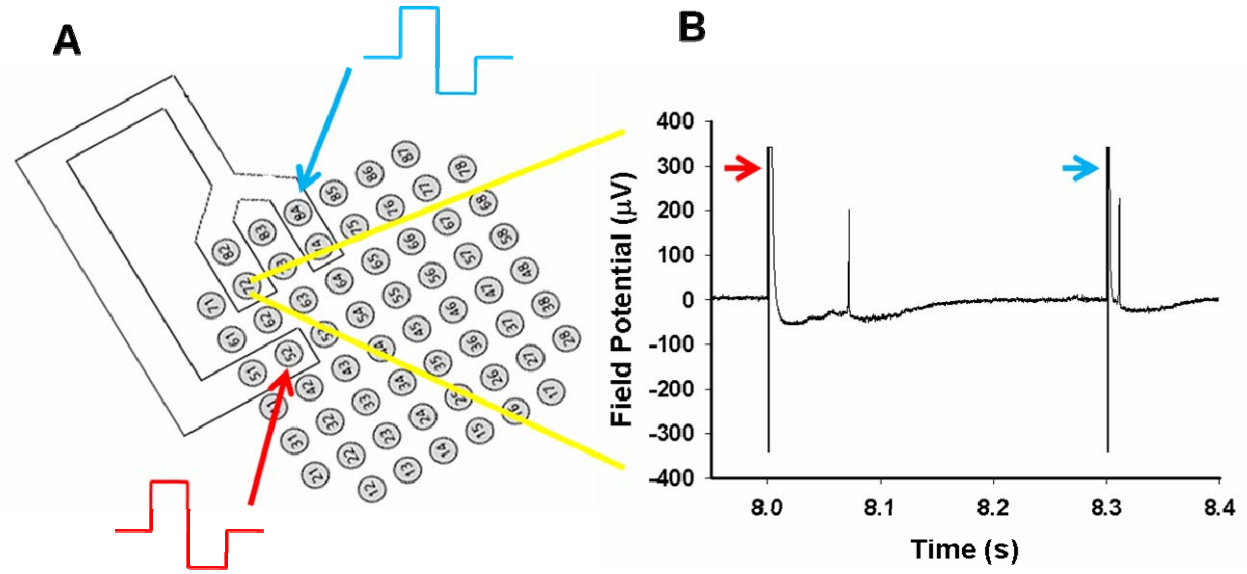


**Figure 3-4: Measurement of conduction velocity in patterned cardiac myocyte monolayers with electrical stimulation.**

**A: Electrodes 52 and 84 were stimulated alternatively with a time delay of 300 ms and the response was recorded at electrodes 72. B: E72 exhibited both long and short time delays in FP generation based on the distance the AP had to travel from the stimulation site.**

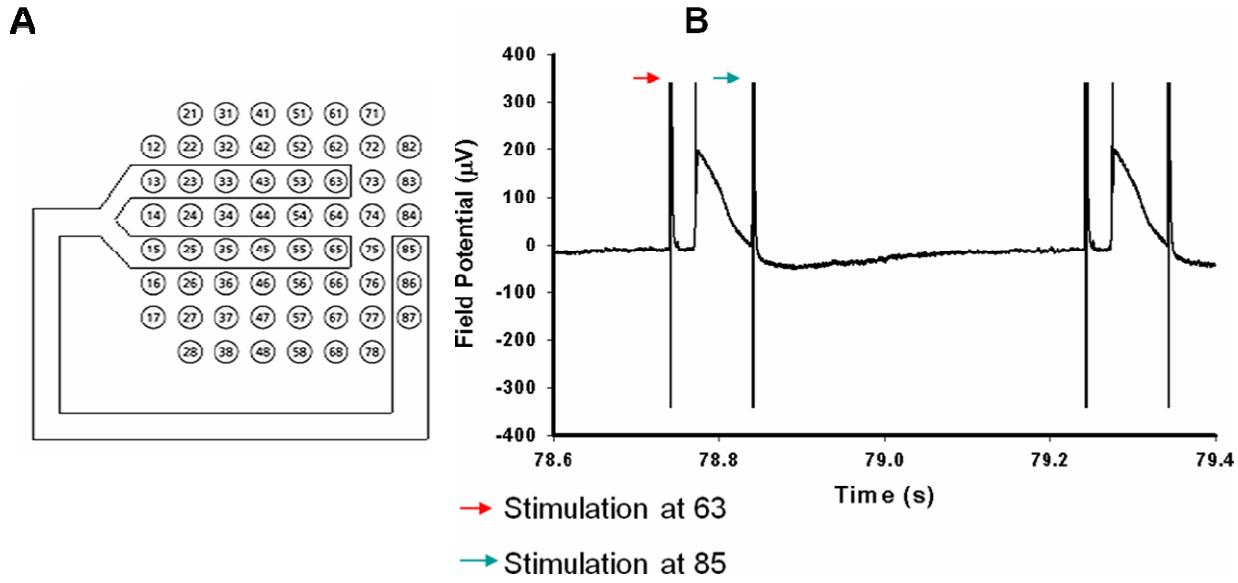


**Figure 3-5: Measurement of refractory period after cardiac action potential.**

**Electrodes 63 and 85 (see pattern geometries on the left) were stimulated alternatively according to the following protocol: E63, 100 ms delay, E85, 400 ms delay, E63 again. Right panel shows recording at electrode 87. Stimulating E85 100 ms after the stimulation of E63 failed to evoke an AP because this delay was too short, cells were stimulated in their refractory period. By chance, cell electrode coupling on electrode E85 was especially strong in this experiment, thus the extracellular recording approximately replicated the shape of the intracellular action potential illustrating the relationship of the action potential and the stimulation.When the stimulation delay between E63 and E85 was 250 ms, both stimulations evoked an action potential at electrode 87.**

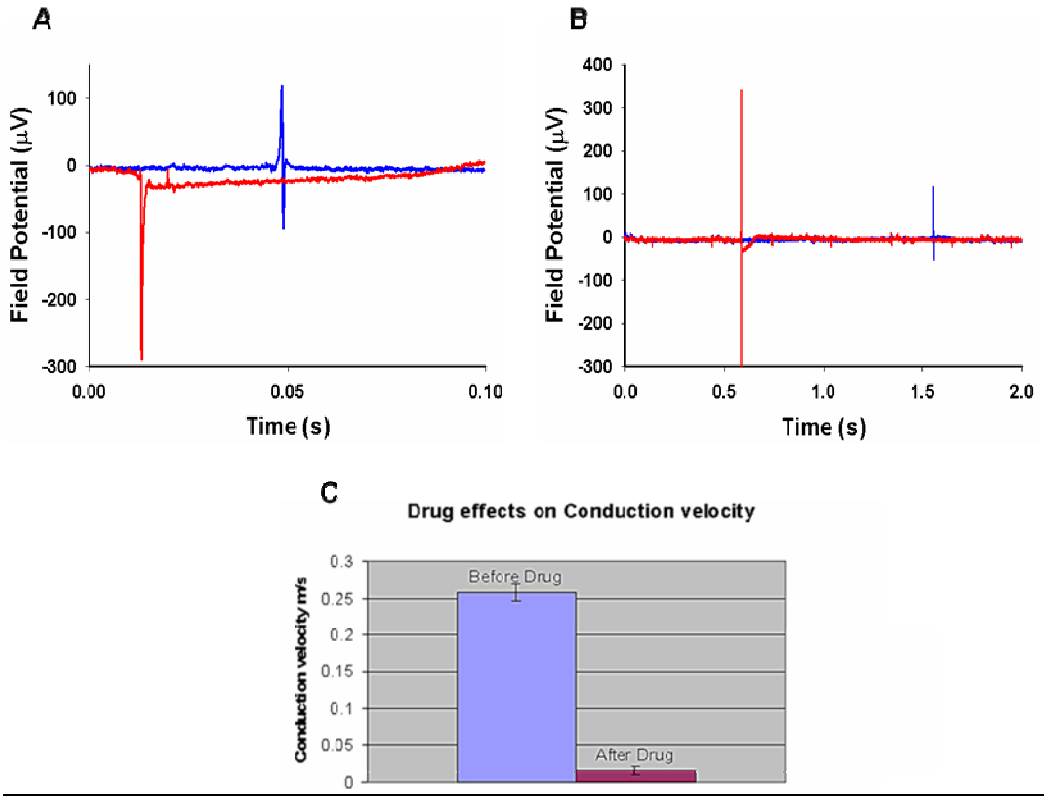


**Figure 3-6: Effect of the gap junction blocker 1-Heptanol.**

**A: Propagation of excitation between the two end points in the pattern (Electrodes 84 and 52) before addition of the drug. The conduction velocity (CV) was measured to be 0.217 m/sec B: Propagation of excitation after the drug. The CV was calculated as 0.006 m/sec C: Drug effect on CV measured over 5 MEAs.**

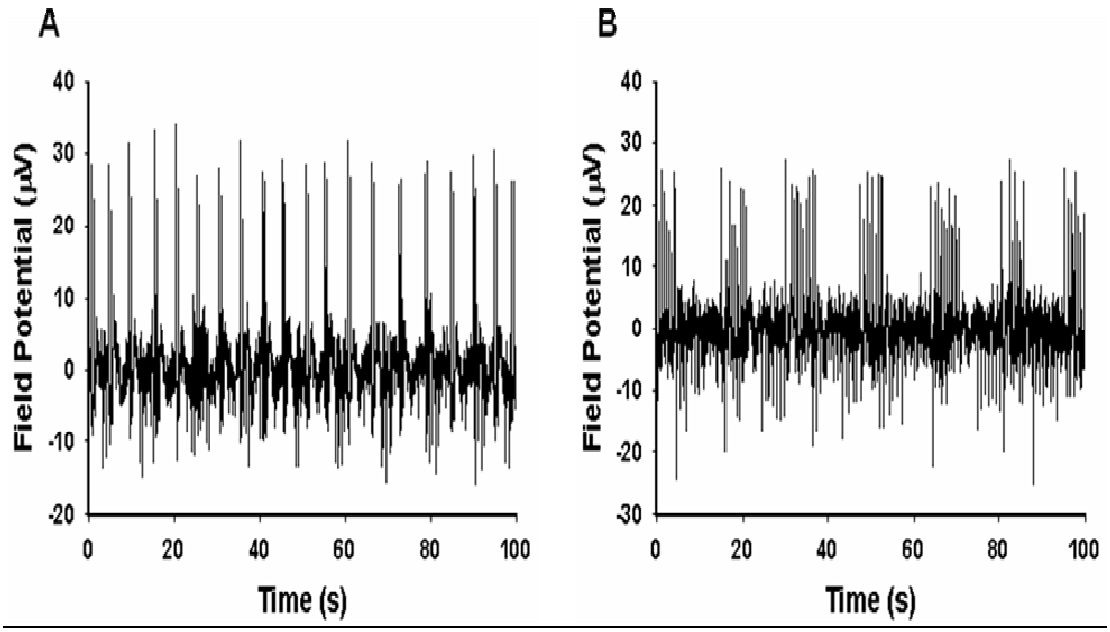


**Figure 3-7: Effect of the HERG channel antagonist Sparfloxacin.**

**A: Field potential recordings before addition of Sparfloxacin indicated stable beating frequencies and synchronous activity B: Field potential recording after the addition of 2 μM Sparfloxacin showed burst like activity with higher intra-burst frequencies and no synchrony between electrodes.**

# References


[1] J. H. t. Jackson, F. Frech, R. Ronen, L. Mullany, B. Lennert, and V. Jhaveri, "Assessment of drug therapy management and the prevalence of heart failure in a managed care population with hypertension," *J Manag Care Pharm,* vol. 10, pp. 513-20, Nov-Dec 2004.

[2] M. P. Nash, A. Mourad, R. H. Clayton, P. M. Sutton, C. P. Bradley, M. Hayward, D. J. Paterson, and P. Taggart, "Evidence for multiple mechanisms in human ventricular fibrillation," *Circulation,* vol. 114, pp. 536-42, Aug 8 2006.

[3] M. GK, "On the multiple wavelet hypothesis of atrial fibrillation," *Arch Int Pharmacodyn Ther,* pp. 183–188, 1962.

[4] D. A. Pijnappels, J. van Tuyn, A. A. de Vries, R. W. Grauss, A. van der Laarse, D. L. Ypey, D. E. Atsma, and M. J. Schalij, "Resynchronization of separated rat cardiomyocyte fields with genetically modified human ventricular scar fibroblasts," *Circulation,* vol. 116, pp. 2018-28, Oct 30 2007.

[5] J. W. Lin, L. Garber, Y. R. Qi, M. G. Chang, J. Cysyk, and L. Tung, "Region [corrected] of slowed conduction acts as core for spiral wave reentry in cardiac cell monolayers," *Am J Physiol Heart Circ Physiol,* vol. 294, pp. H58-65, Jan 2008.

[6] M. Recanatini, E. Poluzzi, M. Masetti, A. Cavalli, and F. De Ponti, "QT prolongation through hERG K(+) channel blockade: current knowledge and strategies for the early prediction during drug development," *Med Res Rev,* vol. 25, pp. 133-66, Mar 2005.

[7] M. Sala, M. Lazzaretti, G. De Vidovich, E. Caverzasi, F. Barale, G. d'Allio, and P. Brambilla, "Electrophysiological changes of cardiac function during antidepressant treatment," *Ther Adv Cardiovasc Dis,* vol. 3, pp. 29-43, Feb 2009.

[8] H. R. Lu, E. Vlaminckx, A. Van de Water, J. Rohrbacher, A. Hermans, and D. J. Gallacher, "In-vitro experimental models for the risk assessment of antibiotic-induced QT prolongation," *Eur J Pharmacol,* vol. 553, pp. 229-39, Dec 28 2006.

[9] R. R. Shah, "Pharmacogenetic aspects of drug-induced torsade de pointes: potential tool for improving clinical drug development and prescribing," *Drug Saf,* vol. 27, pp. 145-72, 2004.

[10] L. M. Hondeghem, "Relative contributions of TRIaD and QT to proarrhythmia," *J Cardiovasc Electrophysiol,* vol. 18, pp. 655-7, Jun 2007.

[11] T. J. Campbell and K. M. Williams, "Therapeutic drug monitoring: antiarrhythmic drugs," *Br J Clin Pharmacol,* vol. 52 Suppl 1, pp. 21S-34S, 2001.

[12] H. V. van Rijen, T. A. van Veen, D. Gros, R. Wilders, and J. M. de Bakker, "Connexins and cardiac arrhythmias," *Adv Cardiol,* vol. 42, pp. 150-60, 2006.

[13] W. Suter, "Predictive value of in vitro safety studies," *Curr Opin Chem Biol,* vol. 10, pp. 362-6, Aug 2006.

[14] A. Natarajan, P. Molnar, K. Sieverdes, A. Jamshidi, and J. J. Hickman, "Microelectrode array recordings of cardiac action potentials as a high throughput method to evaluate pesticide toxicity," *Toxicol In Vitro,* vol. 20, pp. 375-81, Apr 2006.

[15] M. Reppel, P. Igelmund, U. Egert, F. Juchelka, J. Hescheler, and I. Drobinskaya, "Effect of cardioactive drugs on action potential generation and propagation in embryonic stem cell-derived cardiomyocytes," *Cell Physiol Biochem,* vol. 19, pp. 213-24, 2007.
[16] T. Meyer, K. H. Boven, E. Gunther, and M. Fejtl, "Micro-electrode arrays in cardiac safety pharmacology: a novel tool to study QT interval prolongation," *Drug Saf,* vol. 27, pp. 763-72, 2004.
[17] V. Dhir, A. Natarajan, M. Stancescu, A. Chunder, N. Bhargava, M. Das, L. Zhai, and P. Molnar, "Patterning of diverse mammalian cell types in serum free medium with photoablation," *Biotechnol Prog,* vol. 25, pp. 594-603, Mar-Apr 2009.
[18] M. Das, P. Molnar, C. Gregory, L. Riedel, and J. J. Hickman, "Long-term Culture Of Embyonic Rat Cardiomyocytes on an Organosilane Surface in a Serum Free Medium," *Biomaterials,* vol. 25, pp. 5643-5647, 2004.
[19] F. Morin, N. Nishimura, L. Griscom, B. Lepioufle, H. Fujita, Y. Takamura, and E. Tamiya, "Constraining the connectivity of neuronal networks cultured on microelectrode arrays with microfluidic techniques: a step towards neuron-based functional chips," *Biosens Bioelectron,* vol. 21, pp. 1093-100, Jan 15 2006.
[20] A. Khademhosseini, C. Bettinger, J. M. Karp, J. Yeh, Y. Ling, J. Borenstein, J. Fukuda, and R. Langer, "Interplay of biomaterials and micro-scale technologies for advancing biomedical applications," *J Biomater Sci Polym Ed,* vol. 17, pp. 1221-40, 2006.
[21] H. Andersson and A. van den Berg, "Microfabrication and microfluidics for tissue engineering: state of the art and future opportunities," *Lab Chip,* vol. 4, pp. 98-103, Apr 2004.
[22] R. S. Kane, S. Takayama, E. Ostuni, D. E. Ingber, and G. M. Whitesides, "Patterning proteins and cells using soft lithography," *Biomaterials,* vol. 20, pp. 2363-76, Dec 1999.
[23] T. Xu, C. A. Gregory, P. Molnar, X. Cui, S. Jalota, S. B. Bhaduri, and T. Boland, "Viability and electrophysiology of neural cell structures generated by the inkjet printing method," *Biomaterials,* vol. 27, pp. 3580-8, Jul 2006.
[24] J. J. Hickman, Bhatia, S.K., Quong, J.N., Shoen, P., Stenger, D.A., Pike, C.J. and Cotman, C.W, "Rational pattern design for in vitro cellular networks using surface photochemistry," *J. Vac. Sci. Technol. A,* vol. 12, pp. 607–616, 1994.
[25] M. S. Ravenscroft, K. E. Bateman, K. M. Shaffer, H. M. Schessler, D. R. Jung, T. W. Schneider, C. B. Montgomery, T. L. Custer, A. E. Schaffner, Q. Y. Liu, Y. X. Li, J. L. Barker, and J. J. Hickman, "Developmental neurobiology implications from fabrication and analysis of hippocampal neuronal networks on patterned silane- modified surfaces," *Journal of the American Chemical Society,* vol. 120, pp. 12169-12177, 1998.
[26] D. A. Stenger, C. J. Pike, J. J. Hickman, and C. W. Cotman, "Surface determinants of neuronal survival and growth on self-assembled monolayers in culture," *Brain Res,* vol. 630, pp. 136-47, Dec 10 1993.
[27] D. A. Stenger, J. H. Georger, C. S. Dulcey, J. J. Hickman, A. S. Rudolph, T. B. Nielsen, S. M. McCort, and J. M. Calvert, "Coplanar Molecular Assemblies of Aminoalkylsilane and Perfluorinated Alkylsilane - Characterization and Geometric Definition of Mammalian-Cell Adhesion and Growth," *Journal of the American Chemical Society,* vol. 114, pp. 8435-8442, 1992.

[28] J. M. Corey, B. C. Wheeler, and G. J. Brewer, "Compliance of hippocampal neurons to patterned substrate networks," *J Neurosci Res,* vol. 30, pp. 300-7, Oct 1991.
[29] M. Das, N. Bhargava, A. Bhalkikar, J.-F. Kang, and J. J. Hickman, "Temporal neurotransmitter conditioning restores the functional activity of adult spinal cord neurons in long-term culture," *Experimental Neurology,* vol. 209, pp. 171-180 2008.
[30] M. Das, C. A. Gregory, P. Molnar, L. M. Riedel, and J. J. Hickman, "A defined system to allow skeletal muscle differentiation and subsequent integration with silicon microstructures.," *Biomaterials,* vol. 27, pp. 4374-4380 2006.
[31] M. Das, P. Molnar, H. Devaraj, M. Poeta, and J. J. Hickman, "Electrophysiological and morphological characterization of rat embryonic motoneurons in a defined system," *Biotechnol Prog,* vol. 19, pp. 1756-61, Nov-Dec 2003.
[32] A. Lochter, J. Taylor, K. H. Braunewell, J. Holm, and M. Schachner, "Control of neuronal morphology in vitro: interplay between adhesive substrate forces and molecular instruction," *J Neurosci Res,* vol. 42, pp. 145-58, Oct 1 1995.
[33] K. C. Popat, S. Sharma, and T. A. Desai, "Quantitative XPS Analysis of PEG-Modified Silicon Surfaces," *The Journal of Physical Chemistry B,* vol. 108, pp. 5185-5188, 2004.
[34] K. C. Popat, G. Mor, C. A. Grimes, and T. A. Desai, "Surface modification of nanoporous alumina surfaces with poly(ethylene glycol)," *Langmuir,* vol. 20, pp. 8035-41, Sep 14 2004.
[35] A. R. Natarajan, Q. Rong, A. N. Katchman, and S. N. Ebert, "Intrinsic cardiac catecholamines help maintain beating activity in neonatal rat cardiomyocyte cultures," *Pediatr Res,* vol. 56, pp. 411-7, Sep 2004.
[36] A. Sathaye, N. Bursac, S. Sheehy, and L. Tung, "Electrical pacing counteracts intrinsic shortening of action potential duration of neonatal rat ventricular cells in culture," *J Mol Cell Cardiol,* vol. 41, pp. 633-41, Oct 2006.
[37] P. Molnar, J. F. Kang, N. Bhargava, M. Das, and J. J. Hickman, "Synaptic connectivity in engineered neuronal networks," *Methods Mol Biol,* vol. 403, pp. 165-73, 2007.
[38] P. Molnar, W. Wang, A. Natarajan, J. W. Rumsey, and J. J. Hickman, "Photolithographic patterning of C2C12 myotubes using vitronectin as growth substrate in serum-free medium," *Biotechnol Prog,* vol. 23, pp. 265-8, Jan-Feb 2007.
[39] A. E. Schaffner, J. L. Barker, D. A. Stenger, and J. J. Hickman, "Investigation of the factors necessary for growth of hippocampal neurons in a defined system," *J Neurosci Methods,* vol. 62, pp. 111-9., 1995.
[40] A. Papra, N. Gadegaard, and N. B. Larsen, "Characterization of Ultrathin Poly(ethylene glycol) Monolayers on Silicon Substrates," *Langmuir,* vol. 17, pp. 1457-1460, 2001.
[41] K. L. Prime and G. M. Whitesides, "Adsorption of proteins onto surfaces containing end-attached oligo(ethylene oxide): a model system using self-assembled monolayers," *Journal of the American Chemical Society,* vol. 115, pp. 10714-10721, 1993.
[42] R. W.-C. M. D. N. P. M. A. Galtayries, "Fibronectin adsorption on Fe-Cr alloy studied by XPS," *Surface and Interface Analysis,* vol. 38, pp. 186-190, 2006.
[43] D. G. C. S. L. G. B. D. R. K. M. B. H. A. B. Caren D. Tidwell, "Static time-of-flight secondary ion mass spectrometry and x-ray photoelectron spectroscopy characterization of adsorbed albumin and fibronectin films," *Surface and Interface Analysis,* vol. 31, pp. 724-733, 2001.

[44] M. C. Poon, C. W. Kok, H. Wong, and P. J. Chan, "Bonding structures of silicon oxynitride prepared by oxidation of Si-rich silicon nitride," *Thin Solid Films,* vol. 462-463, pp. 42-45, 2004.
[45] M. S. Spach, "The role of cell-to-cell coupling in cardiac conduction disturbances," *Adv Exp Med Biol,* vol. 161, pp. 61-77, 1983.
[46] M. S. Spach and J. F. Heidlage, "The stochastic nature of cardiac propagation at a microscopic level. Electrical description of myocardial architecture and its application to conduction," *Circ Res,* vol. 76, pp. 366-80, Mar 1995.
[47] B. K. Egert U, Meyer T, "Analysis of cardiac myocyte activity dynamics with microelectrode arrays," in *Advances in network electrophysiology using multi electrode arrays*, B. M. Taketani M, Ed.: Springer, 2006, pp. 274-290.
[48] M. Halbach, U. Egert, J. Hescheler, and K. Banach, "Estimation of action potential changes from field potential recordings in multicellular mouse cardiac myocyte cultures," *Cell Physiol Biochem,* vol. 13, pp. 271-84, 2003.
[49] C. K. Yeung, F. Sommerhage, G. Wrobel, A. Offenhausser, M. Chan, and S. Ingebrandt, "Drug profiling using planar microelectrode arrays," *Anal Bioanal Chem,* vol. 387, pp. 2673-80, Apr 2007.
[50] S. Iravanian, Y. Nabutovsky, C. R. Kong, S. Saha, N. Bursac, and L. Tung, "Functional reentry in cultured monolayers of neonatal rat cardiac cells," *Am J Physiol Heart Circ Physiol,* vol. 285, pp. H449-56, Jul 2003.
[51] E. K. Entcheva, Y. Tchernev, E. Tung, L., "Fluorescence imaging of electrical activity in cardiac cells using an all-solid-state system" *IEEE Transactions on Biomedical Engineering*, vol. 51, pp. 331-341, 2004.
[52] J. Stinstra, S. Roberts, J. Pormann, R. Macleod, and C. Henriquez, "A Model of 3D Propagation in Discrete Cardiac Tissue," *Comput Cardiol,* vol. 33, pp. 41-44, 2006.
[53] R. E. Klabunde, *Cardiovascular physiology concepts*, illustrated ed.: Lippincott Williams & Wilkins, 2004.
[54] N. Inoue, T. Ohkusa, T. Nao, J. K. Lee, T. Matsumoto, Y. Hisamatsu, T. Satoh, M. Yano, K. Yasui, I. Kodama, and M. Matsuzaki, "Rapid electrical stimulation of contraction modulates gap junction protein in neonatal rat cultured cardiomyocytes: involvement of mitogen-activated protein kinases and effects of angiotensin II-receptor antagonist," *J Am Coll Cardiol,* vol. 44, pp. 914-22, Aug 18 2004.

# CHAPTER 4: CREATING FUNCTIONAL NEURONAL NETWORKS ON MICROELECTRODE ARRAYS TO STUDY SYNAPTIC

## Introduction

Studying the electrophysiology of electrically active cells has long been a basis for understanding neuronal cell function and various disease pathologies. In the vertebrate brain plasticity, specifically long term potentiation (LTP) and long term depression (LTD), have been widely studied as a cellular model for learning [1]. LTP is defined as a significant strengthening or enhancement in signal transmission between two synchronously stimulated neurons that is long lasting or persistent and is thought to be the synaptic basis underlying learning and memory. Although LTP was discovered in 1966 in the rabbit hippocampus the precise molecular mechanism involved in the enhancement or depression of synaptic transmission between two neurons is not clearly understood in part due to variation in species and brain region [2]. A clearer definition of LTP would also help in better understanding the pathology of diseases like Alzheimer's and brain injuries.

Hippocampal slices are currently the most widely used preparations and models for studying synaptic plasticity and LTP. LTP has been demonstrated in slice preparations in each major subsector of the rodent hippocampus [3, 4]. Experiments in the last decade have shown that LTP in CA3 neurons innervated by the Mossy Fiber pathway follows the Hebbian learning rule [5-7]. LTP at this synapse is defined by 'an increase in amplitude and maximal initial slope of the extracellular field potential and a decrease in the threshold and latency of action potentials elicited by the stimulation of the potentiated projection' [4, 8, 9].

In order to better understand LTP, it is essential to characterize the cellular and molecular changes that underlie enhancement of synaptic transmission. Disassociated hippocampal neuronal cultures not only allows us to control and define cell environment, cell connections and synapses but also makes it possible to closely monitor and study two-way communications between single cells.

The traditional methods of functional electrophysiological studies involve extracellular field potential recordings and intracellular patch clamp techniques [10-12]. But patch clamp electrophysiology does not allow for long term continuous monitoring of changes associated with injury or chemical effects over several days. The last three decades has therefore seen an increase in research using silicon-based microelectrode arrays (MEA) and field effect transistors (FET). MEAs are being increasingly used not only as a high-throughput biosensor devices [13] to study drug and toxin effects but also to examine the major physiological properties of electrical active cells such as neurons and cardiomyocytes [14, 15]. These silicon-cell hybrids allow for multi-site recordings from different parts of tissue slices or from many interconnected neuronal cells at the same time. They give both temporal and spatial information and because they are non-invasive, facilitate long term experiments. More importantly for the study of LTP, the simultaneous stimulation, recording and monitoring at different sites of the tissue or functional neuronal network provides more information about the plasticity of synaptic transmission.

In this study it was shown that engineering a directed functional neuronal network on MEAs allows for the study of synaptic plasticity and can be further extended to examine two cells and individual cell physiology during LTP and LTD. For these experiments surface

patterning was used and serum-free medium to both guide cells and create an ideal system for cell growth and differentiation and provide a defined environment. Surface patterning techniques have been used over the last two decades to try to create a functional neuronal network. The techniques have varied over the years [16-20] as researchers established simpler and more efficient means to create patterned cells that have longer survival rates and better cell firing activity, with the goal of using them for high throughput pharmacological and toxicology research, including serving as tools to study disease models. Patterning allows the cells to grow in a more ordered way, thus mimicking the structured networks of the brain and representing a more accurate study. To this end, significant research has been done in this area, indicating that patterned neurons synapse and form electrical circuits [21, 22] with defined polarity [22] depending on the pattern. We have now designed directional patterns on MEAs that result in specific unidirectional axonal and dendritic growth.

The activity of the neuronal networks was analyzed by studying the functional connectivity between two neurons. For our study, functional connectivity is defined by the ability of communicating neurons to fire almost synchronously and can be observed by cross-correlation of the spike trains of the corresponding cells [6]. The time delays, if any, in spike activity, of concurrently firing neurons was measured and displayed using statistical tools. LTP in our system was defined as a significant and persistent change in functional connectivity that is expressed as a decrease in directional synaptic delay in the activation of a post-synaptic neuron by pre-synaptic stimulation. This could be measured using a cross-correlation diagram or as an increase in the directional granger causality as calculated from neuronal data.

## Materials and Methods

### *Surface cleaning*

Glass coverslips were cleaned using an acid wash protocol. Briefly a ceramic rack containing glass slips were soaked in a solution of 50/50 methanol (HPLC grade)/ hydrochloric acid (Reagent grade) or 15-30 min. They were then rinsed with deionised ultra filtered (DUIF) water three times and placed in a beaker containing concentrated sulfuric acid (reagent grade from fisher) for a minimum of 30 minutes. The rack of coverslips was rinsed thoroughly again and boiled in DUIF water for at least 30 minutes. The rack and slips were then rinsed in two final solutions of acetone and oven dried at 110 °C for 10-15 min or until dry. The contact angle was then confirmed to be less than 5 deg. Microelectrode arrays were plasma cleaned for 10 minutes.

### *Surface modification*

The method used for surface modification is as described [22]. Briefly, Ceramic racks with the cleaned surfaces (Glass slips and MEAs) were immersed in a 0.1% (v/v) DETA ( N-1[3-(Trimethoxysilyly)propyl] Diethylenetriamine ) in HPLC-graded Toluene solvent and heated to just below the boiling temperature for 30 minutes. It was then allowed to cool down to room temperature. HPLC-graded Toluene was then used to rinse the slips and the slips were reheated for 30 minutes as before. The surfaces are then oven dried for 2 hrs to overnight. After DETA ablation using deep UV laser (mentioned below), backfilling the ablated region was done using 0.1% tridecafluoro-1,1,2,2-tetrahydrooctyl-1-trichlorosilane (13F) in chloroform solution.

Briefly the racks with the slips were immersed in the 13f solution for 5 minutes, rinsed in chloroform and oven dried for 15 minutes.

### *Photolithographic patterning*

Patterns were made photolithographically by exposing the DETA monolayer to ArF laser irradiation through a quartz mask. The microelectrode arrays were patterned using a deep UV (193 nm) excimer laser (Lambda Physik) at a pulse power of 230 mW and a frequency of 10 Hz for 45 seconds through a quartz photomask (Bandwidth foundry, Eveleigh, Australia)

### *Surface characterization*

The XPS characterization of the MEA's as received, $O_2$ plasma cleaned MEAs, DETA-coated MEAs, laser ablated DETA and 13F-coated MEAs was done with a Thermo ESCALAB 220i-XL X-Ray photoelectron spectrometer equipped with an aluminum anode and a quartz monochromator. The surface charge compensation was achieved by using a low-energy electron flood gun and when necessary by masking the samples with Al foil (a small area was left un-covered for analysis). Survey scans were recorded in order to determine the relevant elements (pass energy of 50 eV, step size = 1 eV). High resolution spectra were recorded for Si 2p, C 1s, N 1s, and O 1s (pass energy of 20 eV, step size = 0.1 eV). The spectrometer was calibrated against the reference binding energies of clean Cu, Ag and Au samples. In addition, the calibration of the binding energy (BE) scale was made by setting the C 1s BE of carbon in a

hydrocarbon environment at 285 eV. N 1s and Si 2p peak deconvolution were performed with Avantage version 3.25 software, provided by Thermo Electron Corporation.

For surface wettability, a static drop (5 μL) of deionized water was applied to the sample surface at three different spots for three different readings and the average value was taken.

## *Cell culture*

Hippocampal neurons were obtained from day 18 old rat embryos and prepared as previously described [23]. Briefly, hippocampi were dissected from the fetuses of timed-pregnant Sprague-Dawley rats. The tissue was mechanically dissociated in a cold serum free dissection Hibernate E medium supplemented with B27 (2% v/v; Invitrogen), glutamax (1% v/v; Invitrogen) and antibiotic/antimycotic (1% v/v; Invitrogen). Prior to cell plating, patterned MEAs were sterilized with absolute ethanol and dried. Cells were plated on the MEAs at a density of approximately 75 or 200 cells/mm$^2$, depending on the pattern. The serum free culture media was neurobasal medium supplemented with B27 (2% v/v; Invitrogen), glutamax (1% v/v; Invitrogen) and antibiotic/antimycotic (1% v/v; Invitrogen).

## *Extracellular microelectrode recordings*

The Hippocampal neurons were cultured on patterned metal microelectrode arrays (planar 10 μm electrodes, separated by 200 μm, Multichannelsystems). A 60 channel amplifier (MEA1040, Multichannelsystems) was used to record electrical activity from the cells. The same electrodes were also used for stimulation using a stimulus generator (STG 1002, Multichannel systems). Stimulation experiments were done using a high frequency tetanic pulse at 100 Hz, 500

mV. The recording medium was the same as the plating medium with the pH adjusted to 7.3 using HEPES buffer. After a 30 minute incubation and stabilization period, field potentials were detected and recorded using built in functions of the multichannel software. For chemical induction of synaptic plasticity, 30 μM 1S,3R ACPD (Aminocyclopentane-1S, 3R-dicarboxylic acid) was added to the recording medium and recordings were taken every 15 minutes. Data was then analyzed using Matlab and Clampfit (Axon Instruments) and statistical significance was determined using a student's t test.

## Results

### *Surface modification and patterning of hippocampal neurons on microelectrode arrays*

Our laboratory routinely uses self-assembled monolayers to modify and pattern glass coverslips for cell culture applications [24-29]. Surface modification of MEAs for creating neuronal networks was done using two self-assembled monolayers, DETA and 13F. Since neuronal networks using these SAMs were successfully created on glass coverslips we replicated the procedure on MEAs. XPS is a surface characterization technique with a probing depth of about 10 nm. It is useful to monitor the surface modification of the top 10 nm layer of the MEA after chemical treatment. The surface modification of an MEA from the initial pristine surface to the final modified surface which contains DETA hydrophilic patterns surrounded by a 13F hydrophobic background is suggestively depicted by the set of XPS survey spectra presented in figure 4-1. The chemical composition of the top 10 nm layer of the MEA as received (Fig 1A (a)) consist of silicon (Si 2p = 102.2 eV), carbon (C 1s = 285 eV), nitrogen (N 1s = 398.2 eV),

and oxygen (O 1s = 533 eV). This chemical composition corresponds to the MEA's insulation layer (500 nm thickness) which is made out of $Si_3N_4$ (silicon nitride). The silicon nitride surface was slightly oxidized, since a significant O 1s peak is detected by XPS (Fig 4-1A (a)). The presence of C in a hydrocarbon environment (C 1s = 285 eV) is mainly due to carbon contamination most likely through the MEA's handling. By exposing the MEA to $O_2$ plasma discharge, the surface was cleaned, and only traces of carbon (C 1s) were then detectable by XPS (Fig 4-1A (b)). At the same time there was a noticeable increase of signal from oxygen. The relative O 1s intensity compared to the Si 2p intensity increased by about 60% after the $O_2$ plasma treatment.

The chemical composition of the patterned (DETA-coated) and un-patterned (13F-coated) portions of the MEA's surface are shown in the XPS survey spectra in Fig 4-1A (c) and (e), respectively. A significant C 1s peak centered at 285 eV was present in the XPS survey of the patterned portion of the MEA peak, which proves the DETA incorporation. This peak was almost completely removed in the XPS survey spectrum of the Laser ablated MEA surface, as seen in Figure 4-1A (d). For the un-patterned, 13F-coated portion of the MEA's surface, the XPS survey spectrum showed an F 1s peak at about 689 eV, a binding energy characteristic to an F-C bond. The C 1s peak was much less intense then the C 1s for DETA-coated portion of the MEA, and was split into 2 peaks. Fig 4-1 B indicates a set of high resolution C 1s spectra as described above. Clearly, there are 2 main peaks: the first centered at about 285 eV, and it is either due to adventitious C (b and d) or C in a hydrocarbon environment (c and e); the second line shifted about 6 eV to higher binding energy, and it was due to $CF_2$ groups of the 13 F (e). Fig 4-1 C shows a set of high resolution N 1s spectra for the same samples as described above. In all cases

there was a dominant peak at about 398 eV, due to the $Si_3N_4$ insulation. For the DETA-coated portion of the MEA, besides the $Si_3N_4$ dominant feature, there was a second feature much smaller and shifted towards higher binding energy. Figure D shows the high resolution N 1s spectrum of the DETA-coated portion of the MEA, with the corresponding curve fitting. The $Si_3N_4$ dominant feature is centered at 398.2 eV. The smaller feature consist of 2 lines shifted towards higher binding energy of about 2 eV and 4 eV respectively. These lines are characteristic of amine and protonated amine groups in DETA. Contact angle values were around 51 ± 3°.

Hippocampal neurons were plated at a density of 200 cells/mm$^2$ on the patterned MEAs and formed neuronal networks by day 4 as shown in figure 4-2B

### *Extracellular recordings from patterned neuronal networks*

Spontaneous electrical activity of the patterned Hippocampal neurons was extracellularly recorded by a 60 channel amplifier. Electrical activity of the patterned networks could be seen as early as day 12 and recordings were taken until 21 days in culture. Cell survival and activity on the patterned MEAs after 24 days decreased significantly. Control (unpatterned) MEAs were plated at 300 cells/mm$^2$ while patterned MEAs were plated at 200 cells/mm$^2$ to account for factors such as cell migration and a smaller cell adhesive region on patterned MEAs. Recordings were taken from both control and patterned MEAs on day 14 in 15 minute intervals. Synchronous burst activity was observed in many of the channels on control MEAs, however non-burst spiking activity was also seen as shown in figure 4-3A

As shown in figure 4-3B, the patterned networks tended to synchronously fire and had a significantly higher bursting activity, demonstrating synaptic connectivity and communication.

This could be due to better connectivity brought about by patterning as opposed to random networks as well better recording brought about by the cells being situated on top of the electrodes. To test if LTP like behavior could be chemically induced, the group I/II mGluR agonist 1S, 3R ACPD (30μM) was added to the recording medium and activity was monitored over 5 hours. ACPD significantly increased bursting activity in both patterned and random networks (n = 5). In addition there was a significant difference between electrical activity in general between the control and patterned networks (Fig 4-3C). This could indicate increased connectivity in patterned networks as well as more robust cell culture due to the presence of a more structured network. To calculate the percentage of spikes in the bursts, the number of spikes in each burst was divided by the total number of overall spikes over a 2 minute block.

*Data analysis of burst activity from neuronal networks*

The analysis of data from patterned networks is still a challenging work in progress. Certain basic programs were used to try to extract the information from the data sets. To identify firing patterns, analysis of spiking data was done using Peri-stimulus histograms (PST histogram) and Granger causality in Matlab. PST histograms allows for an analysis of the spiking order and directionality of the network resulting in the identification of a pre- and post-synaptic cell as indicated by the positive and negative correlation of the two channels

The effect of ACPD in this system was further analyzed by looking at neuronal interactions before and after drug addition using the Granger causality algorithm. Figure 4-4A shows the interaction between the different channels on the patterned MEAs before the addition of ACPD. Figure 4-4B depicts the interaction among different channels on the same patterned MEA five hours after exposure to ACPD. The different colors represent the different synaptic

strengths between communicating neurons on the electrodes. In traditional slice electrophysiology, LTP is defined by the increase in the size of the postsynaptic cells response to presynaptic stimulation following a specific stimulus pattern or chemical induction. Here it was observed that ACPD application increased neuronal connectivity and decreased interspike intervals though the directionality of the connections was not defined. A decrease in synaptic delay was observed between directionally connected channels following incubation of the patterned MEA with ACPD for after one hour.

In addition to increases in granger causality and decreases in directional synaptic delay, in some cases it was also observed that ACPD introduced a decrease in synaptic efficacy or a depression. Further probing of the literature indicated that ACPD has been shown in some cases to induce LTD at the Schaffer collateral – CA1 synapse of rodent brain slices. Indeed, selective activation of group I mGluRs results in LTD at this synapse which may account for the observed depression in some of our experiments since ACPD also actives group I mGluRs.

In addition to chemical induction of LTP in our system, LTP was induced by applying a high frequency tetanic pulse using the stimulus generator. Though the stimulation caused an immediate effect increasing the synaptic efficacy of the network the effect was not long lasting.

## Discussion

In this study we showed that creating an engineered neuronal network on microelectrode arrays helps facilitate the study of synaptic plasticity in disassociated neurons. Though recent researchers have looked towards studying LTP and LTD in cell culture systems, most of this work involves random networks rather than patterned networks [30, 31]. The vast majority of current research into LTP includes hippocampal slice electrophysiology as opposed to cell

culture models. Using patterned neuronal networks provides a structured organization of the neurons allowing for a low level mimicking of certain functions of the brain. By providing ideal geometric constraints and cell growth conditions, including a defined environment, cell growth, differentiation, migration and synaptic connectivity was controlled. The ability to induce LTP in our system will allow us to further probe the mechanisms of LTP at the cellular and molecular level. Previous research in this area has shown LTP like activity in random networks with the addition of chemicals such as Bicuculine [32], but analyzing specific synaptic interactions between cells is almost impossible in such networks. The specific geometric pattern used for our experiments allows for the analysis of interspike intervals and synaptic changes between specifically connected cells rather than in a random network. In the future this could provide more information of how LTP is involved in communication between individual cells.

Our results indicate that commercial microelectrodes can be modified with silanes. The electrode arrays can be re-used several times leading to the efficiency of the system. Cells grow and are viable for at least 3 weeks with good electrical activity on the patterns. Furthermore, an increase in synchronized activity in the patterned networks was demonstrated. This suggests that patterning reduces random cross-talk between cells and directs synaptic formation in a more constrained and organized manner. Significant increases in bursting activity with the patterned networks were also observed, a phenomenon generally seen with mature neurons in random networks. This agrees with previous work indicating that patterned networks generally tend to be more robust and electrically active than random networks [17]. In addition, our results also indicated that LTP induction in our system is more pronounced in patterned rather than random networks.

One of the major difficulties of this study was to define Synaptic plasticity and LTP induction in disassociated hippocampal cell culture models using extracellular recordings as opposed to traditional patch clamp intracellular signals. Traditional analysis of the changes in amplitude (patch clamp recordings) or slope (extracellular field recordings) of the postsynaptic potential becomes difficult in this situation. Though the study of LTP or LTD using this method allows for a simple, efficient and less time consuming protocol, the information gained is more limited. Changes in synaptic strength was measured by Granger causality, a method recently used to look at neuronal communication in the brain [33]. Granger causality is a concept based on predicting the actions of one time series based on the actions of another. We use this concept to see if one layer of neurons brings about a change in the second layer of neurons to which it is connected in a unidirectional manner or in other words to determine if there is a causal relationship between the two layers of chattering neurons. The use of neurons connected in a specific manner helps narrow down parameters and allows us to examine if there is a change in granger causality with regard to communicating cells.

Here we demonstrate that patterned neuronal networks provide a simple, efficient, high-throughput method to study synaptic plasticity at the cellular level. Currently we are working toward extending this model to a 2 cell system to narrow down LTP and LTD analysis to a single cell level. This system could find further uses in studying disease pathologies and drug effects on synaptic plasticity.

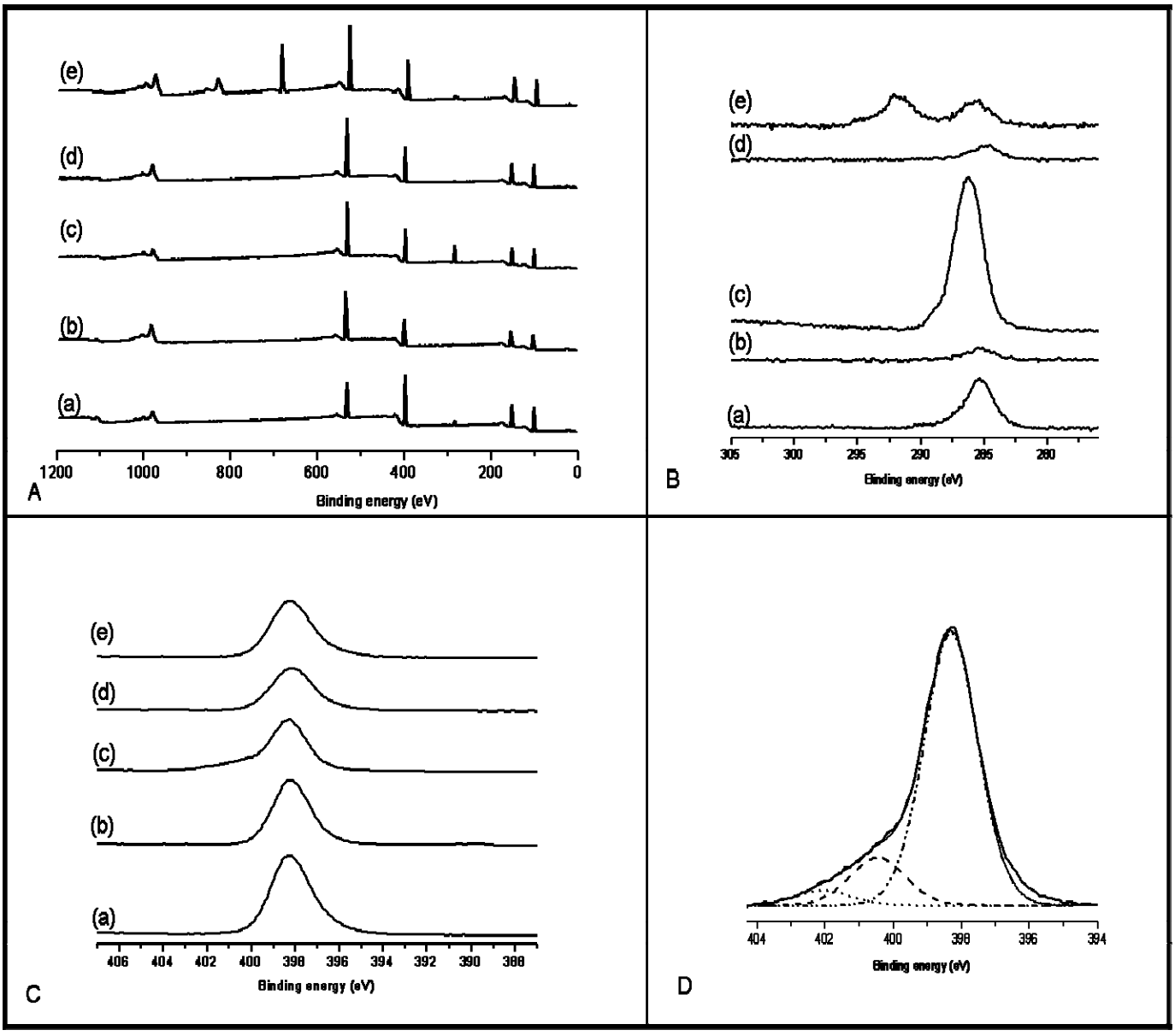


**Figure 4-1: XPS analysis of MEAs before and after surface modification with SAMs**

**A (a-e): the MEA as received (a), the MEA after $O_2$ plasma cleaning treatment (b), with DETA (c) and 13 F (e) As a control, the MEA surface has been also examined after exposing it to the LASER irradiation (d). C 1s, Si 2p, N 1s and O 1s high resolution spectra for the same set of samples (a-e) were also recorded and presented in Fig 1 B, C, D and E respectively.**

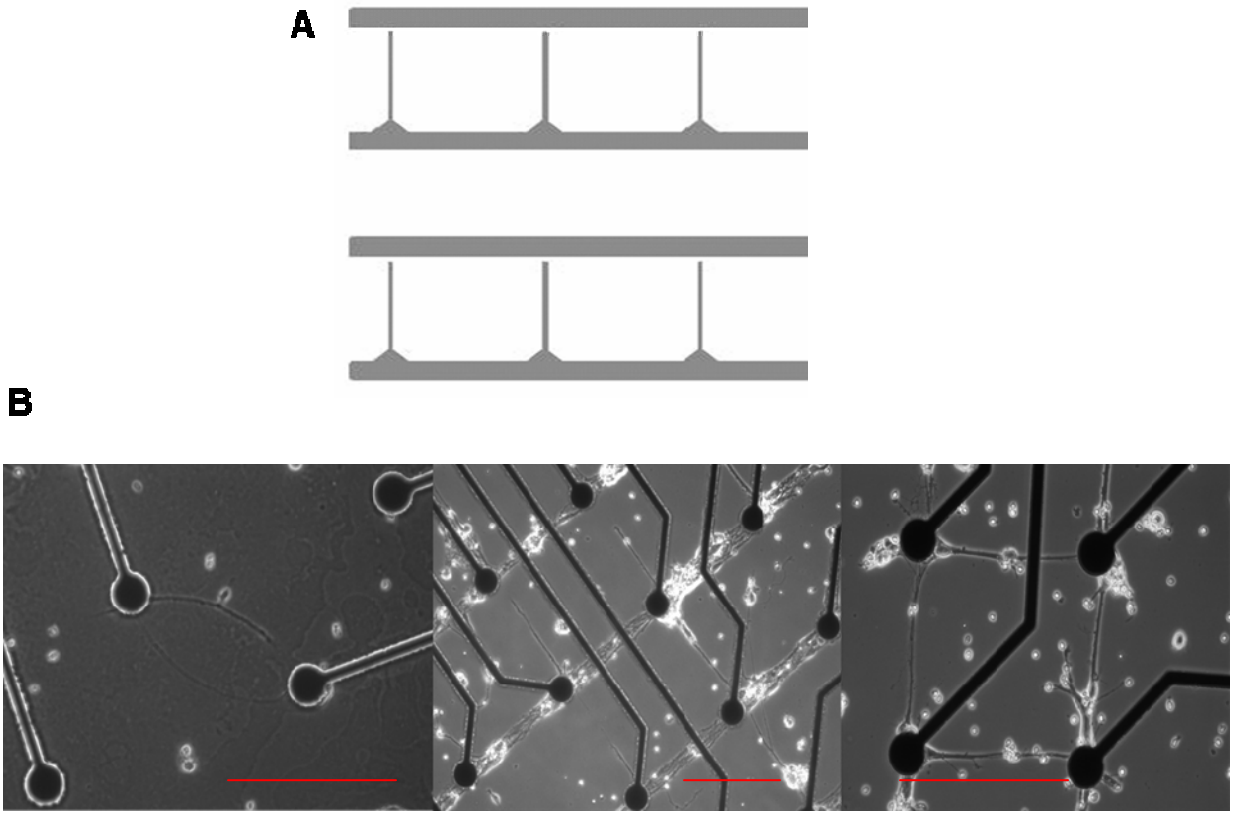


**Figure 4-2: Pattern design and patterned embryonic hippocampal neurons.**

**A: mask design for studying network activity, B: Phase pictures of patterned neuronal networks and two cell networks on microelectrode arrays on day 7 after culture. Extreme left image shows a two cell hippocampal network, center figure shows a grid like pattern of hippocampal cells. Scale bar: 200 µm.**

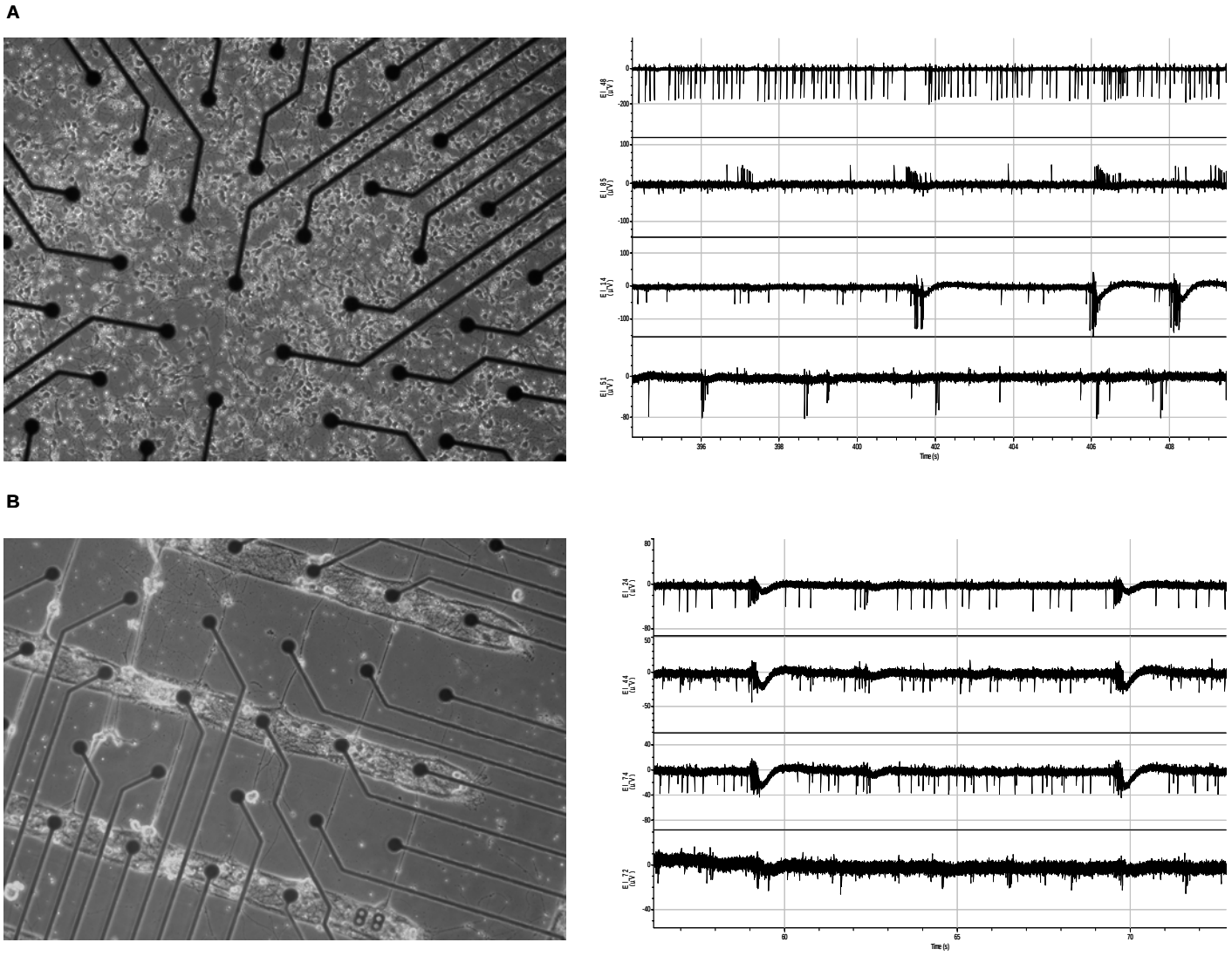


**Figure 4-3: Induction of LTP like activity in cultured Hippocampal networks.**

**A: Left: Random network of Hippocampal neurons on day 14, Right: Recordings taken from 4 different electrodes from the random network show both burst and non-burst spike activity. A burst is defined as a collection of spikes which are indicated by the single vertical lines. Each panel indicates recordings from an electrode on the MEA. Degree of synchronous spiking is not high, B: Left: Patterned networks on day 14, Right: Recordings taken from 4 directionally connected channels showing a stronger and higher degree of synchronous burst activity.**

**1S, 3R ACPD: 1-Aminocyclopentane-1,3-dicarboxylic acid**

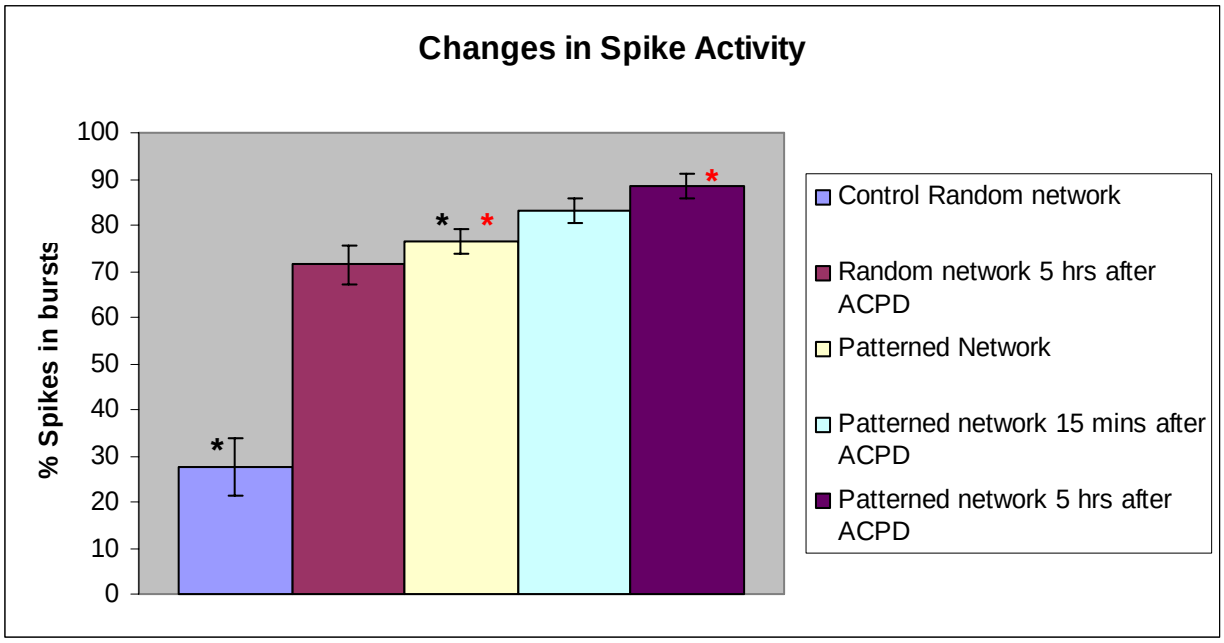


*** p<0.01, * p< 0.05 N=5**

**Figure 4-4: Induction of LTP like activity in cultured hippocampal networks.**

**C: Recordings taken 15 minutes after addition of 30 µM ACPD. Representative traces show more organized and increased synchronous spike activity. D: Recordings taken 5 hours after addition of 30uM ACPD show increased and synchronous bursting activity between interconnected neurons E: Bar graph representing the percentage of spikes in bursts of the different treatment conditions (Mean ± SEM; n = 5).**

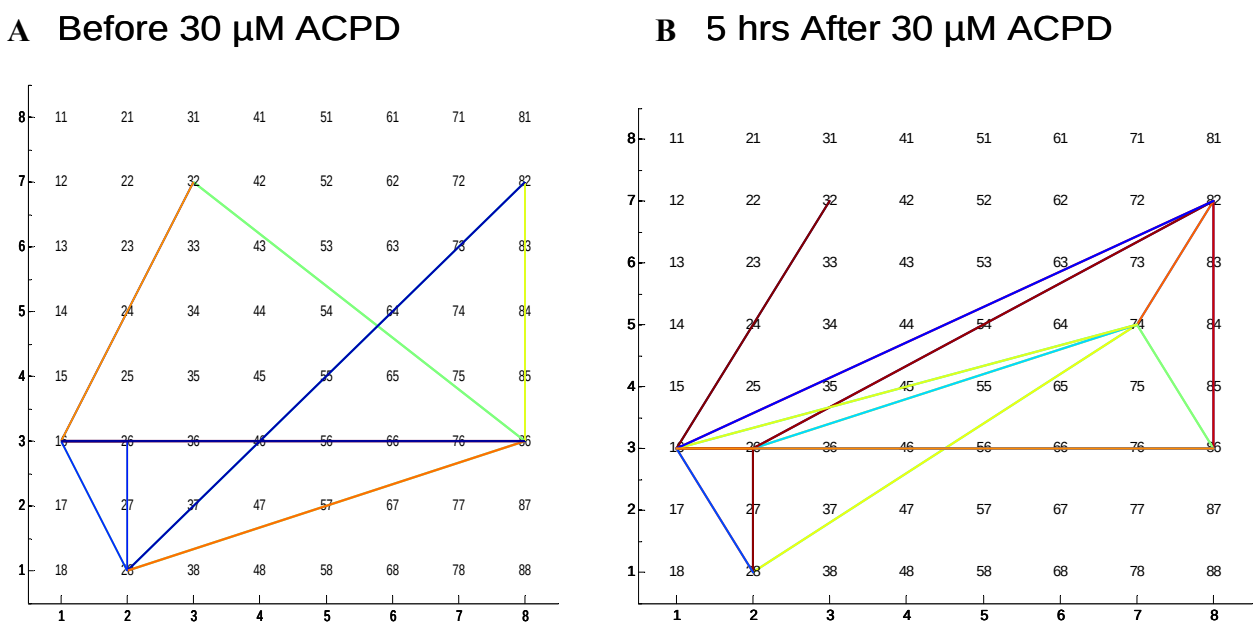


**Figure 4-5: Analysis of synaptic restructuring after ACPD addition.**

**A: Granger Causality showing synaptic communication between the interconnected neuronal layers on the electrodes before ACPD addition B: Granger causality showing increased network activity after ACPD addition. The lines are color coded to indicate the strength of the synaptic activity with blue indicating a weaker synaptic strength and red the strongest synaptic strength.**

## References:


[1] H. Bading, "Transcription-dependent neuronal plasticity the nuclear calcium hypothesis," *Eur J Biochem,* vol. 267, pp. 5280-3, Sep 2000.

[2] R. C. Malenka and M. F. Bear, "LTP and LTD: an embarrassment of riches," *Neuron,* vol. 44, pp. 5-21, Sep 30 2004.

[3] B. E. Alger and T. J. Teyler, "Long-term and short-term plasticity in the CA1, CA3, and dentate regions of the rat hippocampal slice," *Brain Res,* vol. 110, pp. 463-80, Jul 16 1976.

[4] P. A. Schwartzkroin and K. Wester, "Long-lasting facilitation of a synaptic potential following tetanization in the in vitro hippocampal slice," *Brain Res,* vol. 89, pp. 107-19, May 16 1975.

[5] J. C. Lopez-Garcia, O. Arancio, E. R. Kandel, and D. Baranes, "A presynaptic locus for long-term potentiation of elementary synaptic transmission at mossy fiber synapses in culture," *Proc Natl Acad Sci U S A,* vol. 93, pp. 4712-7, May 14 1996.

[6] S. H. Yun, D. S. Lee, H. Lee, E. H. Baeg, Y. B. Kim, and M. W. Jung, "LTP induction modifies functional relationship among hippocampal neurons," *Learn Mem,* vol. 14, pp. 190-4, Mar 2007.

[7] R. A. Zalutsky and R. A. Nicoll, "Comparison of two forms of long-term potentiation in single hippocampal neurons," *Science,* vol. 248, pp. 1619-24, Jun 29 1990.

[8] T. V. Bliss and A. R. Gardner-Medwin, "Long-lasting increases of synaptic influence in the unanesthetized hippocampus," *J Physiol,* vol. 216, pp. 32P-33P, Jul 1971.

[9] T. V. Bliss and A. R. Gardner-Medwin, "Long-lasting potentiation of synaptic transmission in the dentate area of the unanaestetized rabbit following stimulation of the perforant path," *J Physiol,* vol. 232, pp. 357-74, Jul 1973.

[10] T. P. Yu, H. A. Lester, and N. Davidson, "Requirement of a critical period of GABAergic receptor blockade for induction of a cAMP-mediated long-term depression at CA3-CA1 synapses," *Synapse,* vol. 49, pp. 12-9, Jul 2003.

[11] M. P. Thomas, M. I. Davis, D. T. Monaghan, and R. A. Morrisett, "Organotypic brain slice cultures for functional analysis of alcohol-related disorders: novel versus conventional preparations," *Alcohol Clin Exp Res,* vol. 22, pp. 51-9, Feb 1998.

[12] C. O. Aptowicz, P. E. Kunkler, and R. P. Kraig, "Homeostatic plasticity in hippocampal slice cultures involves changes in voltage-gated Na+ channel expression," *Brain Res,* vol. 998, pp. 155-63, Feb 20 2004.

[13] A. Natarajan, P. Molnar, K. Sieverdes, A. Jamshidi, and J. J. Hickman, "Microelectrode array recordings of cardiac action potentials as a high throughput method to evaluate pesticide toxicity," *Toxicol In Vitro,* vol. 20, pp. 375-81, Apr 2006.

[14] J. Pine, "Recording action potentials from cultured neurons with extracellular microcircuit electrodes," *J Neurosci Methods,* vol. 2, pp. 19-31, Feb 1980.

[15] G. W. Gross, B. K. Rhoades, H. M. Azzazy, and M. C. Wu, "The use of neuronal networks on multielectrode arrays as biosensors," *Biosens Bioelectron,* vol. 10, pp. 553-67, Summer 1995.
[16] D. W. Branch, J. M. Corey, J. A. Weyhenmeyer, G. J. Brewer, and B. C. Wheeler, "Microstamp patterns of biomolecules for high-resolution neuronal networks," *Med Biol Eng Comput,* vol. 36, pp. 135-41, Jan 1998.
[17] J. C. Chang, G. J. Brewer, and B. C. Wheeler, "A modified microstamping technique enhances polylysine transfer and neuronal cell patterning," *Biomaterials,* vol. 24, pp. 2863-70, Aug 2003.
[18] Y. Nam, J. C. Chang, B. C. Wheeler, and G. J. Brewer, "Gold-coated microelectrode array with thiol linked self-assembled monolayers for engineering neuronal cultures," *IEEE Trans Biomed Eng,* vol. 51, pp. 158-65, Jan 2004.
[19] A. E. Schaffner, J. L. Barker, D. A. Stenger, and J. J. Hickman, "Investigation of the factors necessary for growth of hippocampal neurons in a defined system," *J Neurosci Methods,* vol. 62, pp. 111-9, Nov 1995.
[20] D. A. Stenger, C. J. Pike, J. J. Hickman, and C. W. Cotman, "Surface determinants of neuronal survival and growth on self-assembled monolayers in culture," *Brain Res,* vol. 630, pp. 136-47, Dec 10 1993.
[21] Ravenscroft, M. S., Bateman, K. E., Shaffer, K. M., Schessler, H. M., Jung, D. R., Schneider, T. W., Montgomery, C. B., Custer, T. L., Schaffner, A. E., Liu, Q. Y., Li, Y. X., Barker, J. L., and Hickman, J. J. (1998) Developmental Neurobiology Implications from Fabrication and Analysis of Hippocampal Neuronal Networks on Patterned Silane-Modified Surfaces, *Journal of the American Chemical Society 120*, 12169-12177.
[22] D. A. Stenger, J. J. Hickman, K. E. Bateman, M. S. Ravenscroft, W. Ma, J. J. Pancrazio, K. Shaffer, A. E. Schaffner, D. H. Cribbs, and C. W. Cotman, "Microlithographic determination of axonal/dendritic polarity in cultured hippocampal neurons," *J Neurosci Methods,* vol. 82, pp. 167-73, Aug 1 1998.
[23] G. J. Brewer and C. W. Cotman, "Survival and growth of hippocampal neurons in defined medium at low density: advantages of a sandwich culture technique or low oxygen," *Brain Research,* vol. 494, pp. 65-74, 1989.
[24] M. Das, P. Molnar, C. Gregory, L. Riedel, and J. J. Hickman, "Long-term Culture Of Embyonic Rat Cardiomyocytes on an Organosilane Surface in a Serum Free Medium," *Biomaterials,* vol. 25, pp. 5643-5647, 2004.
[25] V. Dhir, A. Natarajan, M. Stancescu, A. Chunder, N. Bhargava, M. Das, L. Zhai, and P. Molnar, "Patterning of diverse mammalian cell types in serum free medium with photoablation," *Biotechnol Prog,* vol. 25, pp. 594-603, Mar-Apr 2009.
[26] P. Molnar, J. F. Kang, N. Bhargava, M. Das, and J. J. Hickman, "Synaptic connectivity in engineered neuronal networks," *Methods Mol Biol,* vol. 403, pp. 165-73, 2007.
[27] P. Molnar, W. Wang, A. Natarajan, J. W. Rumsey, and J. J. Hickman, "Photolithographic patterning of C2C12 myotubes using vitronectin as growth substrate in serum-free medium," *Biotechnol Prog,* vol. 23, pp. 265-8, Jan-Feb 2007.
[28] M. S. Ravenscroft, K. E. Bateman, K. M. Shaffer, H. M. Schessler, D. R. Jung, T. W. Schneider, C. B. Montgomery, T. L. Custer, A. E. Schaffner, Q. Y. Liu, Y. X. Li, J. L. Barker, and J. J. Hickman, "Developmental neurobiology implications from fabrication

and analysis of hippocampal neuronal networks on patterned silane- modified surfaces," *Journal of the American Chemical Society,* vol. 120, pp. 12169-12177, 1998.

[29] A. E. Schaffner, J. L. Barker, D. A. Stenger, and J. J. Hickman, "Investigation of the factors necessary for growth of hippocampal neurons in a defined system," *J Neurosci Methods,* vol. 62, pp. 111-9., 1995.

[30] F. J. Arnold, F. Hofmann, C. P. Bengtson, M. Wittmann, P. Vanhoutte, and H. Bading, "Microelectrode array recordings of cultured hippocampal networks reveal a simple model for transcription and protein synthesis-dependent plasticity," *J Physiol,* vol. 564, pp. 3-19, Apr 1 2005.

[31] H. Bading and M. E. Greenberg, "Stimulation of protein tyrosine phosphorylation by NMDA receptor activation," *Science,* vol. 253, pp. 912-4, Aug 23 1991.

[32] F. Hofmann and H. Bading, "Long term recordings with microelectrode arrays: studies of transcription-dependent neuronal plasticity and axonal regeneration," *J Physiol Paris,* vol. 99, pp. 125-32, Mar-May 2006.

[33] S. L. Bressler, W. Tang, C. M. Sylvester, G. L. Shulman, and M. Corbetta, "Top-down control of human visual cortex by frontal and parietal cortex in anticipatory visual spatial attention," *J Neurosci,* vol. 28, pp. 10056-61, Oct 1 2008.

# CHAPTER 5: DESIGNING PATTERN FEATURES TO STUDY TWO CELL HIPPOCAMPAL NETWORKS AND CELL MIGRATION IN SERUM FREE MEDIUM

## Introduction

Neuronal cultures have traditionally been grown from disassociated cells where the basic structure of the brain is destroyed. These *in vitro* systems form random synaptic connections and Patch-clamp electrophysiology has been extensively used to study single cell and network activity. The inherent drawbacks to this approach are the invasiveness of the cell isolation techniques which basically destroys the pre existing networks found in the CNS. Patch clamp electrophysiology also cannot be used to monitor large populations of cells. Planar microelectrode arrays (MEA) have been utilized over the last two decades in an attempt to record non-invasively from neuronal cells (*1-3*) to overcome some of the limitations in established techniques. However random cultures on microelectrode arrays present new challenges as the cells tend to not always establish themselves on top or near electrodes making specific site recording difficult in these cultures. Placing the cells directly on top of the electrode would better facilitate the proper study of the neuronal connectivity between neuronal cells *in vitro*. Surface modification and patterning would help in not only providing a solution to this problem but also establishes interconnections and aids in long term survival (*4-7*).

A critical part of patterning is to provide the cell with two types of adhesion options. The foreground or the cell attractive region generally consists of molecules that include amino silanes

or ECM proteins including Fibronectin (*8, 9*). The background is a cell repulsive region that includes alkylsilanes, fluorinated silanes and polyethylene glycol moities that provides a protein cytophobic surface (*8, 10*). Previous research has (*8, 11, 12*) indicated that photolithographic patterning of SAMs can help create engineered neuronal networks.

The ideal engineered connectivity to reproduce some of the basic functions of neuronal networks would consist of two cell patterns. Studying synaptic plasticity and interactions between these cells could yield information about Long term potentiation (LTP), drug effects and cell migration at the cellular level. In this study the geometric requirements needed for creating two cell networks was invetsigated. It is challenging to establish artificial neuronal circuits that precisely comply with pre-designed MEA circuit geometry by controlling individual neuronal migration and positioning in vitro thereby simulating the process of directed neuronal migration in vivo. In this study, we demonstrated that neuron migration to a predetermined pathway and destination can be achieved by appropriate manipulation of substrate surface chemistry and pattern geometry in embryonic hippocampal neuronal cultures.

## Materials and Methods

### *Surface cleaning*

Glass coverslips were cleaned using an acid wash protocol. Briefly a ceramic rack containing glass coverslips were soaked in a solution of 50/50 methanol (HPLC grade)/ hydrochloric acid (Reagent grade) for 15-30 min. They were then rinsed with deionised ultra filtered (DUIF) water three times and placed in a beaker containing concentrated sulfuric acid (reagent grade from fisher) for a minimum of 30 minutes. The racks of coverslips were rinsed

thoroughly again and boiled in DUIF water for at least 30 minutes. The rack and slips were then rinsed in two final solutions of acetone and oven dried at 110C for 10-15 min. The contact angle was confirmed to be less than 5 deg.

### *Surface modification of the acid washed slips*

The method used for surface modification was based on that of previous protocols (*8*). Briefly, ceramic racks with the cleaned glass slips were immersed in a 0.1% (v/v) DETA ( N-1[3-(Trimethoxysilyly)propyl] Diethylenetriamine ) in HPLC-graded Toluene solvent and heated to just below the boiling temperature for 30 minutes. It was then allowed to cool down to room temperature. HPLC-graded Toluene was used to rinse the slips and the slips were reheated for 30 minutes as before. The slips were then oven dried for 2 hrs to overnight.

After DETA ablation using deep UV laser irradiation (mentioned below), backfilling the ablated region was done using a 0.1% tridecafluoro-1,1,2,2-tetrahydrooctyl-1-trichlorosilane (13F) SAM in chloroform solution. Briefly, the racks with the slips were immersed in the 13f solution for 5 minutes, rinsed in chloroform and oven dried for 15 minutes

### *Photolithographic patterning*

The required pattern was designed using either AutoCAD or CLEWIN software and the design was used to construct a quartz mask. Patterns were made photolithographically by exposing the DETA monolayer to ArF laser irradiation through the quartz mask. Deep UV ablation of DETA was done using a 193 nm Ar/F excimer LPX2001 laser beam (Lambda Physik,

Ft.Lauderdale, Fl) combined with a beam homogenizer (Microlas, Ft.Lauderdale, Fl). The ablation was done for a minimum of 30 seconds.

## *Surface characterization*

The surface analysis of the modified slips was done using X-Ray photoelectron spectroscopy (XPS) and contact angle measurements. Three spots on a sample slip were analyzed using XPS. For each sample, survey scans and high resolution scans for the individual peaks of Fluorine (1s), Oxygen (1s), Carbon (1s) and Silicon (2p) and Nitrogen (1s) was performed. Using a standard curve fitting technique for the high resolution peaks, the individual elemental compositions, the relative values of fluorine with respect to the rest of the elements, and the ratio of nitrogen to silicon were calculated. More details were given in the previous chapter. XPS analysis is shown in figure 2. The wettability of the SAM surfaces was determined by contact angle goniometry (KSV Instruments, Cam 200). A static sessile drop of ultra pure deionized water (5µl) was dispensed on the monolayer surface (DETA and 13F SAMs). The angle at which the water drop contacts the surface was measured. The reported values represent the average of three independent measurements taken across the surface.

*Pd-Cu electroless metallization***.** The formation of DETA/13F SAMs pattern was confirmed by electroless metallization. The metallization process is an indirect method for visualization of organosilane patterns, because direct examination of patterns is difficult with a microscope. This method was adapted from Kind et al.(*15*) and slightly modified to better suit our system

(DETA/13F patterns). Copper (Cu) binds only to the amine groups of the DETA monolayer through a series of chemical reactions, but not to the 13F monolayer. In brief, the patterned substrates were first immersed in a disodium tetrachloropalladate ($Na_2PdCl_4$) solution for 15 min to allow the palladium chloride ions ($PdCl_4^{-2}$) to directly bind to the amino groups of DETA. The solution was made with 10 mg $Na_2PdCl_4$ and 1.75 g sodium chloride (NaCl) dissolved in 50 ml distilled water, whose pH was adjusted to 1.0 with concentrated HCl. The substrates were then rinsed thoroughly with distilled water and immersed for 15 min in a solution of dimethylamine borane (DMAB) to allow the reduction of palladium chloride ions to palladium metal (Pd). The DMAB solution was prepared by dissolving 1.7 g of DMAB in 50 ml distilled water. The substrates were again rinsed thoroughly with distilled water and subsequently immersed in a third solution called copper bath solution. This solution was prepared by dissolving 3 g of copper sulfate ($CuSO_4$), 14 g sodium potassium tartrate ($KNaC_4H_4O_6 \cdot 4H_2O$) and 2 g sodium hydroxide (NaOH) in 100 ml distilled water, followed by slow addition of formaldehyde (37.2%) (10 µl/ml of CBS). The formaldehyde functions as a reducing agent during metallization. Ultimately this leads to copper metal (Cu) deposition onto DETA. The palladium ions, which were bound to the amino groups of the DETA, served as the precursor for the deposition of copper ions. This process allows metallization of Cu only on the DETA regions (i.e. patterned surfaces), which can be visualized by a light microscope. Figure 3 shows the metallized images of different kinds of patterns.

## *Cell culture*

Hippocampal neurons were obtained from day 18 old rat embryos and prepared as previously described (*13*). Briefly, hippocampi were dissected from timed-pregnant Sprague-Dawley rats. The tissue was mechanically dissociated in a cold serum free dissection Hibernate E medium supplemented with B27 (2% v/v; Invitrogen), glutamax (1% v/v; Invitrogen) and antibiotic/antimycotic (1% v/v; Invitrogen).

Prior to cell plating, patterned glass coverslips were sterilized with absolute ethanol and dried. Cells were plated on the glass coverslips at a density of approximately 75 cells/$mm^2$. The serum free culture media was neurobasal medium supplemented with B27 (2% v/v; Invitrogen), glutamax (1% v/v; Invitrogen) and a antibiotic/antimycotic (1% v/v; Invitrogen).

## *Time lapse recording*

Time lapse recordings were performed immediately after the cells were plated. The neurons were observed under an inverted microscope (Zeiss-Axiovert 100) equipped with Plan-Neofluar 10x objective (Zeiss, Oberkochen, Germany) and in a humidified incubation chamber to achieve a constant temperature of 37ºC in a 5% $CO_2$ atmosphere. Time-lapse pictures were captured with a Hamamatsu C8484-05G digital charge-coupled device camera (Hamamatsu Photonics, Shizuoka, Japan). Time-lapse experiments were run under the control of Okolab software (OKO-lab, Ottaviano, NA, ITALY). Live cell image sequences were exported using NIH ImageJ software to create the movies.

## Results

The surface characterization of the SAMs indicated successful surface modification with incorporation of both DETA and 13F (Figure 5-1). Further characterization was done using electroless metallization and as shown the fidelity of the patterns was confirmed (Figure 5-2). Surface wettability was determined using contact angle measurements. The average contact angle of DETA was 48 ± 2° and for 13F was 85± 2°. Dissociated hippocampal neurons from embryonic rats were cultured on patterns of different dimensions, in a defined serum-free medium. The cells were found to attach to these patterns in a manner indicating their geometric preferences for cell body adhesion sites as well as process outgrowth. The design criteria of the neuronal circuit were simple and yet served multiple functionalities. The two-neuron circuit was designed to study synaptic connectivity (*16*), and to immobilize two neurons at determined sites. Ideally, each individual neuron adhered to the circular region or solid dot provided and put out an axon and dendrites along designated pathways. The two neurons thus formed synaptic connections that could then be used for studying circuit functionality. For the circuit geometry, each broken or dashed line comprised of two 2 μm X 10 μm bars separated by a 10 μm gap allowing for the shorter dendritic outgrowth (*8*). The solid dot also acted as the destination of the migrating neuron and became the somal adhesion site with a size of 20 μm in diameter. The distance between two somal adhesion sites was varied between a 100μm to 500 μm and the line width for process growth was varied between 1 and 4 μm. The continuous line and dashed or broken line on either side of the somal adhesion sites were designed so that axonal growth was in a specific, unidirectional pathway toward the second neuron in the circuit. The arc shape design of the continuous line was to eliminate any other geometry influences (e.g. angles in a

rectangular shape circuit) on the migration process of the neurons. To determine the optimal cell density for seeding, the cells were plated on the patterned surfaces at cell concentrations ranging from 50 to 200 cells/mm$^2$. The cell culture results suggested that the lower the cell density (less than 75 cells/mm$^2$), the higher the restriction of cell attachment on the patterned surfaces. Conversely with higher cell densities (greater than 100 cells/mm$^2$), then the greater the cell attachment and spreading over the patterned surfaces, which led to unwanted cluster formation at the cell adhesion sites (i.e. growth of multiple cells on the circular pad of the network geometry where single cell growth was optimal) and, as a result, complex network formation (Data not shown). The optimal cell density chosen for this study was 75 cells/mm$^2$. The results also suggested that the line width between 2 and 3 μm provided the best environment for the axonal pathway. We have not noticed much difference on the line length of the pattern, which means cells send their axons typically to any length tested (100 and 500 μm). However, the line width between 200 and 300 μm provided more reproducible results for the axonal pathway as shown in the figure 5-3. These results indicate that geometrical dimensions of patterns greatly influence cell behaviors, in particular cell localization and migration. The cells cultured on the patterned surfaces survived up to 24 days on the patterned surfaces, which is more than sufficient for the study of electrophysiological behaviors of excitable neurons.

Patterning using the two cell network also allowed for initial studies of cell migration. To observe how the neuronal circuits were formed on the chemically patterned glass substrate, time lapse recording was performed immediately after the hippocampal neurons were plated on surfaces. Initially, the neurons were uniformly distributed on the entire surface. The majority of neurons were located on the 13F background area and at different distances to the DETA

geometry cues. Some of the neurons were close to the dashed lines and some were near the continuous lines. Time lapse sequences revealed how a typical two-neuron circuit was formed on the patterned surface by directed neuron migration (Figure 5-4). We observed that the dashed line – dot combined geometry cues provided a somal translocation mode migration pathway and destination. At a specific time point, the neurons close to the dashed line were observed to quickly extend a leading process towards the somal adhesion site followed by a fast soma movement along the leading process. Finally, the cell body extended a neurite to form the axon along the continuous line and neurites along the smaller dashed lines (*17*) that form dendrites. The following neurite growth along the continuous lines established physical connection between two adhered neurons at somal adhesion sites leading to the formation of a two-neuron circuit.

## Discussion

As shown in the previous chapters we have successfully modified the surfaces of not only clean glass coverslips but also commercial electrode arrays (that can be reused over time) with SAMs to form engineered neuronal networks with functional connectivity. In this study the pattern features were refined such that limit cell adherence was limited to the patterns of two cells. This would allow not only the study of cell-cell interaction, but also synaptic responses to enable investigations of synaptic plasticity phenomenon such as LTP at the single cell level. It also for the exploration of the concept of cell migration and neuronal process outgrowth, which is as of yet not clearly defined. As shown in the results the patterned surfaces provided adequate support for adhesion, survival, orientation, neurite outgrowth, and synapse formation for the mammalian embryonic hippocampal cells. This study helps determine the ideal parameters

needed for the formation of two cell networks providing the required pattern dimensions as well as cell culture optimal density requirements. It also indicated neuronal cell migration on a DETA/13F SAM surface for the first time.

We have developed an in vitro system that allows for pyramidal neuron migration which can then be spatially and temporally analyzed. Neurite outgrowth was controlled by both environmental signals and geometric constraints which is different from what occurs in vivo. This raises the interesting question of whether these neurites are different in terms of cell surface receptors, motor proteins, signaling pathways, post-translational tubulin modification, etc. The presence of chemical groups on the surface leading to covalent attachments can modify the present of catalytic enzymes which can significantly alter the amount of tubulin within the cell (*18*). Further studies would involve a closer look at hippocampal neurites in this system and whether traditional neurite inhibitors can cause an effect and if so, in what way. The blocking of motor proteins such as Kinesin 1 which determine axon identity could also help in distinguishing these in vitro pyramidal cell neurites compared to those found in the brain. These experiments would then yield further information that can be used in in vitro studies involving stem cells differentiating into neurons.

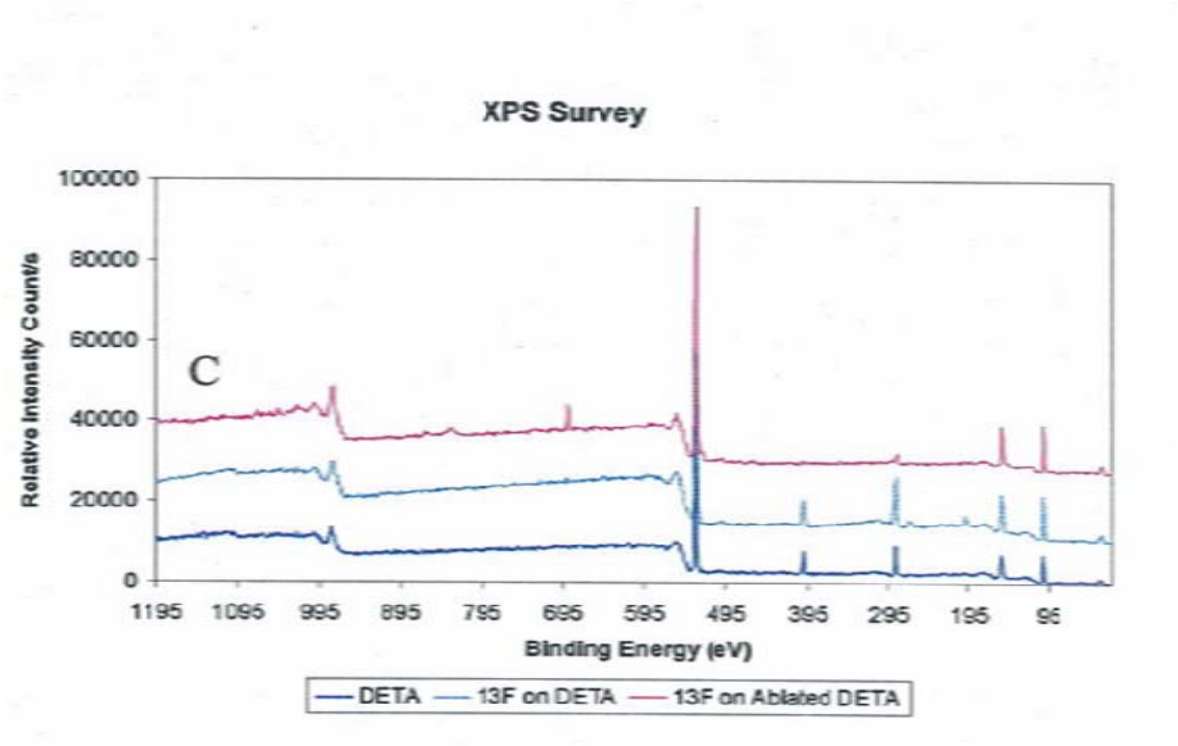


**Figure 5-1: Chemically patterned surface chemistry characterization using XPS**

**XPS survey scans of the DETA control (blue), 13F on DETA (green) and 13F on ablated DETA (red). The scan of 13F on DETA showed very little incorporation of the 13F into the DETA monolayer. The scan of 13F on ablated DETA had negligible nitrogen peak but significant fluorine peak. Scale bar, 50μm.**

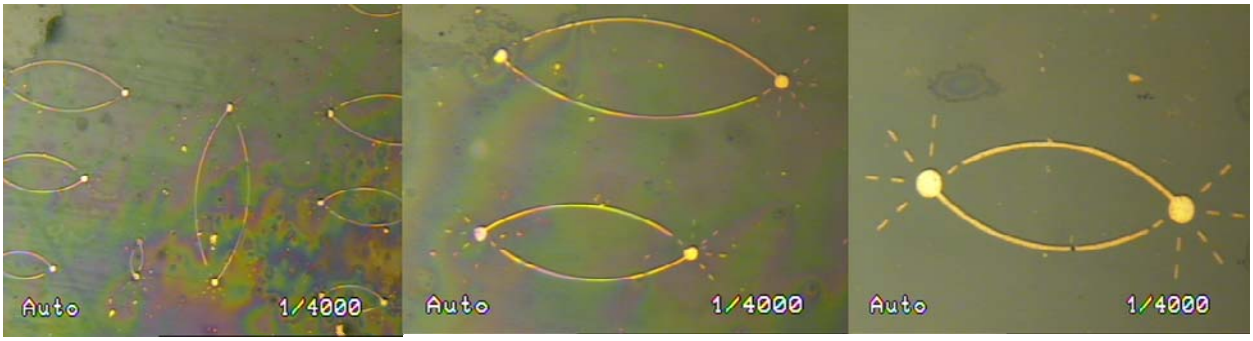


**Figure 5-2: Metallized image of the two-neuron circuit design with different dimensions**

**Each solid dot has a diameter of 20 µm and the distance between the two dots varied from 200 µm to 500 µm. Each dashed line contained two 2 µm x 10 µm bars separated by 10 µm gap. The two continuous lines had a maximum distance of 75 µm and each had 1 to 4 µm width.**

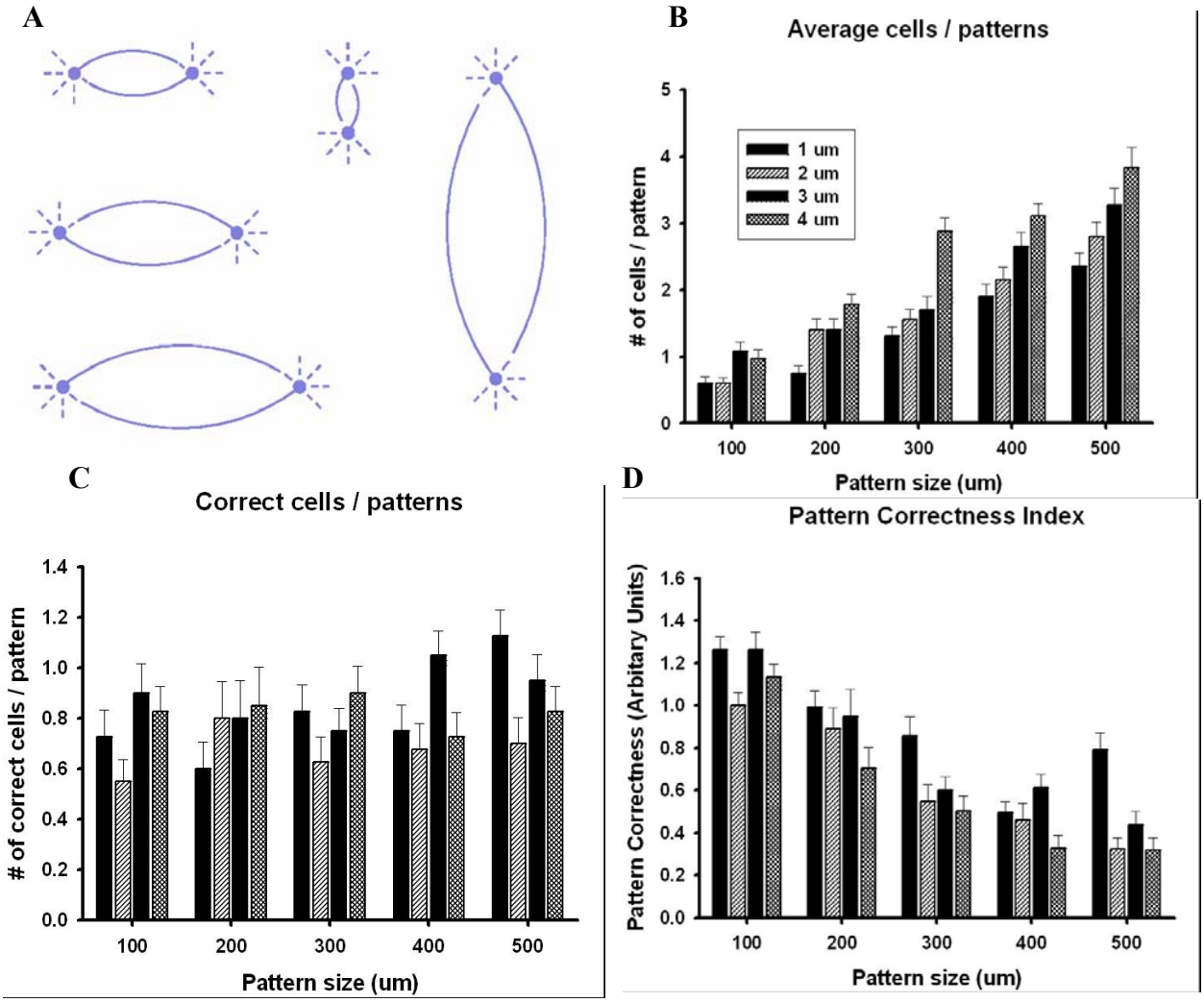


**Figure 5-3: Characterization of the effect of feature size and line width on cellular pattern formation.**

**A: Combination "fish pattern" design with 100,200,300,400 and 500 µm pattern diameters. Line width was also varied between 1 and 4 µm on different parts of the mask. B: The total number of cells on the patterns was approximately linearly related to the diameter of the patterns C: The number of correct cells (Sitting on the cell attachment sites) practically was not affected by any of the measured parameters D: The ratio of the correct patterns measured by the 'pattern correctness index' (Calculated as correct cells*correct cells/ total**

**cells) declined with increasing feature size, but it was only slightly dependent on the line width.**

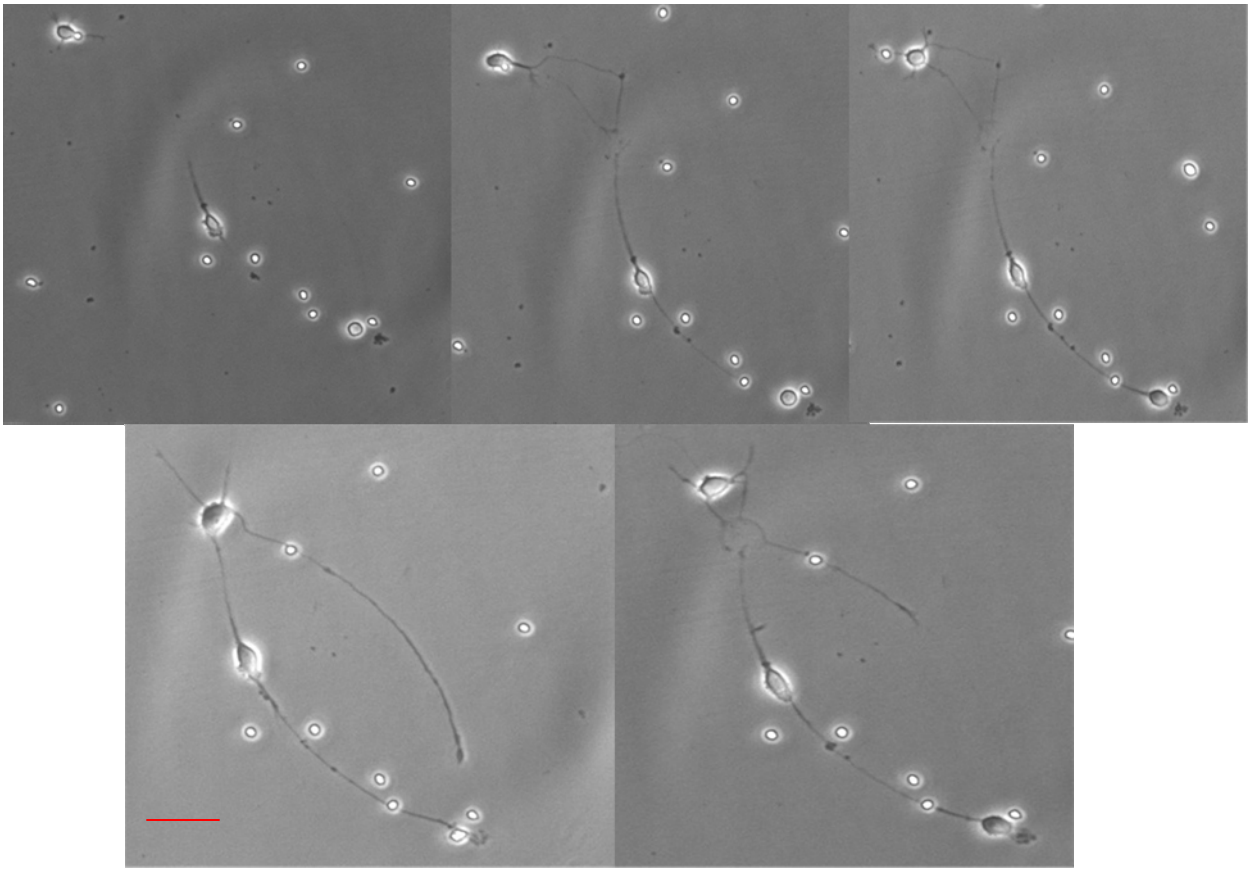

**Figure 5-4: Time lapse sequences over 48 hours of a two-neuron circuit formation by somal translocation mode neuron migration.**

**From left to right in a clockwise direction: Within 23 hours after plating, the neuron on the 13F region but close to the DETA dashed line developed short mutipolar processes. One short process randomly detected the DETA dashed line, and then it grew fast along the dashed line towards the somal adhesion site. When the tip of the leading process reached the somal adhesion site, it stopped growing but adhered and formed a circular growth cone with a diameter nearly identical to the size of the somal adhesion site. Around 12 hours later, soma translocated quickly through the leading process towards the somal adhesion site. After the soma reached the somal adhesion site, it assumes a flat and circular morphology with a diameter nearly identical to the somal adhesion site size. Axonal outgrowth starts along the continuous DETA line till it reached the neuron on the left side. Scale bar: 50 µm**

# References


1. Morin, F. O., Takamura, Y., and Tamiya, E. (2005) Investigating neuronal activity with planar microelectrode arrays: achievements and new perspectives, *J Biosci Bioeng 100*, 131-143.
2. Pine, J. (1980) Recording action potentials from cultured neurons with extracellular microcircuit electrodes, *J Neurosci Methods 2*, 19-31.
3. Potter, S. M. (2001) Distributed processing in cultured neuronal networks, *Prog Brain Res 130*, 49-62.
4. Chang, J. C., and Wheeler, B. C. (2006) Pattern Technologies for Structuring Neuronal Networks on MEAs, in *Advances in Network Electrophysiology: Using Multi-Electrode Arrays* (Taketani, M., and Baudry, M., Eds.), pp 153-189, Springer, New York.
5. Chang, J. C., Brewer, G. J., and Wheeler, B. C. (2001) Modulation of neural network activity by patterning, *Biosens Bioelectron 16*, 527-533.
6. Kleinfeld, D., Kahler, K. H., and Hockberger, P. E. (1988) Controlled outgrowth of dissociated neurons on patterned substrates, *J Neurosci 8*, 4098-4120.
7. Ma, W., Liu, Q. Y., Jung, D., Manos, P., Pancrazio, J. J., Schaffner, A. E., Barker, J. L., and Stenger, D. A. (1998) Central neuronal synapse formation on micropatterned surfaces, *Brain Res Dev Brain Res 111*, 231-243.
8. Stenger, D. A., Hickman, J. J., Bateman, K. E., Ravenscroft, M. S., Ma, W., Pancrazio, J. J., Shaffer, K., Schaffner, A. E., Cribbs, D. H., and Cotman, C. W. (1998) Microlithographic determination of axonal/dendritic polarity in cultured hippocampal neurons, *J Neurosci Methods 82*, 167-173.
9. Clark, E. A., and Brugge, J. S. (1995) Integrins and signal transduction pathways: the road taken, *Science 268*, 233-239.
10. A. Galtayries, R. W.-C. M. D. N. P. M. (2006) Fibronectin adsorption on Fe-Cr alloy studied by XPS, *Surface and Interface Analysis 38*, 186-190.
11. Ravenscroft, M. S., Bateman, K. E., Shaffer, K. M., Schessler, H. M., Jung, D. R., Schneider, T. W., Montgomery, C. B., Custer, T. L., Schaffner, A. E., Liu, Q. Y., Li, Y. X., Barker, J. L., and Hickman, J. J. (1998) Developmental Neurobiology Implications from Fabrication and Analysis of Hippocampal Neuronal Networks on Patterned Silane-Modified Surfaces, *Journal of the American Chemical Society 120*, 12169-12177.
12. James, J. H., Suresh, K. B., Judy, N. Q., Paul, S., David, A. S., Christian, J. P., and Carl, W. C. (1994) Rational pattern design for in vitro cellular networks using surface photochemistry, *Journal of Vacuum Science & Technology A: Vacuum, Surfaces, and Films 12*, 607-616.

13. Brewer, G. J., and Cotman, C. W. (1989) Survival and growth of hippocampal neurons in defined medium at low density: advantages of a sandwich culture technique or low oxygen, *Brain Research 494*, 65-74.
14. Kind, H., Bittner, A. M., Cavalleri, O., Kern, K., and Greber, T. (1998) Electroless deposition of metal nanoislands on aminothiolate-functionalized Au(111) electrodes, *J. Phys. Chem. B 102*, 7582-7589.
15. Kind, H., Bittner, A. M., Cavalleri, O., Kern, K., and Greber, T. (1998) Electroless Deposition of Metal Nanoislands on Aminothiolate-Functionalized Au(111) Electrodes, *The Journal of Physical Chemistry B 102*, 7582-7589.
16. Molnar, P., Kang, J. F., Bhargava, N., Das, M., and Hickman, J. J. (2007) Synaptic connectivity in engineered neuronal networks, *Methods Mol Biol 403*, 165-173.
17. Stenger, D. A., Hickman, J. J., Bateman, K. E., Ravenscroft, M. S., Ma, W., Pancrazio, J. J., Shaffer, K., Schaffner, A. E., Cribbs, D. H., and Cotman, C. W. (1998) Microlithographic determination of axonal/dendritic polarity in cultured hippocampal neurons, *Journal of Neuroscience Methods 82*, 167-173.
18. Laferriere, N. B., MacRae, T. H., and Brown, D. L. (1997) Tubulin synthesis and assembly in differentiating neurons, *Biochem Cell Biol 75*, 103-117.

# CHAPTER 6: GENERAL DISCUSSION

The combination of nanotechnology, surface chemistry and biomedical sciences provides numerous opportunities to develop hybrid systems that will play a significant role in the future of modern science (*1, 2*). This dissertation, done in two parts, showed the development of this prototypical system, which was relatively simple and can be further developed in industry for use in multiple applications. These include not only drug development and an understanding of how cells interact with each other and surfaces, but also as toxin sensors and in tissue engineering by demonstrating the interaction of cells with appropriate materials that can act as scaffolds that aid long term cell growth and survival (*3-5*). This was done primarily by controlling two vital parameters, the surface on which the cells grow and the defined environment, namely the medium in which the cells are cultured. The control and manipulation of the surface using SAMs had a three fold purpose. It was used to improve cell growth and survival, study surface effects on cell function and development, and most importantly, for patterning. Patterning, the technique of providing the cells two different kinds of surfaces, control their movement and growth according to a specific design, is an important part of the development of these hybrid systems. It was significant in that it not only directed the formation of ordered networks of cells that mimics the more structured tissue in the body, but also helped situate the electrically active cells on recording/stimulating electrodes in microelectrode arrays. The use of serum-free

medium also defined the environment of the system and was critical in analyzing the output or response of the cells to different kinds of stimuli, be it to chemical or electrical.

The first part of this project used cardiomyocytes to develop two kinds of high-throughput platforms. By manipulating surface chemistry and patterning, a simple method was devised to (a) study surface effects on cell growth and differentiation and (b) developed a system that can act as a drug side effect screening tool. First, to understand the effect of scaffold degeneration on cardiac mycoytes, the growth of embryonic rat cardiomyocytes on surfaces functionalized with SAMs was studied with SAMs that had hydroxyl and carboxyl functional groups to mimic the surface degradation of three biodegradable polymers, Poly (lactic acid) (PLA), poly (lactic-co-glycolic acid) (PLGA) and poly (glycolic acid) (PGA). Using simple surface modification techniques 4 different types of surfaces were prepared and embryonic rat cardiomyocytes, in serum free medium were cultured on these surfaces. The morphology, physiology and survival was then characterized. The effects of these surfaces on cell morphology, beating and physiology was examined and quantified. Results indicated that there were definite differences in cell electrophysiology, significantly in the case of surfaces functionalized with hydroxyl functional groups and the survival of cells on this surface was the lowest. This finding supported the work done in 3 dimensional scaffolds and hydrogels, which showed the dependence of cell survival on scaffold degeneration. Our results are significant in showing the increase in action potential duration of cells cultured on hydroxyl surfaces and showed the efficiency of such a system to study surface effects and could easily be reproduced to facilitate the study of implants and prosthetic devices as well as other applications in tissue engineering.

The vital part of any hybrid system is the interface and the first series of experiments in the chapter three delve into understanding what types of surface and environmental controls are necessary for the ideal growth of cardiomyocytes in defined patterns. It was found that embryonic rat cardiomyocytes did not form monolayer sheets on patterned MEAs that were functionalized with DETA/13F. The adsorption of the proteins Fibronectin or vitronectin to the DETA/13 patterns did not prove successful either as the proteins uniformly adsorbed everywhere including on the 13F. This led to the development, as shown in chapter three, of a new type of surface modification of the MEAs, using neonatal rat cardiomyocytes. Poly-ethylene glycol (PEG) has been shown to be very resistant to protein adsorption (*6*) and proved to be ideal for a Fibronectin/PEG modification of the MEAs for supporting patterned cardiomyocytes growth and survival in serum-free conditions. The series of experiments indicate the feasibility of such a system to determine vital cardiac parameters at the cell and tissue level. Conduction velocity was measured to a high degree of accuracy and the system was used to study the effects of different toxins on these parameters. The results showed that this system can be used to study cardiac disease models, conduction block, QT interval, refractory period and changes in these parameters when exposed to a drug. This is highly significant, as this system can be developed into a high throughput drug development platform that could reduce animal testing and analyze drug side effects at the cell and tissue levels. Such a system would even advance the study of side effects on human cells..

The next two chapters used the technique of patterning to study a high throughput neuronal platform. Experiments were done to functionalize the surface of commercial microelectrode arrays with SAM patterns. Initial studies involved pattern design, to improve the

resolution of patterns that would best support network formation and cell survival in serum-free conditions. We designed, optimized and characterized two cell networks *in vitro*. The results indicated cell migration onto such patterns and the electrophysiology demonstrated the synaptic connectivity. Such two cell networks would be extremely useful in not only studying developmental behavior at the cellular level but would also give information concerning cell interactions. The design was further changed into a uni-directional grid pattern to study synaptic plasticity. Though decades of research have gone into understanding memory formation and the phenomenon underlying it termed Long term potentiation (LTP) and Long term depression (LDP)(*7-10*), there are still many questions that are unanswered in this field especially at the cellular level. Studies into LTP thus far have looked at hippocampal tissue slices (*7, 11*). In this study, we have attempted to demonstrate LTP in an ordered network of disassociated cells, so that the effects of cell responses on factors such as memory formation could be better understood at the cellular level. Using an engineered network of cell layers positioned on electrodes with a unidirectional functional connectivity, these experiments demonstrated synaptic responses similar to LTP. The structural re-organization of the network and the synaptic strengthening of cell interactions, by chemical induction, showed the efficacy of this system to study drug effects in disease models. Such a system would help make significant strides in understanding LTP in Alzheimer's and be used for drug screening and testing.

In conclusion, this dissertation outlined the steps involved in the successful development and testing of high throughput hybrid systems that have varied applications ranging from implant development, understanding cell developmental behavior, and most importantly in disease models and as a fast, efficient, high-throughput *in vitro* drug side effect screening

platform. Information from such a system can lead to significant improvements in technology utilized by the pharmacology industry and give valuable insight into many diseases.

## References


1. Kubinova, S., and Sykova, E. Nanotechnologies in regenerative medicine, *Minim Invasive Ther Allied Technol 19*, 144-156.
2. Buzanska, L., Zychowicz, M., Ruiz, A., Ceriotti, L., Coecke, S., Rauscher, H., Sobanski, T., Whelan, M., Domanska-Janik, K., Colpo, P., and Rossi, F. Neural stem cells from human cord blood on bioengineered surfaces--novel approach to multiparameter bio-tests, *Toxicology 270*, 35-42.
3. Hassell, T. J., Jedlicka, S. S., Rickus, J. L., and Irazoqui, P. P. (2007) Constant-current adjustable-waveform microstimulator for an implantable hybrid neural prosthesis, *Conf Proc IEEE Eng Med Biol Soc 2007*, 2436-2439.
4. McKnight, T. E., Ericson, M. N., Jones, S. W., Melechko, A. V., and Simpson, M. L. (2007) Vertically aligned carbon nanofiber arrays: an electrical and genetic substrate for tissue scaffolding, *Conf Proc IEEE Eng Med Biol Soc 2007*, 5381-5383.
5. Teixidor, G. T., Gorkin, R. A., 3rd, Tripathi, P. P., Bisht, G. S., Kulkarni, M., Maiti, T. K., Battacharyya, T. K., Subramaniam, J. R., Sharma, A., Park, B. Y., and Madou, M. (2008) Carbon microelectromechanical systems as a substratum for cell growth, *Biomed Mater 3*, 034116.
6. C.D. Tidwell, D. G. C., S.L. Golledge, B.D. Ratner, K. Meyer, B. Hagenoff, and A. Benninghoven. (2001) Static ToF SIMS and XPS Characterization of Adsorbed Albunim and Fibronectin Films, *Surface and Interface Analysis 31*, 724-733.
7. Alger, B. E., and Teyler, T. J. (1976) Long-term and short-term plasticity in the CA1, CA3, and dentate regions of the rat hippocampal slice, *Brain Res 110*, 463-480.
8. Malenka, R. C., and Bear, M. F. (2004) LTP and LTD: An Embarrassment of Riches, *Neuron 44*, 5-21.
9. Peter W. Kalivas, C. D. B. (1988) *Sensitization in the Nervous System* 1 edition ed., CRC.
10. Kandel, E., Schwartz, J., and Jessell, T. (2000) *Principles of Neural Science*, 4 ed., McGraw-Hill Medical.
11. Schwartzkroin, P. A., and Wester, K. (1975) Long-lasting facilitation of a synaptic potential following tetanization in the in vitro hippocampal slice, *Brain Res 89*, 107-119.